VALIDATION OF A NAVIGATED HIP REPLACEMENT SURGERY SYSTEM

By

Shanika Mihirani Arumapperuma Arachchi

This thesis is submitted in partial fulfillment of the requirements

For the degree of

Master of Philosophy in Bioengineering

18/07/ 2012

Bioengineering Unit
University of Strathclyde
Glasgow, UK

DECLARATION

This thesis is the result of the author's original research. It has been composed by the author and has not been previously submitted for examination which has led to the award of a degree. The copyright of this thesis belongs to the author under the terms of the United Kingdom Copyright Acts as qualified by University of Strathclyde Regulation 3.50. Due acknowledgement must always be made of the use of any material contained in, or derived from, this thesis.

Signed:

Date:

ACKNOWLEDGEMENTS

First and foremost, I would like to express my gratitude to Professor Philip Rowe, my supervisor at Bioengineering, University of Strathclyde, for his technical guidance, support and timely encouragement during this research. I would not have been able to pursue this degree without his patience, insight, and plentiful advice.

I would also like to express my gratitude to those who have contributed significantly to this research work, in particular to:

- OrthoPilot™ BBraun Aesculap, Tuttlingen, Germany
- Dr. Angela Deakin, Golden Jubilee National Hospital, Clydebank, for her kind support and guidance throughout my research
- Golden Jubilee National Hospital, Clydebank, for supporting me in different ways, including financial support for conferences, providing necessary experimental equipments and many more to state here
- Those who were with me during this time, encouraging me and helping me in various ways

Finally I am grateful to Upaka Rathnayake for his help and encouragement in any number of ways.

Shanika Mihirani Arumapperuma Arachchi

DEDICATION

This thesis is dedicated to my loving father A.A Bandupala and my loving mother Chandra Senanayake.

ABSTRACT

Navigation of surgical instruments and implants plays an important role in the computer assisted surgery. OrthoPilot™ Hip Suite (BBraun Aesculap) is one such system used for hip navigation in orthopedic surgery. However the accuracy of this system remains to be determined independently of the manufacturer. The manufacturer supplies a technical specification for the accuracy of the system (± 2 mm and ± 2°) and previous research has been undertaken to compare its clinical accuracy against conventional hip replacements by x-ray. This clinical validation is important but contains many sources of error or deviation from an ideal outcome in terms of the surgeons' use of the system, inaccurate palpation of landmarks, variation in actual cup position from that given by the navigation system and measurement of the final cup position. It is therefore not possible to validate the claims of the manufacturer from this data. There is no literature evaluating the technical accuracy of the software i.e. the accuracy of the system given known inputs. The main aims of this study were to validate the OrthoPilot data capturing and to validate the cup navigation algorithm. The OrthoPilot was compared with the gold standard of a VICON movement analysis system. An aluminium pelvic phantom was machined with high accuracy to perform the experiments. Data were captured simultaneously from both OrthoPilot and VICON systems. Distances between the anatomical land marks, which defines the anterior pelvic plane on the pelvic phantom were compared to test the accuracy and the repeatability of the OrthoPilot data capturing. The accuracy of the hip navigation algorithm was tested by applying similar algorithm to calculate the native anteversion and inclination angles of the acetabulum using the VICON system. Both systems produce comparable results with small standard deviations. Finally, it can be concluded that from the laboratory based data, the OrthoPilot system, if used correctly, for the radiographic definition of the acetabular alignment using passive trackers, are sufficiently accurate for the orthopedic applications.

LIST OF PUBLICATIONS ARISING FROM THIS WORK

Journal paper

S.M.A. Arachchi, A. Augustine, A.H. Deakin, F. Picard, P.J. Rowe, "Validation of a CT-free navigation system for the measurement of native acetabular alignment", Journal of Orthopaedic Surgery, (in the process of submission)

Extended abstract

S.M.A. Arachchi, A. Augustine, A.H. Deakin, F. Picard, P.J. Rowe (2011). "Technical validation of the accuracy of measurement of pelvic planes and angles with a navigation system" for British Journal of Bone and Joint Surgery (in press)

Conferences

S.M.A. Arachchi, A. Augustine, A.H. Deakin, F. Picard, P.J. Rowe (2011). "Technical validation of the accuracy of the OrthoPilot cup navigation software-measurement of native acetabular alignment" at Institute of Mechanical Engineers, Engineers and Surgeons: Joined at the Hip III November 1-3, London, UK

S.M.A. Arachchi, A. Augustine, A.H. Deakin, F. Picard, P.J. Rowe (2011). "Technical validation of the accuracy of measurement of pelvic planes and angles with a navigation system" at 11th Annual Meeting of the International Society for Computer Assisted Orthopedic Surgery, June 15-19, London, UK

S.M.A. Arachchi, P.J. Rowe (2011) "Technical validation of the accuracy of the navigated hip replacement surgery system" University Research Day, June 7, Barony Hall, University of Strathclyde, Glasgow, UK

TABLE OF CONTENT

LIST OF FIGURES

LIST OF TABLES

ABBREVIATIONS

APP	Anterior Pelvic Plane
APC	Anterior Pelvic Coordinate
ASIS	Anterior Superior Iliac Spine
LASIS	Left Anterior Superior Iliac Spine
RASIS	Right Anterior Superior Iliac Spine
PS	Pubic Symphysis
Ant	Anteversion Angle
Inc	Inclination Angle
ϕ	Rotational angle around X axis
θ	Rotational angle around Y axis
φ	Rotational angle around Z axis
A	Transformation matrix of position sensor
A^{-1}	Inverse matrix of A
B	Transformation matrix of position sensor
P	Transformation matrix of any point
R_{ij}	Any Component of Rotational matrix of any point
T_k	Any translation components of matrix P
R_p	Rotational matrix of P
T_p	Translation matrix of P
R_x	Rotational matrix around X axis
R_y	Rotational matrix around Y axis
R_z	Rotational matrix around Z axis
T_r	Transformation matrix of the surgical tool
x_p	X component of any point P
y_p	Y component of any point P
z_p	Z component of any point P
$(x_{col}, y_{col}, z_{col})$	Coordinates of the collateral ASIS (Ipsilateral)
$(x_{con}, y_{con}, z_{con})$	Coordinates of the Contralateral ASIS
$(x_{cen}, y_{cen}, z_{cen})$	Coordinates of pubic Symphysis, central

Chapter 1

INTRODUCTION

1.1 Background

Computer assisted surgery is becoming more frequently used in the medical world. Navigation of surgical instruments and implants plays an important role in orthopedic surgery. OrthoPilot™ Hip Suite (BBraun Aesculap) is one such system used for navigation in total hip replacement surgery. However the accuracy of this system required to be determined independently of the manufacturer. According to the OrthoPilot manufacturer's technical specification (user manual), the system precision with regard to the computed angles and distances is $\pm 2^0$ and ± 2 mm respectively. Previous research (Kiefer, 2003) has been undertaken to compare OrthoPilot's clinical necessity against conventional hip replacements using x-ray. This clinical validation is important; however it contains many sources of error or deviation from an ideal outcome in terms of the surgeons' use of the system, inaccurate palpation of landmarks, variation in actual cup position from that given by the navigation system and measurement of the final cup position. It is therefore not possible to validate the claims of the OrthoPilot manufacturer about the accuracy of the system easily from these data. There is no literature evaluating the technical accuracy of the system i.e. the ability of the system to measure known inputs.

1.2 Aims of the research

The main aim of this study was to examine the accuracy of the OrthoPilot system. In order to achieve this aim, the research was carried out with two sub aims. These two sub aims are to

- Assess the accuracy of the OrthoPilot system, while navigating the surgical instruments

- Assess the accuracy of the hip navigation algorithm which is used in the OrthoPilot system to orientate and position the acetabular cup.

Accuracy was assessed out using the gold standard VICON system by comparing the data from both systems.

1.3 Scope of the research

Total hip replacement (THR), total knee replacement (TKR) and anterior cruciate ligament (ACL) replacement are the major usages of the OrthoPilot system. With the limited time and the available resources, OrthoPilot cup only navigation, which is a section of the total hip replacement procedure, was considered during this study as misalignment of the cup can lead to dislocation of the replacement hip and major complication as a result. This experimentation was performed and compared against the gold standard of a VICON movement analysis system to achieve the above stated aims. All the experiments were conducted using accurately made pelvis phantom for the radiographic definition of the acetabular alignment and passive trackers were used for data palpation.

1.4 Layout of the thesis

Layout of the thesis is explained in this paragraph. Chapter 1 of the thesis is to give brief introduction of the research aims and the thesis layout. Chapter 2 of the thesis is dedicated to literature review. Background information on hip anatomy, hip replacement, reasons behind hip failures, computer assisted navigation and problems in applying navigational techniques in real surgeries are presented in this chapter. Detailed discussions on content validity of the OrthoPilot system and mathematical representation during the data palpation and surgical navigation processes are discussed in the Chapter 3. The next chapter, Chapter 4 discusses validation of the OrthoPilot system. Detailed experimental procedures and their results are discussed in this chapter. Discussions of the results and the future works are presented in the chapter 5. Finally, Chapter 6 highlights the concluding remarks.

Chapter 2

LITERATURE REVIEW

2.1 Introduction

The hip joint is known as the coxal articulation in medical terminology. It is located, where the thigh bone (femur) articulates with the pelvis. The head of the femur and a cavity in the pelvis bone (acetabulum) form the hip joint. The hip joint allows a wide range of motion. This is greater than would appear to be required for daily activities (Radin 1980).

Walking is one of the major human daily activities in which the hip joint plays an essential part. In normal level walking, the pelvis rotates alternatively to the right and to the left, relative to the line of progression. In the stance phase of gait, this rotation occurs alternatively at each hip joint. Each hip joint passes from internal to external rotation and is reciprocated by the other hip (Saunders et. al 1953).

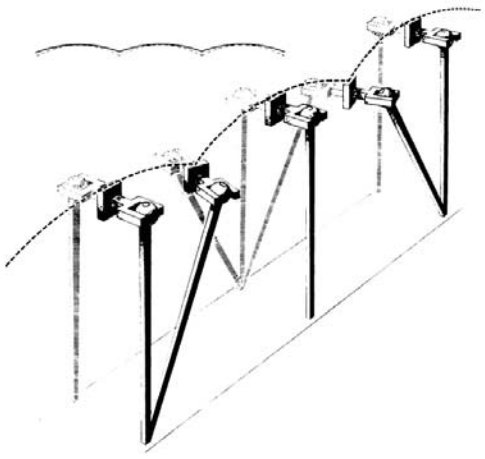

Figure 2.1: Pelvic rotation (Saunders et. al 1953)

Referring to the figure 2.1, the pelvic rotation flattens the arc of the center of gravity. Because of this, the energy consumption in locomotion is reduced. In addition, the angular rotation at the hip is reduced hence saving energy required for oscillation of the trunk and limbs (Saunders et. al 1953). Therefore, rotation of the hip is essential for a smooth bipedal gait.

The pelvis is tilted in normal locomotion. The displacement of the hip joint produces an equivalent relative adduction of the extremity in the stance phase. In addition, it produces relative abduction of the extremity in the swing phase. The knee joint of the non weight-bearing limb must flex to allow the clearance for the swing-through of delay to accommodate for pelvic tilt (Saunders et. al 1953).

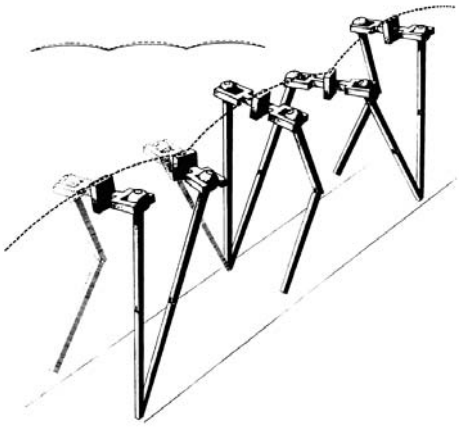

Figure 2.2: Pelvic tilt (Saunders et. al 1953)

2.2 Necessity of hip replacement

In the UK, approximately 15% of the female and 10% of the male population over the age of 65 have radiographic evidence of moderate to severe osteoarthritis of the hip joint (Erhardt 1995). According to the Frankel et al (1999), 12.7-17.8 people per 1000 aged 35-85 years are suffering from hip diseases, which require surgery.

According to Erhardt (1995) and Frankel et al (1999), hip replacement surgery is conducted to relieve the arthritic pain and restore range of motion. A diseased hip joint not only causes pain, but also limits the ability to perform normal activities. Hip

replacement is a surgical procedure to replace the hip joint by a prosthetic implant. The objectives of the hip replacement are to minimize or to eliminate the pain and to improve the mobility.

Dandy & Edwards, (2003) described in their studies that, the most common diseases leading to hip replacement are Osteoarthritis, Rheumatoid arthritis, Osteonecrosis and Hip disorders or fractures. These authors further explained that, Osteoarthritis is the gradual deterioration of the cartilage within the joint. Pursuant to cartilage wear, irregularities have occur on the surrounding joint surface. Rheumatoid arthritis is an inflammation of the tissues surrounding the joint and this leads to wear the cartilage and a painful swollen joint. Deterioration of the cartilage and destruction of the joint are the results of this decease. Osteonecrosis occurs due to the loss of blood supply to the ball of the hip joint. Hip disorders or fractures occur due to falls or accidents and hip replacement surgery is performed to treat the associated fractures. Both ball and socket are replaced in a total hip replacement. The acetabulum is replaced by a plastic, ceramic, or metallic cup, while the femoral head is replaced by a ball attached to a long stem, usually of metal. The stem is fixed into the femur either by a porous bone in growth surface or cement.

2.3 Reasons for implant failure

DiGioia et. al (2002) stated in his studies that, the most common complication of hip arthroplasty is mal-positioning of the implant. Mal-positioning of the components is linked with dislocations, impingement, pelvic osteolysis, acetabular migration, leg length discrepancy, early implant wear and malfunction of the hip due to loosening. Numair et al. (1997) described 15% revision rate of the acetabular component in the group of high hip dislocation, based on his study at Wrightington hospital, Wigan, UK. Furthermore, authors described cup loosening seems to be a general complication of THA in high hip dislocation and possible loosening of the acetabular component was 16%. According to the Fender et. al (1999), the main reasons for implant failure were aseptic loosening (2.3%), deep infection (1.4%) and general loosening (5.2%). In addition, a Swedish study (Herberts and Malchau 200

0) had found 71% of hip replacement revisions were due to aseptic loosening; however, the number of revisions in Sweden had decreased to 3% within 10 years mainly due to improvements of surgical techniques. Improper placement of acetabulum or femoral head or both of them may lead to one or a combination of the above-mentioned problems. Improper acetabular component positioning is linked to impingement and dislocations (Kennedy et. al 1998).

According to Wolf. et al. (2005), implant impingement leads to restrict range of motion and higher stress on bearing surfaces and bone implant interfaces. Mal-positioning of the acetabular cup causes inappropriate tensional forces and these forces lead to prosthesis wear and loosening. In addition, authors mention that, if the abduction angle of the cup is more vertical than normal, load per unit area in the superior aspect of the polyethylene increases linearly leading to a higher wear. Errors introduced during landmark palpation have a substantial effect on the final cup orientation and hence on impingement, dislocation, wear and loosening (Wolf. et al. 2005).

2.4 Method of guidance

The method of guidance used to implant the cup plays an important role in precise implant positioning. Three main types of guidance methods have been used for hip replacement. These component guidance methods can be categorized as conventional, mechanical and navigational.

Murray, (1993) described conventional hip replacement surgery which exposes the muscles overlying the joint during the surgery. At the end of the replacement procedure, the muscles are repaired. Lewineck et al, (1978) concluded in their studies that, in the conventional method using vision alone, acetabular cup positioning is carried out manually within the safe range of 15^{o} +/- 10^{o} of anteversion and 40^{o}+/- 10^{o} of inclination, this range was arrived through experience. Furthermore, authors stated, main disadvantages of the conventional hip replacement are high possibility of dislocation, early implant wear and long rehabilitation time.

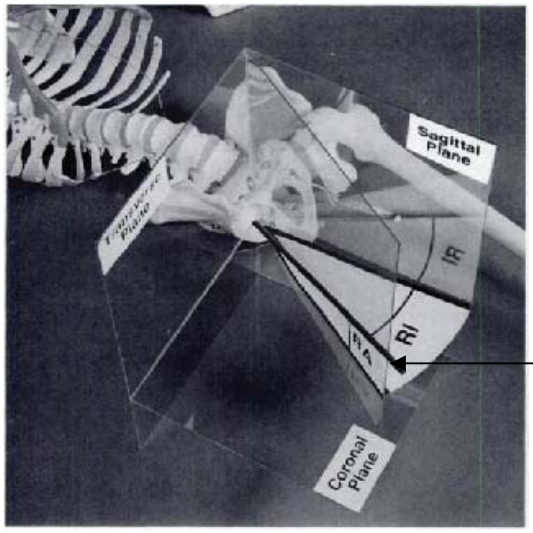

Figure 2.3 Radiographic definition of the acetabular orientation; RI: Radiographic inclination, RA: Radiographic anteversion (Murray 1993)

According to Jaramaz et. al 1998, rigs and jigs are used in mechanical guidance method. Most surgeons are aiming to obtain $40^0$of inclination and $15^0$of anteversion using the mechanical devices provided by the implant manufacturers. These angles are determined relative to the Anterior Pelvic Plane (APP). DiGioia et. al (2002) evaluated the mechanical guidance method for acetabular alignment and concluded it was insufficient to achieve the final acetabular orientation required. Furthermore, they concluded that, there was a significant variation in the range of the implant cup alignment in inclination (46^o +/- 13^o) and in anteversion (10^o +/- 14^o), after examining the post operative radiographs. Incorrect positioning of the mechanical jigs causes mal-alignment and implant mal-positioning (Jaramaz et. al 1998).

Mechanically guided implant positioning is designed to improve the accuracy of the component orientation compared to conventional implant positioning. Proper component orientation is inadequate in mechanically guided hip replacements, as the guides do not account for variations of the patient's position and pelvic motion during the surgery (Ybinger et. al 2007).

Computer assisted navigation systems were developed to provide surgeons with improved methods for intra-operative measuring of the orientation and the alignment, based on anatomical landmarks or on improved mechanical alignment tools (Ybinger et.

al 2007, DiGioia et. al 2002). Also, DiGioia et. al (2002) stated that, computer assisted navigation creates many opportunities; providing the ability to measure intra-operative implant alignment precisely, intra-operatively prepared acetabular surface and bone preparation by resulting optimal acetabular cup alignment.

2.5 Navigation - general use in surgery

Finding the way from one place to another is called Navigation. Sugano (2003) described, surgical navigation as a visualization system, which provides positional information about the surgical tool or the implants' relative to a target organ (bone) on a computer display in real time. Furthermore, he stated that, surgical navigation uses 3D positional sensors to track the targeted organ and surgical instruments or implants. Tran et al, (2009) stated that, navigation systems combined with imaging techniques provide computer-assisted surgery. According to the authors, this makes possible less invasive surgical operations with a smaller scar and reduced rehabilitation time. Furthermore, they stated that, navigational and imaging data and advanced computer graphics algorithms are used to generate a real time 3D anatomical structure, which guides the surgeon throughout the surgery.

Tran et al, (2009) also indicated that, navigation systems could be categorised into three main sections. They are intra-operative imageless navigation systems, pre-operative imaged-based navigation systems (CT and MRI) and intra-operative image-based navigation systems (Ultrasound and Fluoroscopy). In addition, Langlotz et.al (2007) described the systems, based on the different imaging or digitization techniques, these used for acetabular cup placement, namely as computer tomography based (CT- based), fluoroscopy based or imageless navigation.

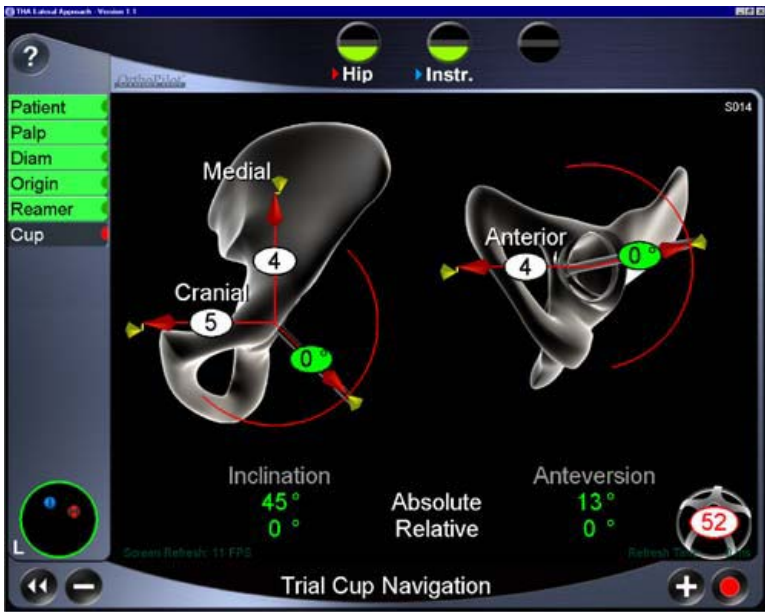

Figure 2.4 Intra-operative screen shot of OrthoPilot (image-less navigation system) hip navigation (Reference: Kiefer 2003)

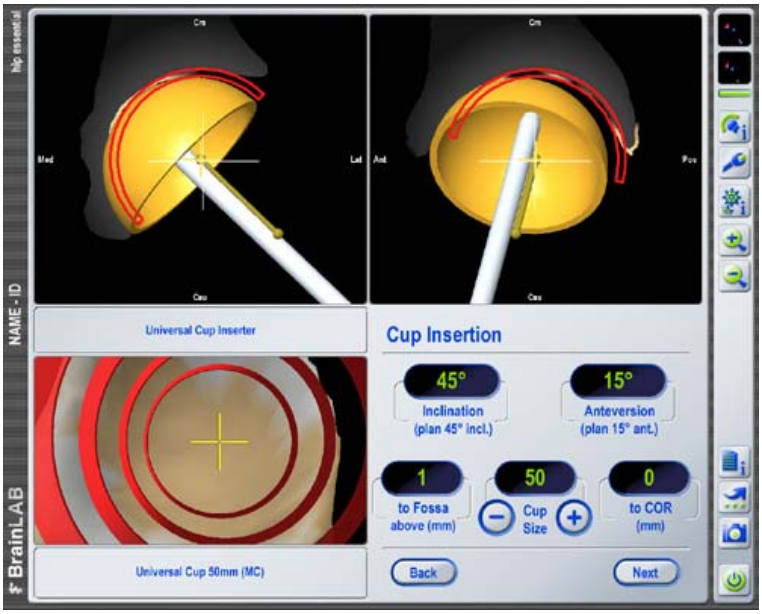

Figure 2.5 Screen shot of Brain LAB system (Image based navigation system) (Reference: www.brainlab.com/ hip-navigation-application/).

According to Sugano (2003) Computer assisted surgery can also be classified into three types; passive systems, semi-active systems and active systems. Sugano described them as follows; passive systems assist the surgeons during preoperative planning, surgical simulation, or intra-operative guidance without performing any

actions on the patients. Semi-active systems assist the surgeon by moving a drill guide sleeve or a cutting jig to the correct position and then the system cuts the bone. Active systems directly contribute to some pre-operatively programmed surgical actions i.e. bone cutting.

Tran et al, (2009) further explained, neither CT nor radiographs are used in the intra-operative image-less navigation systems. However, CT images are used in the pre-operative image-based navigation systems, while radiographs are used in the intra-operative image-based navigation systems. Image-free navigation is more popular because it minimizes the surgical time and surgical cost. In addition, the patient does not need to be exposed to ionizing radiation.

Swiatek-Najwer et al. (2008) indicated that, the position of the surgical tools with respect to the patient's frame is tracked with the navigation system. The purpose of this tracking system is to lead an object to a desired location precisely. In addition, they described, the three main types of tracking systems, which are acoustic tracking systems, optical tracking systems and electromagnetic tracking systems. They indicated that, optical and electromagnetic tracking systems are the most prominent. Electromagnetic tracking system uses an electromagnetic field from a transmitter to generate local magnetic field, which is detected by passive sensors to give their position and orientation to that field. Electromagnetic navigation gives high resolution. However, the main disadvantage of this navigation is the errors introduced by ferrous metallic objects and electromagnetic devices. This means that the surgical field must be kept free of ferrous materials and all the surgical tools must be non-ferrous. Further, the operating room must be free of major sources of electro magnetic radiation.

Sugano (2003) concluded that, optical tracking systems are more frequently used in navigation systems in orthopaedic surgery. He further explained that, in optical tracking systems, charged coupled device (CCD) cameras are used to obtain positional information. These are usually based on infrared light from a dynamic reference frame made from infrared light-emitted diodes (LED) or infrared light-

reflecting markers. The dynamic reference frame is attached to the target organs (or bones) and the surgical tools to be tracked. Highly accurate and fast measurements can be obtained from optical sensors as many LEDs can be tracked simultaneously, although an uninterrupted line of sight must be maintained between the CCD camera and dynamic reference frame. Swiatek-Najwer et al. (2008) described in his article that, an infrared camera tracks both active and passive elements. In an active marker system infrared light emitted by the diodes, an active marker is observed by the camera. In passive marker system, spheres of metal or plastic are coated with reflective tape or paint to give a passive marker, which reflects IR light emitted from diodes around the camera lens. The positions of the rigid bodies that make up the limbs are tracked by in the computer using a cluster of markers attached to the limb with the camera data.

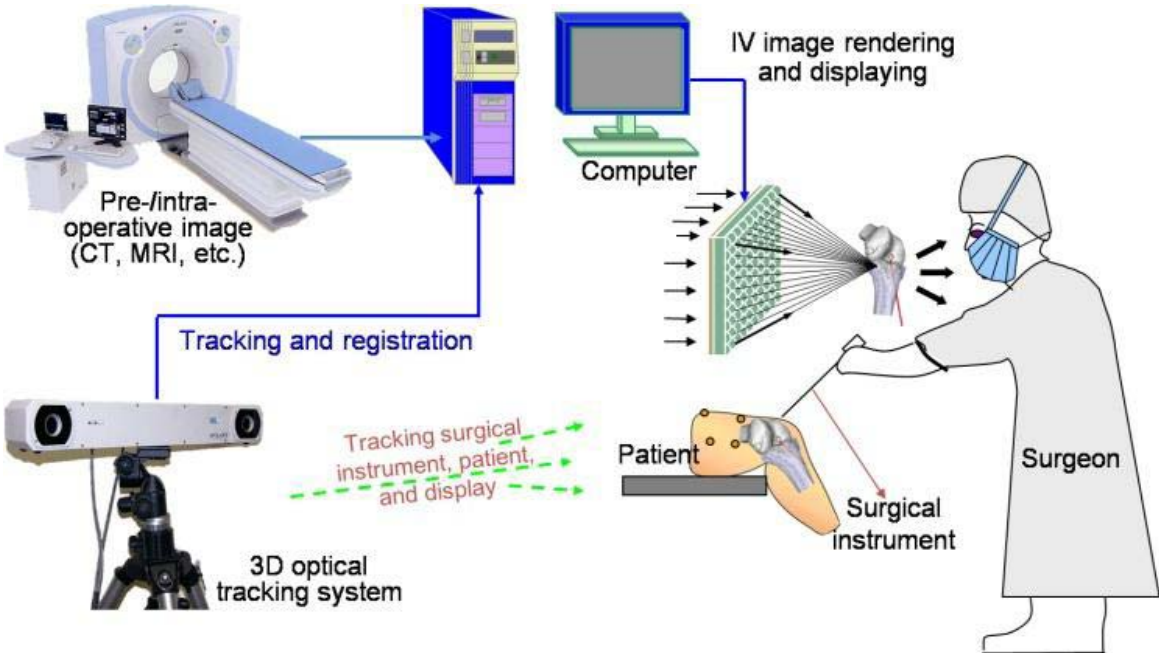

Figure 2.6 Computer assisted navigation system (Tran et al, 2009)

Figure 2.6 shows the configuration of a typical navigation system. This system consists of an image acquisition device (CT- Computer Tomography or MRI- Magnetic Resonance Image), an optical position-tracking device and a computer,

which is used for data segmentation, communication and other computational tasks. The patient is scanned and data are sent to the computer. These data are used to construct a 3D surface model. During the operation, the orientation of optical markers, which are attached to the surgical tool are read by the tracking device and sent to the computer. This data determines the position and orientation of the surgical tool and guides the surgeon to produce accurate instrument and implants' positioning during the operation.

2.6 Hip navigation systems

Navigational techniques are widely used in hip implant surgeries (Kelley et. al (2009), Sugano (2003), Tran et al, (2009)). The systems claims to provide optimal implant positioning and minimize the risk of dislocation and implant wear; hence increasing longevity (Kelley et. al 2009). The first use of these surgical techniques can be traced back to the beginning of the 20th century. Robert Henry Clarke and Sir Victor Horsley developed the first practical stereotactic apparatus for animal research in 1908. Their surgical instruments were localized using a Cartesian coordinate system. Since then, the applications of the computer tomography and magnetic resonance imaging have been developed and facilitated by stereotactic surgery. The first hip navigation system was developed in 1992 by ROBODOC; Integrated Surgical Systems, Davis, California [now Curexo Technology, Sacramento, California] and it was an image based navigation system.

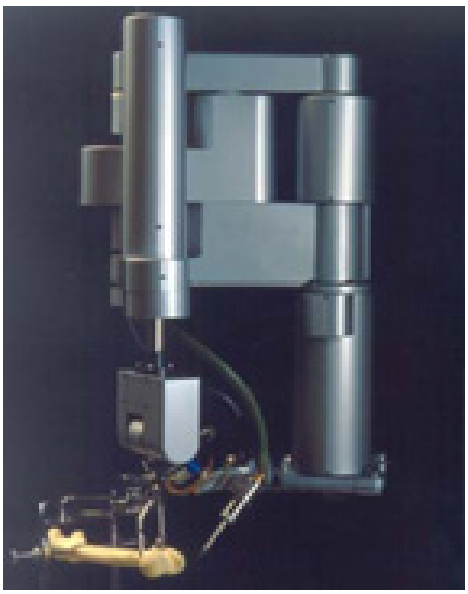

Figure 2.7 Early ROBODOC prototype (Reference: www.robodoc.com/pro_about_history.html)

Recently, a number of surgical navigation systems have been used for the hip replacement surgery (Kelley et. al 2009). These navigation systems enhance the tools to measure acetabular cup positioning intra operatively, most notably the pioneering computer-assisted navigational systems that utilise preoperative planning with computer tomography scans. These systems are thought to be highly successful in improving the acetabular component position to the acceptable range (Ybinger et. al 2007).

2.6.1 Image-based navigation

The Hip Navigational System (HipNav) is an image-guided navigational tool, which can be used to improve the positioning of the acetabular implant in THA (DiGioia et. al 1998). The aim of this development was to address the limitations' inherent in conventional method of component positioning. The HipNav system determines the optimal position and orientation of the acetabulum by the preoperatively generated CT scans of the pelvis. Optical localizer is used for intra-operative guidance. This optical localizer tracks marker with infrared light-emitted diodes it is therefore an active optical image guided system. A cluster of marker is attached to the pelvis and

allow continuous tracking of the pelvis during cup positioning. Jaramaz et. al (1998) showed in a clinical trial that data from the first eight patients enrolled in the HipNav system achieved cup inclination and anteversion closer to that recommended by the implant manufacturer than would have been achieved with mechanical guides.

CT- based navigation uses preoperative CT imaging to create 3-dimensional models of the hip joint (Ecker et al 2007). By using these images, placement of the prosthetic component is planned before the surgery. In addition, this method allows pre-operative prediction of the leg length change and the range of motion of the hip, which will result from the proposed surgery.

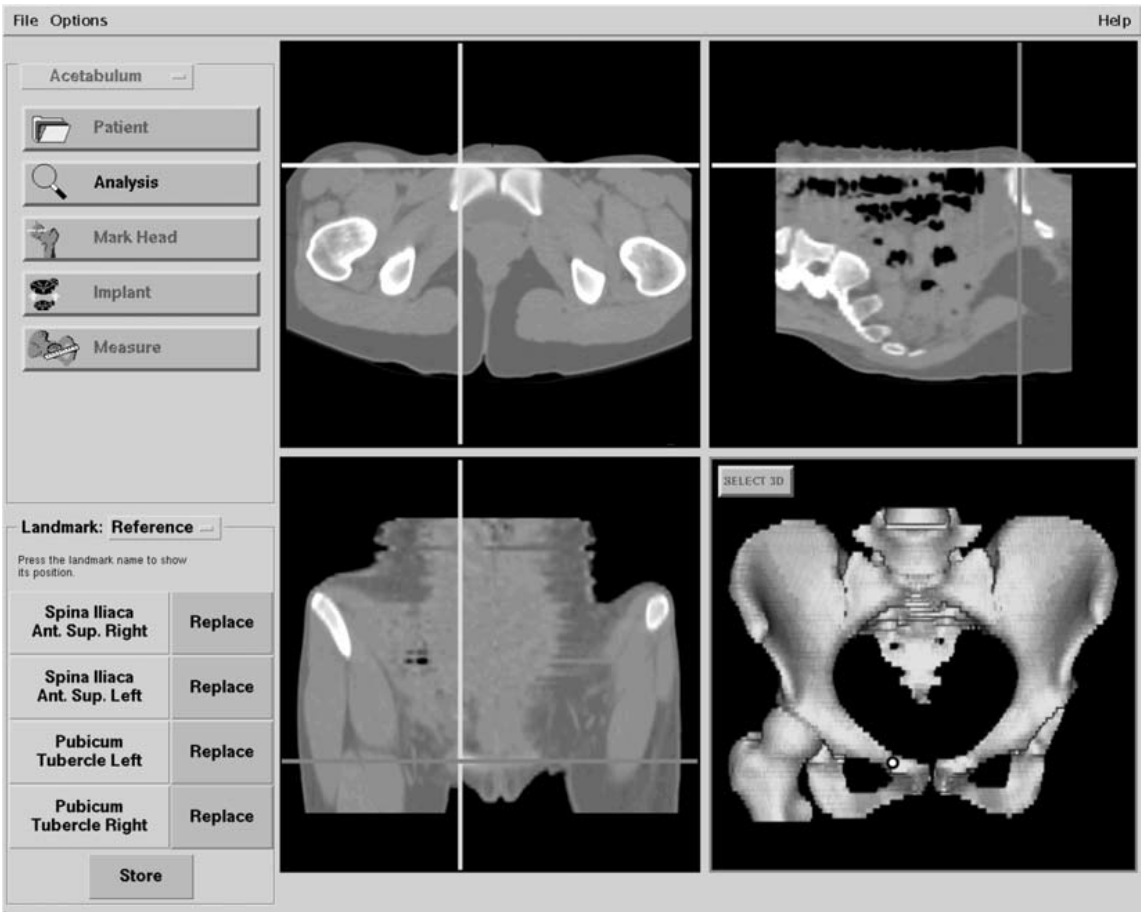

Figure 2.8 CT-based definition of the anterior pelvic plane. Pelvic landmarks (here a right pubic tubercular) are interactively defined in 2D and 3D representations of the anatomy (Langlotz et. al 2007)

2.6.2 Image-free navigation

Image-free navigation is also known as kinematic or landmark-based navigation. The implant alignment in image-free navigation is based only on anatomical landmarks, palpated intra-operatively by the surgeon using a reference pointer (Kalteis et. al. 2005). The surgeon communicates with the kinematic navigation system, via a computer screen, which shows how to guide the surgical instruments and implants. This system is designed to implant the cup in the desired position and orientation with respect to the pelvis, and independent of the patient's position on the table (Kiefer 2003).

Kalteis et. al. (2005) described that, in image-free navigation, the anterior superior iliac spine and pubic tubercles are palpated when implanting the acetabular cup. These data provide the basis for 'Surgeon-defined anatomy' and frontal pelvic plane is defined with that data. Pre-operative or intra-operative image acquisition is not required for image-free navigation. According to the authors, accuracy of the acetabular component positioning using the image-free navigation is as accurate as the CT-based method and both techniques significantly reduce the variation in the positioning of the component compared to the conventional free hand method.

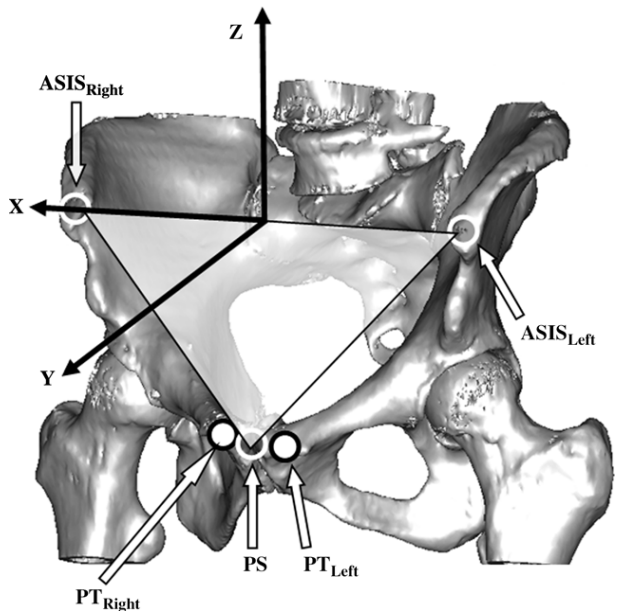

Figure 2.9 Anatomical landmarks of Anterior Pelvic Plane (Reference: Lin et al 2008)

Striker navigation system (Stryker Corporation, Kalamazoo, MI, USA) and OrthoPilot™ Hip Suite (BBraun Aesculap, Tuttlingen, Germany) are two examples of image-free navigation systems. Striker has been used for surgical navigation since August 2000 (www.stryker.com). Accurate and optimal extension and rotation of the hip prosthesis can be quickly determined with this system. It uses active LED based tracking system. In this system, relevant bony landmark positions are determined by the manual palpation and trackers are rigidly fixed to the pelvis and femur (Lin et. al 2008).

Figure 2.10 Screen shot of Striker hip navigation (Reference: www.stryker.com)

OrthoPilot™ was introduced in 1994. It was initially used solely for total knee replacement but from 2000 onwards, it has been used for total hip replacement (http://www.orthopilot.com). It uses an opto-electronic Polaris stereo camera to detect infrared signals from active marker clusters attached to the rigid bodies and a pointer (which is used to palpate anatomical landmark positions), the acetabular reamer and a cup inserter.

Figure 2.11 OrthoPilot navigation system (Reference: Kiefer 2003)

The computer program incorporated in the OrthoPilot system calculates the hip joint centre from the data obtained via surface matching, which is performed by palpating the anatomical landmarks with a pointer and via kinematics (by moving the surgical tool) (Kiefer 2003). With this data, the algorithm within the system calculates the native acetabular orientation, depth of the reaming and orientation of the trial and final cup. During the entire procedure, data in graphical and numerical form, as well as virtual instruments are shown on the computer screen and help to guide the surgeon.

Kiefer (2003) stated that, kinematic cup navigation using the OrthoPilot system demonstrated an improvement in final cup position compared to the conventional cup positioning. Furthermore, their clinical study concluded that, this system leads to reduced dislocation rates, improved joint mobility and reduce incidence of impingement syndrome resulting in a reduction of implant wear. In addition, this system is simple to use and is cost and time efficient.

Figure 2.11 shows the OrthoPilot based cup navigation procedure. Anatomical landmarks for the APP registration is required pre-operatively to navigate the acetabular component, so that the position of the pelvis and the acetabulum in space can be determined by the system. The pelvis is registered by palpating the anterior superior iliac spines and the mid point of Pubic Symphysis. The anterior pelvic plane (APP) is created using these data and then the APP is used as the reference to navigate the implant cup. In imageless navigation systems, registration is made relative to an optical tracker mounted on the pelvis. Anatomical landmarks of anterior superior iliac spines and pubic tubercle are palpated directly over the soft tissue; then registered using an optical pointer. APP palpation is performed while the patient is in the supine position, which allows access to the opposite anterior superior iliac spine. Then, the patient can be turned to the lateral side lying position, after which surgical exposure, acetabular center registration, medial wall palpation, reamer navigation and cup navigation steps follow.

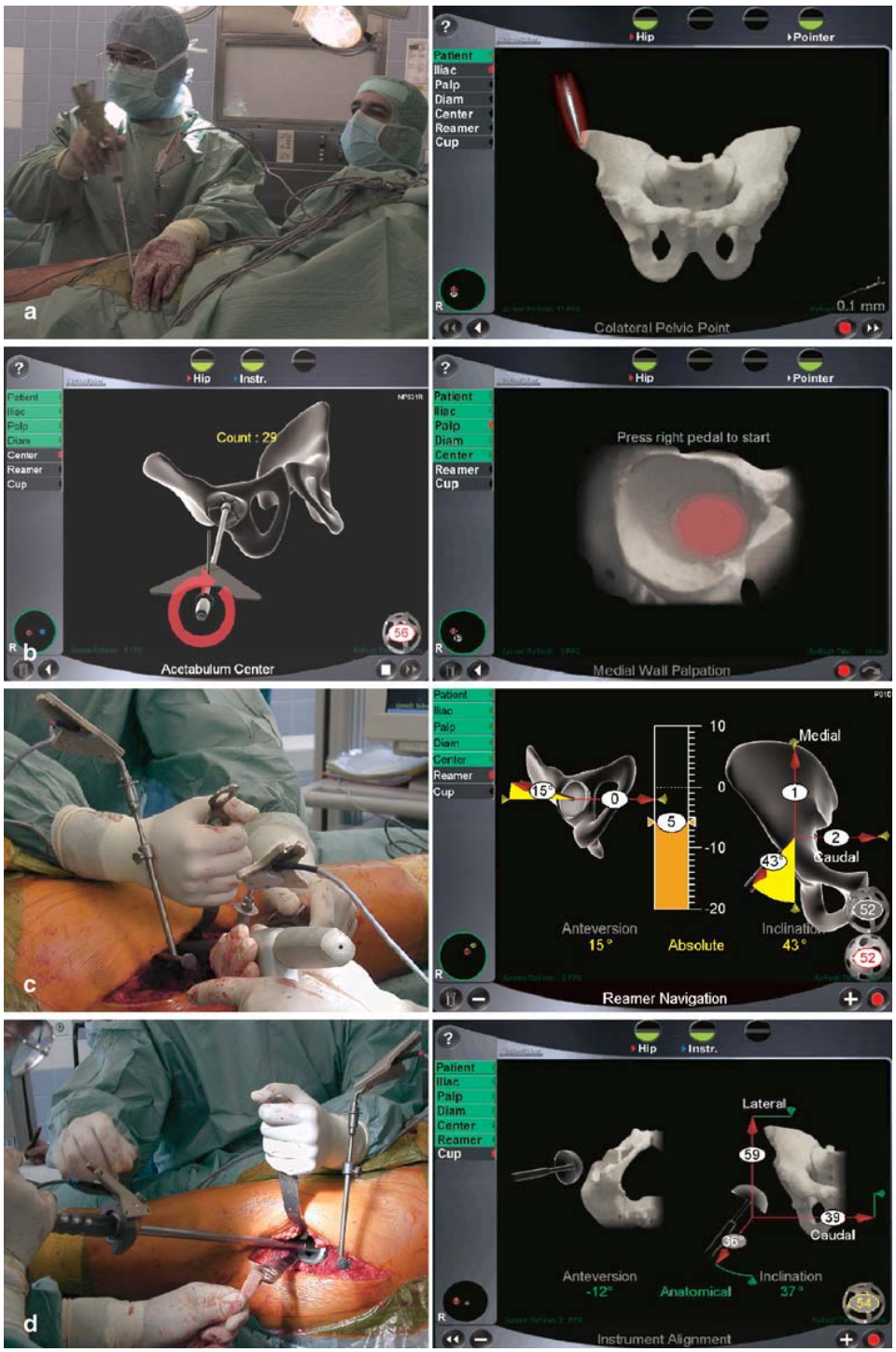

Figure 2.12 OrthoPilot cup navigation, intra-operative workflow: **a** percutaneous registration of the anterior pelvic plane; **b** kinematic registration of the hip centre and palpation of medial wall surface; **c** acetabular preparation by navigated reaming; **d** navigated trial cup insertion and press-fit cup implantation (Reference: Kiefer 2003)

2.6.3 Robotic surgery

Precise execution of a pre-operative plan is not guaranteed by the use of navigated computer assisted surgery as it assists the surgeon in pre-operative and intra-operative planning (Logishetty et. al 2010). The native acetabular reaming and cup implantation is still done by hand. Furthermore Logishetty et. al 2010 have stated that, Surgeons may not position the tools according to the plan as precisely as machines. Robotic systems have been developed to overcome the inaccuracy of the hand-controlled positioning of the surgical tools. In addition, robotic surgery facilitates minimally invasive surgical approaches. It could also be applied for unmanned or remote surgery in the future.

The “da Vinci” tele-robotic platform is the most widely used robotic system. It has been licensed by the US Food and Drug Administration and used in urological procedures since 2001 and gynaecological procedure since 2005 (Logishetty et. al 2010). There are numbers of examples of pilot robotic applications in orthopaedics (Sugano 2003). The Robodoc Surgical Assistant (Curexo) is one such example, which is used to automatically execute the preoperative plan in hip or knee surgery by using pre-operative anatomical information (Sugano 2003). It consists of five-axis robotic arm with high-speed milling device, and helps to mill the bone accurately to achieve precise fit for prosthetic implants. The “Brigit” Bone Resection Instrument is another robotic system, which helps to define cutting limits intra-operatively and assist surgeon in tool positioning (Sugano 2003). According to N. Sugano 2003, both Robodoc and Brigit are semi-active systems. In addition, these semi-active robotic systems can add virtual safety barriers and apply patient-specific templates for the cutters and drills alignment.

Acrobot, London, UK is a haptically guided robotic system used for unicondylar knee replacement, which is thought to improve the precision of implant positioning (Logishetty et. al 2010). Another example is MAKO Tactile Guidance system, which is a haptically guided robotic system (Logishetty et. al 2010). It uses pre-operative imaging to give anatomical information and guides the surgeon intra-operatively to

perform the milling and drilling task precisely. The MAKO system can be used for both hip and knee replacement surgery (Logishetty et. al 2010).

Figure 2.13 A semiactive haptically-guided robotic arm used in total knee arthroplasty—"Makoplasty" (Mako Surgical) (K. Logishetty et. al 2010).

2.6.4 Comparison of acetabular component positioning

Kalteis et. al (2006), which compared the accuracy of acetabular component positioning using free hand, CT-based and imageless navigation and hence results are summarized in Figure 2.14. Their findings were based on examining 90 patients, 30 of them had cup implanted by the free hand method, another 30 with CT based cup navigation, and 30 with imageless cup navigation. In addition, all the patients had a pelvic CT scan five to six weeks after operation in which inclination and anteversion angles were determined. Operation time was measured for all the

surgeries. In CT based navigation, operation time was increased by 17 min compared to the conventional technique (SD< 0.001) and it was increased by 8 min with imageless navigation (SD= 0.11) . This results shows imageless navigation was significantly faster than CT based navigation. According to their experiments, using conventional technique, 53% of the components were out side the Lewineck's safe zone (Inclination of 40^0 +/- 10^0 and Anteversion of 15^0 +/- 10^0). 7% of components were outside the safe zone using imageless navigation (Figure 2.14). They concluded that, when using free hand technique, there is high variability and lack of precision. These inaccuracies can be significantly reduced by using CT based or imageless computer assisted navigations and that imageless navigation is quicker to implement and less costly (DiGioia et al 2002, Kalteis et. al 2006, Kelley et. al 2009).

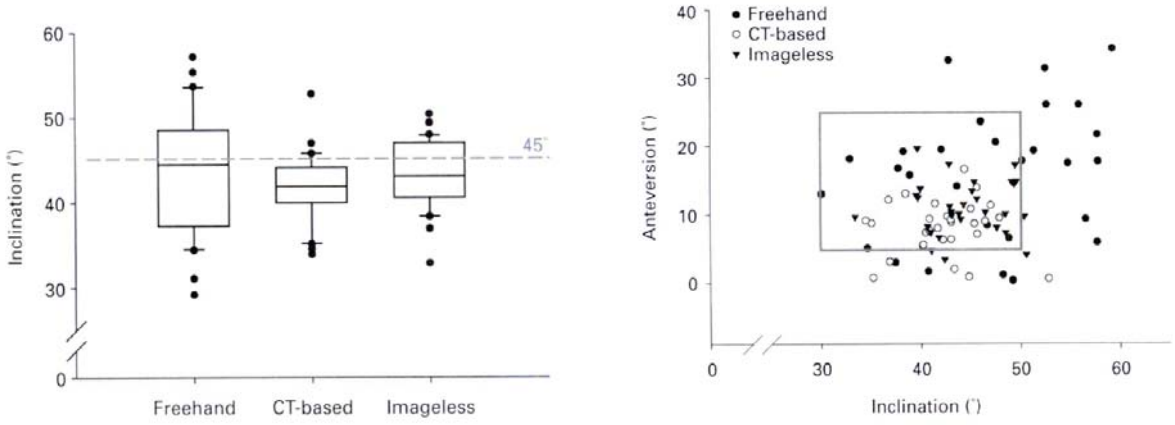

(a) (b)

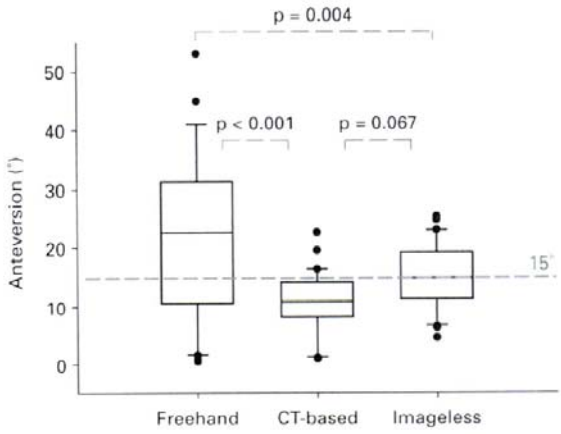

(c)

Figure 2.14 (a), (b), (c) Comparison of acetabular component positioning relative to Lewineck's safe zone using free hand, CT-based and imageless navigation (T. Kalteis et. al 2006).

2.7 Problems with navigation

In summary, it is claimed that, computer assisted navigation leads to more precise implant positioning so benefiting outcome. The main disadvantage of computer-assisted navigation is the time consumption. This navigation increases the intra-operative time by about 10 minutes generally. This directly affects the patient's health in number of ways, such as increasing the anaesthetic time, possible blood

loss. A further 10 minutes is added if image-based navigation systems are used for 3D reconstruction.

In addition, incorrect palpation of the bony landmarks can cause inaccurate implant positioning. As an example; tilting of the APP results in inaccurate acetabular cup implant positioning. A number of reasons for incorrect bony landmark palpation can be identified. The first one is misuse of the surgical pointer. This can happen due to poor pointer registration, bending the pointer or positioning the pointer outside the visible area to the camera. A second reason is related to the patients themselves including fat tissue thickness over the examined position, and the patient's position during the surgery. Fat tissue can cause error in palpation of the exact bony landmarks. Patient's position during the pre-operative data palpation plays an important role. If the patient's position covers some of the anatomical landmarks, which are to be palpated, it would cause inaccurate pointer palpation.

Clear visibility of the pelvic tracking device is very important for all computer navigational systems. Tracking devices should not become in contact with any fluid, which could occlude them and lead to inaccuracy. They should also be within the detectable region of the camera at all the time. All group members of the surgical team need to consider their positions during the surgery, so as not to move the camera or occlude the markers.

Despite these disadvantages, there are many advantages of using computer-assisted navigation for surgery. Most importantly, they improve the outcome of joint replacement surgery (DiGioia et al 2002, Kalteis et. al 2006, Kiefer 2003). However, some surgeons still hesitate to apply navigational techniques. This is partly due to the uncertainty related to the accuracy of these navigational techniques. As a result, it is highly important to validate the navigational system for its accuracy and precision if such systems are to be widely adopted.

Chapter

3

CONTENT VALIDITY

3.1 Introduction

The purpose of this chapter is to establish the content validity of the OrthoPilot based cup navigation process prior to the main study of the accuracy and precision of the system. This section includes the details of the OrthoPilot system, surgical navigation process and mathematical representation during the data palpation process.

According to the previous literature, Computer assisted navigation increases the accuracy and precision of joint replacement surgery. It is claimed that this leads to improved longevity of the implant and functioning of the replaced joint. As a result, Computer assisted navigation is increasing in popularity in total hip replacement (DiGioia et al 2002, Kalteis et. al 2006, Kiefer 2003). OrthoPilot is a user-friendly, image-free, kinematic navigation system. It minimizes the intra-operative time by optimizing the navigation instruments and avoiding pre-operative imaging data (Kalteis et. al 2006). OrthoPilot navigation applications include anterior crucial ligament surgery, total knee replacement and total hip replacement. OrthoPilot™ (BBraun Aesculap) was introduced in 1994. It was initially used solely for total knee replacement but from 2000 onwards, it has been used for total hip replacement using the Hip suite software.

Figure 3.1 OrthoPilot applications in the operation theater
(http://braunoviny.bbraun.cz/clanky/)

The OrthoPilot system consists of a pair of infrared cameras with a control unit, infrared transmitters, a computer system and a foot control switch. Figure 3.1 shown above is an example of the application of OrthoPilot in a surgical environment. It shows femoral registration prior to surgical exposure of the knee. The patient is monitored by the computer via infrared (IR) transmitters that are fixed to the patient using bone pins. The position of the transmitters is detected by the infrared camera, which are connected to the computer. The 3D optical tracking cameras localize the infrared diodes in space. Transmitters are attached to all the surgical instruments. A reference tracker is fixed to the pelvic bone on the affected side. With the IR transmitters, attached to the surgical instrument, the computer defines the position of the surgical instrument with respect to the bones.

The OrthoPilot system has two types of tracker or marker, which are used to communicate the position of the patient and instruments to the computer; passive and

active. The passive trackers contain balls reflecting the IR light emitted by special IR emitters mounted round the camera. All four reflectors should be visible to the camera to define the precise position of the tracker. However, the active IR trackers have six diodes that emit IR and at least three of them must be visible to the camera to determine the precise position of the tracker. The markers are used in sets, usually either all passive or all active. However a third type of marker set, called hybrid, can be used which is a mixture of active and passive markers.

3.2 Surgical navigation process

OrthoPilot™ Hip Suite (BBraun Aesculap, Tuttlingen, Germany) was used during this research study with a spectra camera system from Northern Digital Inc. (Ontario, Canada). Software investigated was the Hip Suite THA cup only navigation software Version 3.1.

In the OrthoPilot system, the positional vectors of each palpated point are stored as transformation matrices. Each transformation matrix consists of both rotational and translation details of each palpated point with respect to the reference on the patient's body. The location and the orientation of the tracker are continuously recorded relative to the tracker fixed in the pelvis of the patient. Generally, the reference tracker is fixed to the affected side of the pelvis. Tracked data are stored and then used for the navigation process. They guide the orientation of the implanted cup. OrthoPilot navigation procedures for landmark palpation, trial cup selection, position recording, reamer navigation and final cup implantation are explained step by step in the following text and illustrated in Figures 3.2 – 3.9.

Step 1**:** Entering Patient data

Figure 3.2 Entering patient data

Before starting the cup navigation procedure, the patient is anaesthetized and prepared for surgery. Initial step of the navigation process is to enter patient's data; it helps to identify the recorded data after performing the surgery. Surgeon's name, patient's name, birthday and gender details are recorded.

Step 2**:** Selecting the implant

Figure 3.3 Implant selections and patient's position selection

Implant selection is one of the most important steps. Several types of implants are available; therefore, it is essential to select the appropriate implant type according to the installed software and availability. The next part is to provide the details of operated side of the pelvis, patient's position throughout the surgery, surgical approach and type of the instrument sets, which is going to be used. Patient's position can be either supine or lateral. Surgical approach is selected according to the patient's position. If it is supine, surgical approach will be anterior, whereas it can be either anterior or posterior with lateral patient's position. Next is to select the tracker type to communicate with the computer. Three types of instrument set are available with the OrthoPilot system; passive, active and hybrid (Section 3.1).

Step 3**:** Anterior Pelvic Plane Palpation

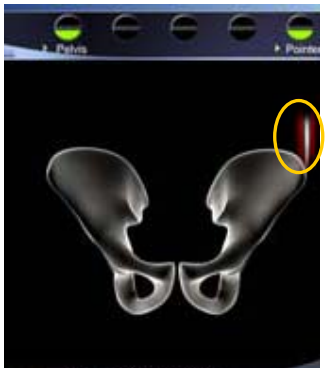

Ipsilateral ASIS

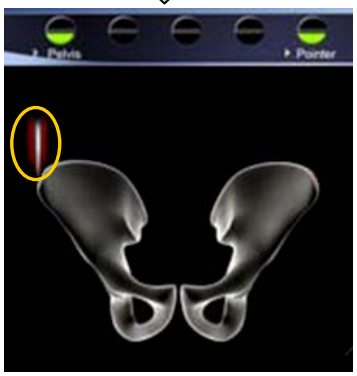

Contralateral ASIS

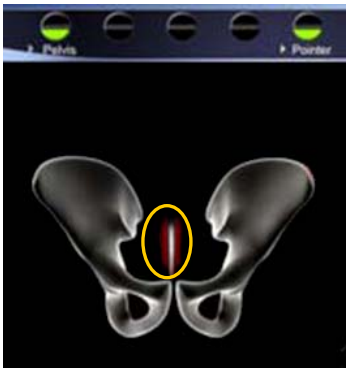

Pubic Symphysis

Figure 3.4 Landmark palpation for APP

Before starting landmark palpation, the reference tracker is fixed to the pelvis wall of the affected hip joint, by penetrating the soft tissue around that area. Procedure for the landmark palpation is as follows. The initial step is to palpate the Anterior Pelvic Plane (APP), which includes three main anatomical points, the left and right Anterior Superior Iliac Supine (ASIS) and the mid point of Pubic Symphysis (PS). These are labeled as ‘Collateral’ (which is the ASIS of the effected hip joint), ‘Contralateral’ (which is the ASIS of the other side) and ‘Central’ (which is the mid point of PS). Above-mentioned anatomical landmarks for the APP, are palpated by penetrating the soft tissue layers at the bony landmarks. With the data for these anatomical landmarks captured the APP of the patient is defined.

Step 4**:** Medial wall palpation / Deepest point of the acetabulum

Figure 3.5 Medial wall palpations

Once the APP bony prominences have been registered, the hip joint area is opened up and the femoral section is taken out from the acetabular cavity and the joint is

dislocated. By doing that, the acetabular cavity is opened for the preparation of cup implanting. The next step is medial wall palpation, which is the location of the deepest point of the native acetabulum. This captured data represents the deepest point of the acetabulum and guides the surgeon during reamer use in order to avoid unplanned reaming of the blood vessels and nerves inside the pelvic bone.

Step 5**:** Pre operative center of rotation/ cup size selection

Figure 3.6 Trial cup registration process

The next step is to register the trial cup. The trial cup size is selected much as close as possible to the original acetabulum. This task is difficult and performed with vision alone and it should be done by a well experienced surgeon. The original hip joint center and the acetabular axis are defined in this stage. All previously palpated data are used to define the anteversion and abduction/inclination angles of the original acetabulum. Calculated angle values are used as reference angle values during reamer navigation and the final cup navigation processes.

Step 6**:** Reamer selection and reamer navigation

Figure 3.7 Reamer navigation process

The sixth step is the process of reamer selection and reamer navigation. The reamer is selected according to the cup size, and it should be slightly smaller than the cup size. The handle of the reamer is fixed to a drill to perform the reaming action. During the reamer use the surgeon is guided by a screen showing the distance from the reamer edge to the medial wall point (indicated in orange). This helps to avoid over reaming of the acetabulum. Unwanted cartilage inside the acetabulum is reamed out during this stage giving a clean bed to place the implant precisely. Anterior-posterior, medial-lateral and caudal-cranial angles of the position of the reamer with respect to the preoperative center of rotation are also given to allow the correct orientation of the reamer.

Step 7**:** Final cup implanting

Figure 3.8 Navigation of acetabular implant

The seventh step is implant positioning. The surgeon is guided during the implant placement by on screen figures of the current anteversion and inclination angles. These data guide the implant cup into position giving a result as close to the native orientation of the acetabulum as possible. Computer screen displays the current position of the implant and the exact position it should be. The surgeon navigates the cup implant to obtain the native acetabular alignment close as much as possible. After positioning the implant, a hammering action is performed to fix the implant into the acetabular bone.

Step 8**:** Recording new center of rotation

Figure 3.9 Recording the new acetabular orientation with implanted cup

The final step is to record the new center of rotation of the implanted acetabulum cup. The anteversion and inclination angles are calculated according to the new hip joint center. These angles represent the final orientation of the acetabulum after implanting the cup. Once completed the cup implantation, hip joint is relocate back by placing the femoral section back inside the acetabular cavity. Here, femoral head is trimmed out to fix it properly to the implanted cup. After relocating the hip joint, surgery comes to the end with closing the wound by stitching the surrounded ligaments and the soft tissues.

3.3 Surgical Recording process

During landmark palpation, all the IR transmitters should be within the visible region of the camera system. Cameras must be within two meters of the patient. Landmark palpation is performed by applying the tip of the pointer to the bone through skin penetration. The palpation process should not be performed in such a way as to cause bending of the pointer. If the pointer is bent, it is indicated at the bottom on the right hand side of the computer screen. The figure displayed at the bottom right hand side of the computer screen should remain less than 2 mm during pointer palpation to avoid inaccurate palpation due to bent instrument. To obtain a sufficient visibility within the sensor volume, the pointer can be rotated around the landmark to be palpated (1 Degree of freedom).

During the registration process, the surgeon performs the palpation. The internal software detects the position of the markers within the registration area. The surgeon holds the pointer still and clicks the right foot pedal. The current position of the pointer tip is calculated and stored as the one of the landmarks.

In this study we aimed to check the content validity of the algorithm used to guide the surgeon as this has not been published or independently verified. To do this, we required to reconstruct the algorithm from the data stored by the system. A typical data file is given below followed by a mathematical explanation of the procedure implemented by the system which has been deduced by unpicking a number of such files. Recorded data are stored in a text document and an example is shown as follows.

Example of recorded data file

The file bellow presents the palpated data obtained from the pelvic phantom, which was used in the experiments and further explained in Chapter 4.

{

AcetabulumRecorder: {

Ant.: 0.24474

Incl.: 0.793349

Size: 48

(

(0.461132, -0.403778, 0.790139, -0.0500267),

(-0.306433, 0.763217, 0.568857, 0.18792),

(-0.832739, -0.504443, 0.228213, -0.0302264)

)

}

AnteriorPlane: (

(0.00702326, -0.987928, -0.154752, 0),

(0.0150834, 0.154843, -0.987824, 0),

(0.999862, 0.00460356, 0.0159888, 0)

)

Central: (

(0.985226, 0.160173, 0.0606231, -0.21121),

(-0.161793, 0.986561, 0.0228034, 0.150647),

(-0.0561559, -0.0322749, 0.9979, 0.0122076)

)

Colateral: (

(0.995084, 0.0956381, 0.0257105, -0.110942),

(-0.0975693, 0.991236, 0.0890607, 0.0445087),

(-0.0169676, -0.0911315, 0.995694, 0.013104)

)

Controlateral: (

(0.996303, 0.00990057, 0.085331, -0.338059),

(-0.0206411, 0.991825, 0.125923, 0.0801058),

(-0.0833867, -0.127219, 0.988363, 0.0141628)

)

Implants: {

Approach: ANTERIOR

Cup: "PLASMACUP SC"

"Cup cementless": YES

"Cup size": 48

"Head Diameter": 28

"Head Material": GENERIC

"Head Neck Size": M

"Inlay Material": CHIRULEN

"Inlay Shape":SYMMETRICAL

Position:SUPINE

Serial:PASSIVE

Stem: ""

"Stem CCD": 135

"Stem antetorsion": 0

"Stem cementless": NO

"Stem size": 0

Taper: 12/14

}

MedialWallPoint: (

(

(-0.0395222, -0.688025, 0.72461, -0.079106),

(0.556417, 0.587186, 0.587889, 0.160514),

(-0.829963, 0.426419, 0.359622, -0.0490489)

)

)

Patient: {

BirthDate: "1999-12-31T00:00:00"

DepartmentName: "B.BRAUN AESCULAP WORKSHOP-SYSTEM"

Gender: FEMALE

PatientFirstName: "TEST TEN MEAN RAD"

PatientLastName: "T TEN"

SurgeonName:DR.D

}

ReamerSelection: {

Position: 0

Reamer: 0

}

SurgeryData: {

InstrumentSetName: ""

IsLeftSide: NO }

3.4 Mathematical representation of the data in the file

During the OrthoPilot hip navigation procedure, initially pelvic anatomical landmarks were palpated and then the native orientation of the acetabulum was recorded. These initial data were stored in the computer to navigate the surgical instruments and implants during the later stages. Palpated data were stored in the computer as transformation matrices, which result in the position vector of each anatomical landmark in the global camera coordinate system. The navigation system transfers the transformation matrices from a camera coordinate system into a navigated rigid body's coordinate system relative to the reference markers in the pelvis. The transformation matrix consists of two components; a rotation matrix and a translation vector.

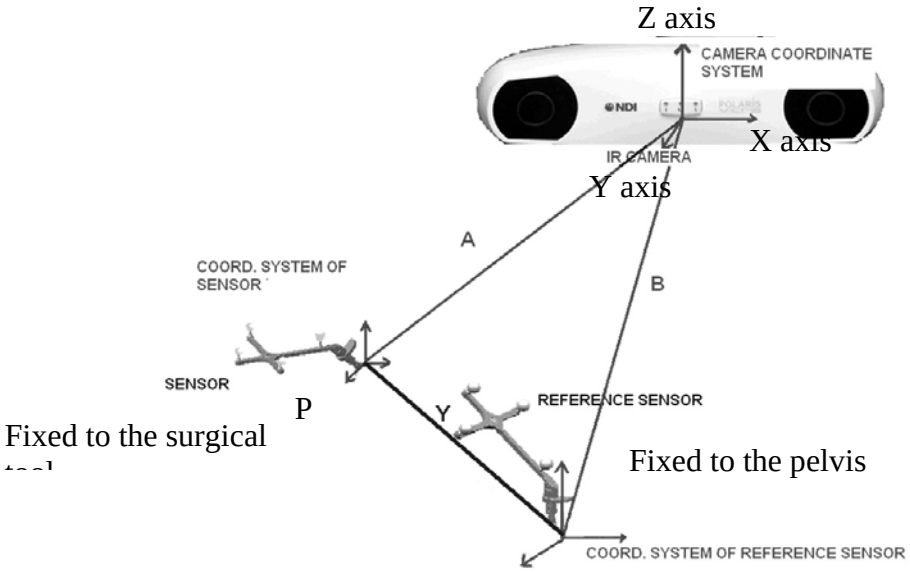

Figure 3.10 Reference coordinate system combined with one of rigid bodies (Swiatek-Najwer et al. 2008)

The figure 3.10 explains how the reference coordinate system relates to the coordinates system of the transmitter. The position of one marker in the coordinate frame of the reference marker is derived according to equation (3.1). ***A*** and ***B*** are the transformation matrices of the position sensor and reference sensor respectively, which are defined from the camera coordinate frame into the rigid body's coordinate frame.

$$AP = B$$
$$P = A^{-1}B \tag{3.1}$$

The following procedure was used to define the position vectors of each marker in the reference coordinate frame. Transformation matrix ***P*** of any point can be shown as the equation (3.2). R_{ij} (i,j = 1,2,3) represents the components of the rotational matrix, while T_k (k = x, y, z) represents the translation components.

$$\begin{bmatrix} R_{11} & R_{12} & R_{13} & T_x \\ R_{21} & R_{22} & R_{23} & T_y \\ R_{31} & R_{32} & R_{33} & T_z \end{bmatrix} = \begin{bmatrix} R_p / T_p \end{bmatrix} \tag{3.2}$$

The coordinate system of the OrthoPilot camera was defined as follows.
Y axis – Towards the OrthoPilot camera direction
Z axis – Vertically upward direction
X axis – Perpendicular direction to both Y and Z (the direction given by the vector multiplication of Y and Z)

Rotational matrix of the surgical instrument derives by rotating the view of the instrument around one of the three coordinates' axes ***X***, ***Y*** and ***Z***. The resulted rotational matrices around the axis of ***X***, ***Y*** and ***Z*** are $\boldsymbol{R_x}$, $\boldsymbol{R_y}$ and $\boldsymbol{R_z}$, and they are explicitly shown in equations (3.3), (3.4) and (3.5) respectively.

$$R_x = \begin{bmatrix} 1 & 0 & 0 & 0 \\ 0 & \cos\phi & -\sin\phi & 0 \\ 0 & \sin\phi & \cos\phi & 0 \\ 0 & 0 & 0 & 1 \end{bmatrix} \tag{3.3}$$

$$R_y = \begin{bmatrix} \cos\theta & 0 & \sin\theta & 0 \\ 0 & 1 & 0 & 0 \\ -\sin\theta & 0 & \cos\theta & 0 \\ 0 & 0 & 0 & 1 \end{bmatrix} \tag{3.4}$$

$$R_z = \begin{bmatrix} \cos\varphi & -\sin\varphi & 0 & 0 \\ \sin\varphi & \cos\varphi & 0 & 0 \\ 0 & 0 & 1 & 0 \\ 0 & 0 & 0 & 1 \end{bmatrix} \tag{3.5}$$

ϕ, ***θ*** and ***φ*** are the rotations around ***X***, ***Y*** and ***Z*** axes respectively. The resultant rotational matrix of the $\boldsymbol{R_x}$, $\boldsymbol{R_y}$ and $\boldsymbol{R_z}$ was obtained by considering the vector multiplication, shown in equations (3.6) and (3.7). Rotation matrix of the surgical instrument is represented by this resultant matrix, ***R***.

$$R = R_x \otimes R_y \otimes R_z \tag{3.6}$$

$$R = \begin{bmatrix} R_{11} & R_{12} & R_{13} & 0 \\ R_{21} & R_{22} & R_{23} & 0 \\ R_{31} & R_{32} & R_{33} & 0 \\ 0 & 0 & 0 & 1 \end{bmatrix} \tag{3.7}$$

Translational matrix, ***T*** is obtained by considering the displacement of the surgical tool with respect to the reference origin defined by the system. Vector multiplication of the rotational and translation matrices provides the transformation matrix, $\boldsymbol{T_r}$ of the surgical tool. This vector multiplication is shown in the equations (3.8) and (3.9).

$$T_r = R \bullet T \tag{3.8}$$

$$T_r = \begin{bmatrix} R_{11} & R_{12} & R_{13} & 0 \\ R_{21} & R_{22} & R_{23} & 0 \\ R_{31} & R_{32} & R_{33} & 0 \\ 0 & 0 & 0 & 1 \end{bmatrix} \bullet \begin{bmatrix} 1 & 0 & 0 & x \\ 0 & 1 & 0 & y \\ 0 & 0 & 1 & z \\ 0 & 0 & 0 & 1 \end{bmatrix}$$

$$T_r = \begin{bmatrix} R_{11} & R_{12} & R_{13} & T_x \\ R_{21} & R_{22} & R_{23} & T_y \\ R_{31} & R_{32} & R_{33} & T_z \\ 0 & 0 & 0 & 1 \end{bmatrix} \tag{3.9}$$

Coordinates vectors were derived for the positions of each surgical instrument and shown in equation (3.10). x_p, y_p and z_p are the coordinates of a particular point. Position vectors of each palpated point were calculated according to the mentioned procedure.

$$\begin{bmatrix} x_p \\ y_p \\ z_p \end{bmatrix} = -\left[R\right]^{-1} * \left[T\right] \tag{3.10}$$

In OrthoPilot cup navigation, acetabular orientation is defined in radiographic, anatomical or operative. This study was conducted by considering the radiographic definition of the acetabular orientation. The Anterior Pelvic plane (APP) was considered as the reference to define orientation. The APP was defined with the two most anterior points, (left and right anterior superior iliac spines (ASIS)) and center of two pubic tubercles (PS). Examined coordinates for the Ipsilateral ASIS, Controlateral ASIS and Pubic Symphysis are shown below.

Coordinates of ASIS of the affected side, collateral = (x_{col}, y_{col}, z_{col})
Coordinates of ASIS of the other side, Contralateral = (x_{con}, y_{con}, z_{con})
Coordinates of pubic Symphysis, central = (x_{cen}, y_{cen}, z_{cen})

Once defined the APP, anterior pelvic coordinate system was constructed. Ipsilateral ASIS was considered as the origin. The Anterior Pelvic coordinates (APC) system was defined as shown in the Figure 3.11. The $\vec{X}$ direction of the APC was obtained with the vector connecting the Ipsilateral ASIS and Controlateral ASIS. This is explicitly shown in the equation (3.11).

$$\vec{X}_{apc} = \begin{pmatrix} (x_{col} - x_{con}) & (y_{col} - y_{con}) & (z_{col} - z_{con}) \end{pmatrix} \quad (3.11)$$

The $\vec{Z}$ direction was determined by the vector multiplication of the linear vector connecting the origin (Ipsilateral ASIS) to the center of the pubic tubercles ($\vec{OP}$) and vector $\vec{X}$, as shown in equations (3.12).

$$\vec{Z} = \vec{OP} \otimes \vec{X} \quad (3.12)$$

$$\vec{Z} = \begin{bmatrix} x - x_{col} & y - y_{col} & z - z_{col} \\ x_{col} - x_{con} & y_{col} - y_{con} & z_{col} - z_{con} \\ x_{col} - x_{cen} & y_{col} - y_{cen} & z_{col} - z_{cen} \end{bmatrix} \quad (3.13)$$

$$Z_{x_{apc}} = (x - x_{col}) \begin{vmatrix} y_{con} - y_{col} & z_{con} - z_{col} \\ y_{cen} - y_{col} & z_{cen} - z_{col} \end{vmatrix} \quad (3.14)$$

$$Z_{y_{apc}} = (y - y_{col}) \begin{vmatrix} x_{con} - x_{col} & z_{con} - z_{col} \\ x_{cen} - x_{col} & z_{cen} - z_{col} \end{vmatrix} \quad (3.15)$$

$$Z_{z_{apc}} = (z - z_{col}) \begin{vmatrix} x_{con} - x_{col} & y_{con} - y_{col} \\ x_{cen} - x_{col} & y_{cen} - y_{col} \end{vmatrix} \quad (3.16)$$

$$z_{x_{app}} = x * \left[(y_{con} - y_{col}) * (z_{cen} - z_{col}) \right] - x_{col} * \left[(y_{cen} - y_{col}) * (z_{con} - z_{col}) \right] \quad (3.17)$$

$$z_{y_{app}} = y * \left[(x_{con} - x_{col}) * (z_{cen} - z_{col}) \right] - y_{col} * \left[(x_{cen} - x_{col}) * (z_{con} - z_{col}) \right] \quad (3.18)$$

$$z_{z_{app}} = z * \left[(x_{con} - x_{col}) * (y_{cen} - y_{col}) \right] - z_{col} * \left[(x_{cen} - x_{col}) * (y_{con} - y_{col}) \right] \quad (3.19)$$

$$\vec{Z} = \begin{pmatrix} Z_{x_{apc}} & Z_{y_{apc}} & Z_{z_{apc}} \end{pmatrix} \quad (3.20)$$

The $\vec{Y}$ direction of the APC was determined by the vector multiplication of $\vec{X}$ and $\vec{Z}$, and shown in equations (3.21) and (3.22). Same calculation method was followed to obtain the equation (3.22) as explained above in the equation (3.20).

$$\vec{Y} = \vec{Z} \otimes \vec{X} \tag{3.21}$$

$$\vec{Y} = \begin{bmatrix} x & y & z \\ Z_{x_{apc}} & Z_{y_{apc}} & Z_{z_{apc}} \\ x_{col} - x_{con} & y_{col} - y_{con} & z_{col} - z_{con} \end{bmatrix}$$

$$\vec{Y} = \begin{pmatrix} Y_{x_{apc}} & Y_{y_{apc}} & Y_{z_{apc}} \end{pmatrix} \tag{3.22}$$

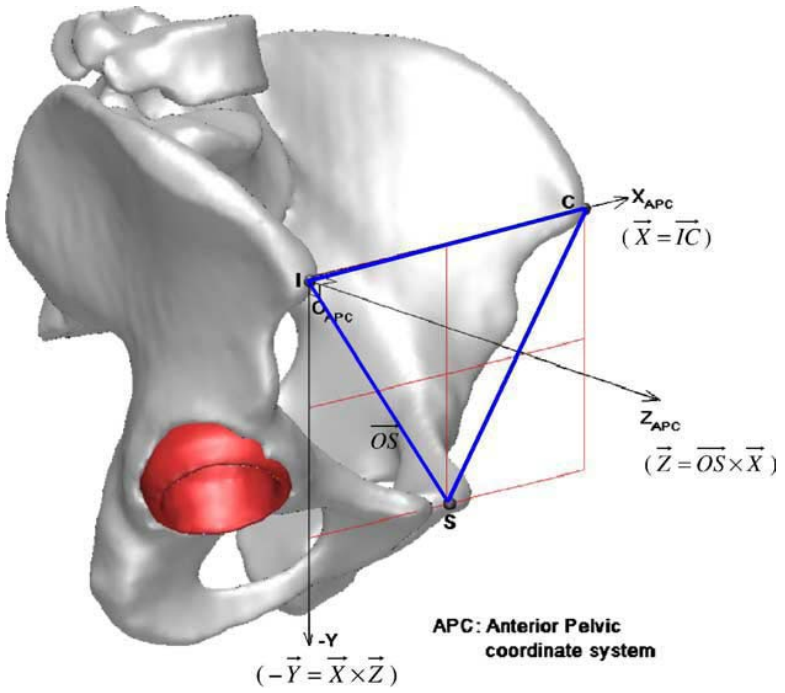

Figure 3.11 Anterior Pelvic Coordinate System (Lee et al. 2008)

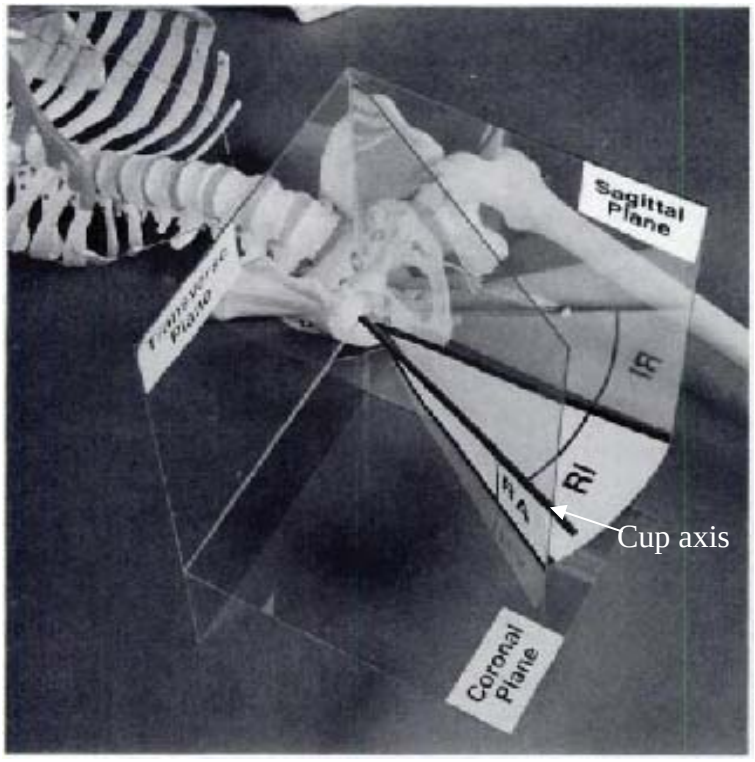

Figure 3.12 Radiographic definitions of anteversion and inclination angles of the acetabular axis (Murray 1992)

3.5 Anteversion angle calculation

The radiographic definition of the anteversion angle is the angle between the acetabular axis and the coronal plane (Lewineck et. al 1978). It is further described by Murray (1992); when the APP projected on to the coronal plane, the angle between the acetabular axis and the axis parallel to the normal of APP is defined as the anteversion angle (Figure 3.12). ***Z*** axis of the APC is parallel to the normal of the APP (Figure 3.12).

Acetabular axis vector was derived with the trial cup registration stage and it is represented as $\left(\vec{a},\vec{b},\vec{c}\right)$. Mathematical representation of the anteversion angle is shown in equation (3.23).

$$antiversion\_angle = \sin^{-1}\left|\left(\frac{\left(Z_{x_{apc}} * a\right)+\left(Z_{y_{apc}} * b\right)+\left(Z_{z_{apc}} * c\right)}{\sqrt{\left(Z_{x_{apc}}\right)^2+\left(Z_{y_{apc}}\right)^2+\left(Z_{x_{apc}}\right)^2} * \sqrt{a^2+b^2+c^2}}\right)\right| \quad (3.23)$$

3.6 Inclination Angle calculation

The radiographic definition of the inclination angle is the angle between the face of the cup and transverse axis (Lewineck et. al 1978), which is further described as the angle between the longitudinal axis and the acetabular axis, when it is projected on to the coronal plane (Murray 1992). This angle is described in the Figure 3.12. Longitudinal axis is parallel to the Y axis of the APC. Therefore, inclination angle is derived as the following equation (3.24).

Mathematical representation of the Inclination angle is

$$inclination - angle = \cos^{-1}\left(\frac{\left(Y_{x_{apc}} * (a/c)\right)+\left(Y_{y_{apc}} * (b/c)\right)+\left(Y_{z_{apc}} * c\right)}{\sqrt{\left(Y_{x_{apc}}\right)^2+\left(Y_{y_{apc}}\right)^2+\left(Y_{z_{apc}}\right)^2} * \sqrt{\left(a/c\right)^2+\left(b/c\right)^2+c^2}}\right) \quad (3.24)$$

3.7 Example using the previously presented data file

After setting up the OrthoPilot system, first step is to palpate the ASIS of the effected side. Data sheet explained at sub section 3.3 was recorded by considering the effected hip at right hand side. Therefore, first pointer palpation was at RASIS. Once surgeon finishes the landmark palpation at RASIS, systems stores its coordinate matrix;

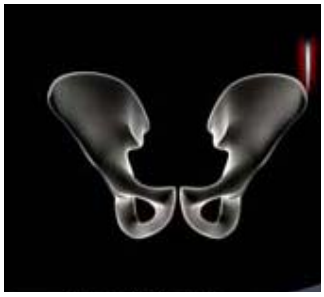

$$\begin{bmatrix} 0.995084 & 0.0956381 & 0.025711 & -0.1109 \\ -0.097569 & 0.991236 & 0.089061 & 0.04451 \\ -0.016968 & -0.091132 & 0.995694 & 0.0131 \end{bmatrix}$$

The next step is to register LASIS. Recorded coordinates matrix is as shown below;

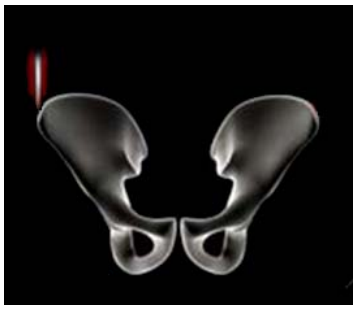

$$\begin{bmatrix} 0.996303 & 0.00990057 & 0.085331 & -0.338059 \\ -0.0206411 & 0.991825 & 0.125923 & 0.080106 \\ -0.0833867 & -0.127219 & 0.988363 & 0.014163 \end{bmatrix}$$

The next step is to register the mid point of PS. Recorded coordinates matrix is as shown below;

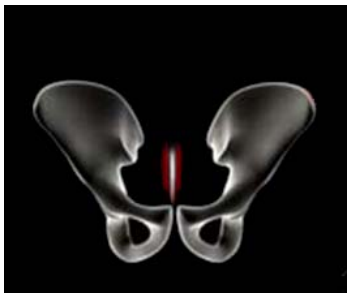

$$\begin{bmatrix} 0.985226 & 0.160173 & 0.0606231 & -0.211214 \\ -0.161793 & 0.986561 & 0.0228034 & 0.150647 \\ -0.0561559 & -0.0322749 & 0.9979 & 0.012208 \end{bmatrix}$$

With the coordinate data for above palpated anatomical landmarks, the APP of the patient is defined.

$$\begin{bmatrix} 0.00702326 & -0.987928 & -0.154752 & 0 \\ 0.0150834 & 0.154843 & -0.987824 & 0 \\ 0.999862 & 0.00460356 & 0.0159888 & 0 \end{bmatrix}$$

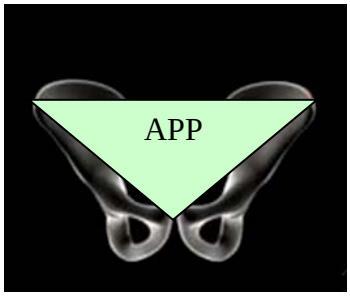

Then, APP was used as a reference to navigate all other surgical instruments.

Next step is medial wall palpation and palpated data is stored as shown below;

$$\begin{bmatrix} -0.0395222 & -0.688025 & 0.72461 & -0.079106 \\ 0.556417 & 0.587186 & 0.587889 & 0.160514 \\ -0.829963 & 0.426419 & 0.359622 & -0.049049 \end{bmatrix}$$

Next step is trial cup registration. Orientation of the surgical tool is recorded with reference to the APP to obtain the orientation of the native acetabulum. From that data, the system calculates the anteversion and inclination angle values for the native acetabulum and they are displayed as;

Ant: 0.244747 radian = 14.02^0

Inc: 0.793349 radian = 45.46^0

Please refer appendix A for an example of anteversion and inclination angle calculations.

3.8 Discussion of the content validity of the OrthoPilot system

The OrthoPilot system is designed to measure acetabular angles similar to radiographic, anatomical or operative definitions. During this study, radiographic definition was used. Optimizing the surgical time is one of the main factors in computer assisted surgery. OrthoPilot navigation procedure has proved to be quick and easy to use (Kalteis et. al. 2006). Proper handling of the tools which are used for surgical recording is another important factor to minimize the errors as well as to save the time. Holding the surgical tool without bending or shaking, it is important as is allowing clear visibility to the IR cameras. In addition, the reference tracker should also be within the visible area of the IR camera. This reference tracker is fixed to the pelvic bone of the operated side of the patient. However, care should be taken not to move the reference tracker during the surgery. This will lead to changes in the reference (APP) of the cup implant and result in an incorrect implant positioning.

OrthoPilot stored the surgical recordings. In addition, to the anatomical data, it records patient's data, implant type, surgeon's name, etc (sub section 3.3). These data can be used to examine the implanted hip joint post operatively. At the end of each palpation it stores data with reference to the camera coordinate frame. The APP registration plays an important role in cup replacement, as it is used as a reference to position the implant cup. Therefore, incorrect APP recording will lead to a poor outcome of the joint replacement. In addition, the surgeon should be able to palpate exact landmarks in order to register the exact APP of the patient.

OrthoPilot accuracy can be improved more by increasing the number of cameras instead of two cameras. In addition, if these cameras can fix on top of the operation bed instead of fixing it on the side of the operation bed, it can reduce the human interference of the IR cameras during the operation. In addition, inaccurate selection of cup size can misguide the surgeon in positioning of the final implant. Special care should be taken in selecting the trial cup size. This should be as close as possible to the native acetabulum. Trial cup selection task can be performed with the vision along by an experienced surgeon. OrthoPilot guides the surgeon throughout the

navigation process. However, it is the user's responsibility to use correct surgical tools and palpating the correct data during the recording and operation process.

OrthoPilot system has been used for hip replacement surgery since 2000 onwards (http://www.orthopilot.com). According to the previous literature application of the OrthoPilot cup navigation is proven to be a simple and safe procedure by improving the final cup position (Kiefer 2003 and http://www.orthopilot.com). The OrthoPilot based data recording is achieved using a foot pedal switch, which is handy in the surgical environment. Cup navigation software is also user-friendly and it guides the relevant surgical tool to be used during each surgical navigation step as explained in subsection 3.2. In addition, it provides the ability to go back and check the previously recorded data. If surgeon uncertainties about the previously recorded data, he can go back to that stage just by clicking the foot pedal switch and delete that data and rerecord it again. This helps to avoid possible inaccuracies occurs due to uncertain landmark registration. Accessing the data file is straightforward and it shows the recorded data clearly. It helps the author, when extracting recorded acetabular angle data from the OrthoPilot as explained in subsection 3.7. With the above mentioned user-friendly features, the author was confident to use OrthoPilot system for the experiments explained in the Chapter 4.

Chapter 4

VALIDATION OF THE ORTHOPILOT SYSTEM

4.1 Aim

To examine the validity of the OrthoPilot system is the main aim of this section of this study. The OrthoPilot validation process has been divided into two sections; one is to assess the accuracy of the OrthoPilot system, while navigating the surgical instruments and the other one is to assess the accuracy of the hip navigation algorithm, which is used in the OrthoPilot system to orientate and position the acetabular cup.

4.2 Introduction and Objectives

A concurrent validity study between the OrthoPilot and VICON system was performed. A calibrated pelvic phantom model, which imitates the average size of the human pelvis, was used as the reference to measure distance and angular parameters. Angular and distance parameters were captured simultaneously from both OrthoPilot and VICON systems and they were then compared. All these measured parameters were based on the pelvic phantom.

Accurate instrument positioning is one of the essential factors during hip replacement surgery. The first stage of the concurrent validity was to answer; is OrthoPilot instrument positioning accurate and repeatable? To answer the above question, distances between the anatomical landmarks were examined to determine the accuracy and repeatability of the instrument positioning using the calibrated pelvic phantom for known distances. Distance data result from both OrthoPilot and VICON

were compared. The Experimental procedure is explained in experiment 1 in subsection 4.4

Inaccuracy in the cup navigation algorithm can also cause poor placement of the cup in hip replacement surgery. Therefore, verifying the accuracy of the cup navigation algorithm is one of the major roles when validating a hip navigation system. The next stage of the concurrent validity was to answer; does the OrthoPilot cup navigation algorithm produce accurate and repeatable results? To answer the above question, the accuracy of the OrthoPilot cup navigation algorithm was observed by using the similar algorithm to calculate the acetabular angles from simultaneously captured VICON data. The Cup navigation algorithm was validated in different ways. Radiographic definitions of the anteversion and inclination angles were examined by palpating the exact landmark points to define the APP on the pelvic phantom. Data were palpated from both OrthoPilot and VICON systems and the angular results compared to determine whether both systems produce similar results when using the same algorithm. This experimental procedure is explained in experiment 2 in subsection 4.5.

The next stage of the cup algorithm validation was to answer; how are the angles affected if the incorrect palpation of the APP during the navigation procedure? And, does the cup navigation algorithm work properly during such situations? To answer the above questions, acetabular angles were obtained by varying APP with known errors. The APP registration was varied in two different ways. The first method was tilting the reference tracker during the APP registration. The other method was varying the dimensions of the APP in the coronal plane. The Angular results from both OrthoPilot and VICON were compared by following the similar angle calculation algorithm. The Acetabular angle results obtained by palpating the exact landmarks to obtain the APP were used as a reference, when examining the acetabular angles for the varying APP by introducing known errors. The APP varying experimental procedures are explained in experiment 3 and 4 in subsections 4.6 and 4.7 respectively.

4.3 Generic Methods

Figure 4.1 shows the Aluminium pelvic phantom which was used to obtain the data. It was built to imitate the average size of the human pelvis with 14 degrees of anteversion and 45 degrees of inclination (as determined by local analysis of pelvic CTs). These angle values were verified by the engineering measuring techniques after the block had been machined.

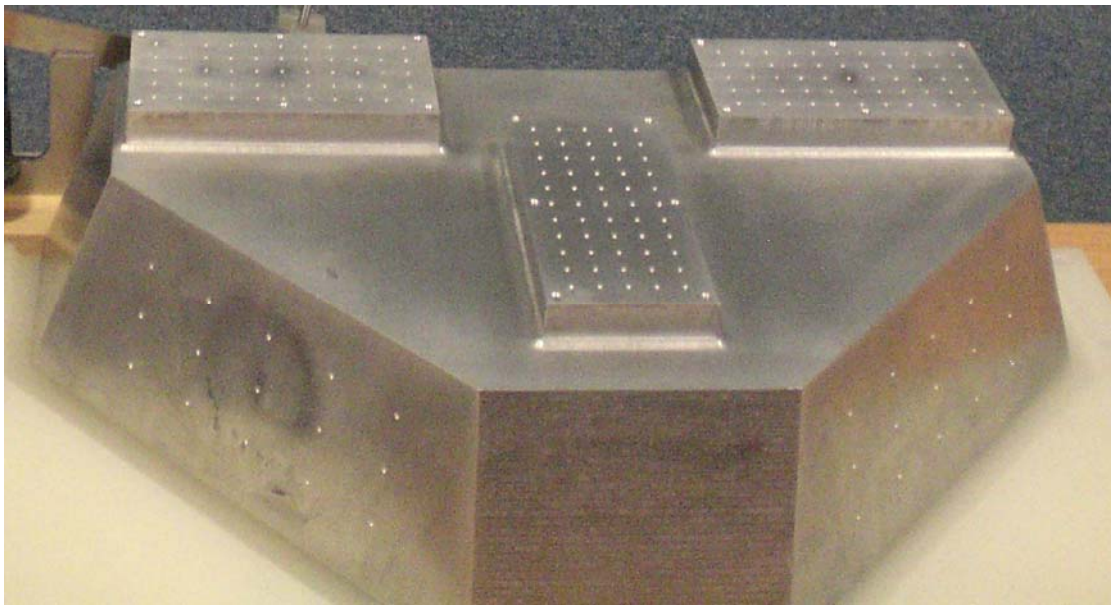

Figure 4.1 Pelvic Phantom model

The physical dimension of the phantom is explained as follows. The average distance between left and right anterior superior iliac supine was 230 mm. The distance between the mid point of anterior superior iliac spines and mid point of the pubic Symphasis was 90 mm. This phantom was machined with a lot of “peg” points around the exact landmark points of RASIS, LASIS and PS. The surrounded peg points were used when changing the landmarks points in different directions which will be explained in subsection 4.7. All the peg points were machined with conical shape and it helped to position the surgical tool tip on top it easily by avoiding the tilting. Detailed CAD drawings of the pelvic phantom are attached in Appendix D.

OrthoPilot™ Hip Suite (BBraun Aesculap) has been explained in detail in Chapter 3. A spectra camera system, from Northern Digital Inc. (Ontario, Canada), was used in

the navigation process. The computer software was Hip Suite THA cup only navigation software version 3.1. The passive instrument set was used in this study.

Pretended patient details, position during surgery, surgical approach and implant type were inputted at the beginning of the OrthoPilot navigation process to initiate the software. During the trial cup registration process, the diameter of the cup was selected close to the native acetabulum. All the data were captured by keeping the five conditions below unchanged through out the experiment.

- Patient's sex – female
- Patient's position during the surgery – supine
- Surgical approach - right hand side anterior approach
- Implant cup type - plasma cup
- Diameter of the trial cup - 48 mm

The OrthoPilot system was compared to data captured using a VICON motion analysis system. The validation was performed and compared against the VICON Nexus (version 1.4.116) with Bodybuilder software (version 3.55) (Oxford metrics Ltd, Oxford, UK). Nexus software was used for data capturing, while Bodybuilder software was used for analysis of the captured data. These data were captured at a frequency of 100 Hz, using twelve MX cameras. Retort stands were used to position and hold steady the surgical tools in known positions, when recording data. The VICON system has been used for concurrent validity studies in different fields varies from life sciences to engineering disciplines (http://www.vicon.com). According to the VICON Nexus manufacturer's technical specification (user manual), the system precision with regard to the positional accuracy and the angular accuracy is ± 0.1 mm and $\pm 0.15^0$ respectively.

4.3.1 Data capturing with VICON motion analysis system

Before capturing data from the VICON system, the environment should be arranged. MX cameras were calibrated with a five marker wand and the test area was cleared of reflective objects.

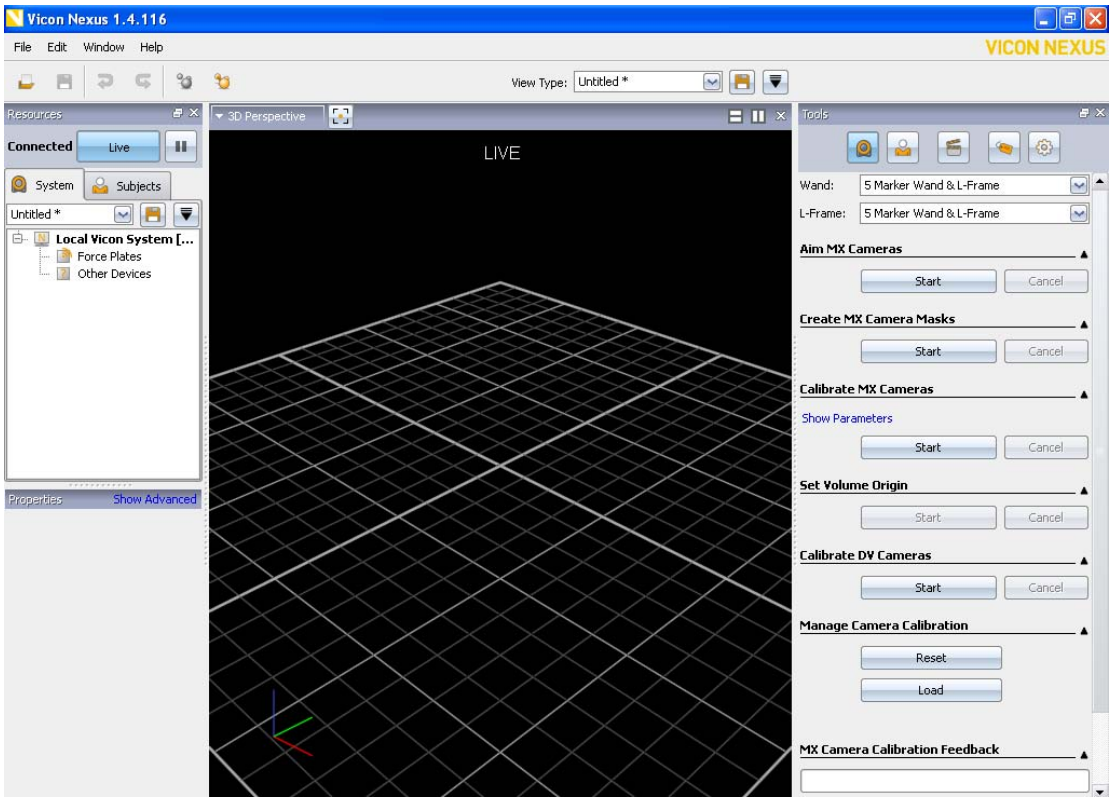

Figure 4.2 Nexus environment to capture VICON data

The MX camera calibration process defines the capture volume of the system, enabling Nexus to determine the position, orientation and lens properties of all the MX cameras. The system uses this information to produce accurate 3D data. The calibration wand was waved within the intended area of the 3D data capture, care must be taken to ensure that the markers on the calibration object are visible to all the cameras. The camera view area of the Nexus software was checked to make sure a good number of wand frames had been captured across the intended 3D capture volume. Once finished camera calibration, the Origin of the VICON coordinate frame was set. This was achieved by placing a five marker wand in the middle of the

force plate system, to set the origin of the lab coordinate frame. The environmental preparation steps are described in detail at appendix B

The next step was phantom preparation. For that, a new subject node was created in the Nexus database based on a VICON Skeleton Template. Once finished preparing the subject environment in Nexus, the phantom was placed within the capture volume and ensuring that all the markers on the phantom were visible to all cameras. The, phantom is ready to capture static trial data. At this stage it was very important to eliminate reflective objects from the experiment environment, as they introduce noise effects to VICON data. In addition, all the lab doors were kept closed during the experiment to eliminate outside noise effects. Then, static trial data were captured for 1-2 seconds.

At the end of data capturing, the Nexus software was switched to offline mode and the captured static trial data was processed. The system was switched to *pipe line*, which is useful for automating the data processing operations. The pipeline performed the *core processing* command for automating the real-time and offline motion capture data processing. The minimum number of cameras per marker was set to three to filter out ghost marks.

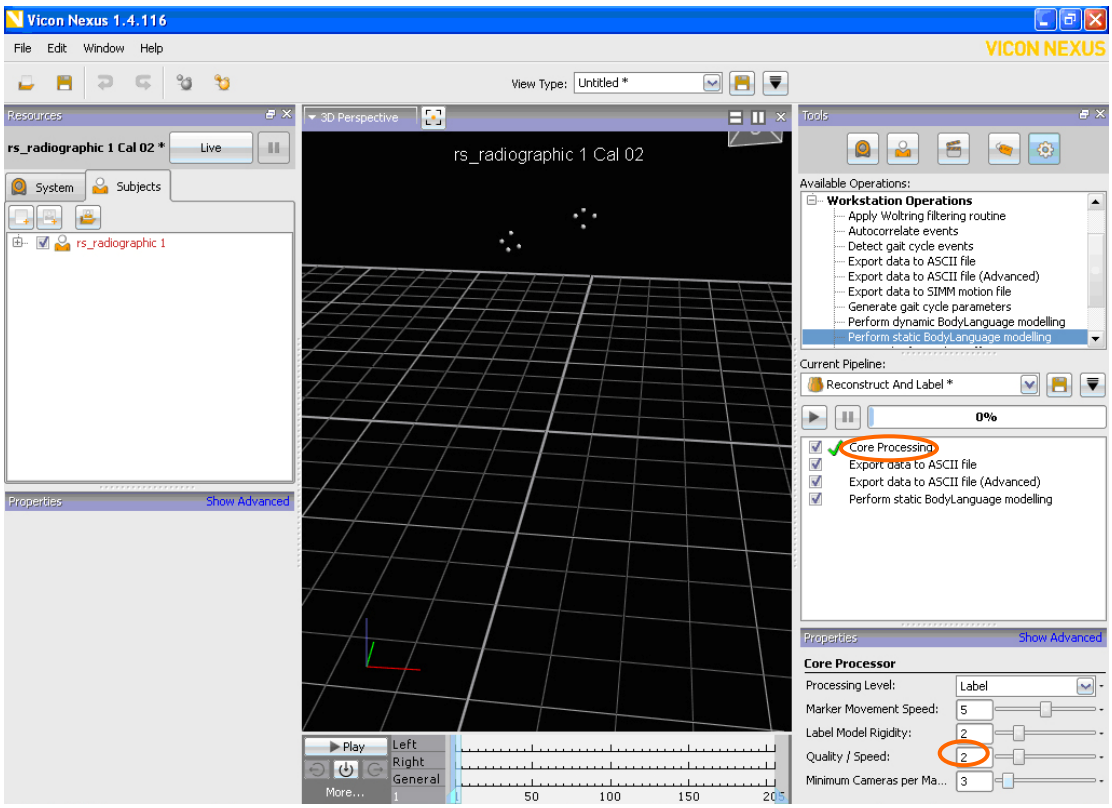

Figure 4.3 Core Processing

The next step was marker labeling. For that, the software was switched to the *subject preparation* section. A labeling template was built by creating a pelvic segment and then used to label the markers. These marker labels were then used in a BodyBuilder model to calculate the results.

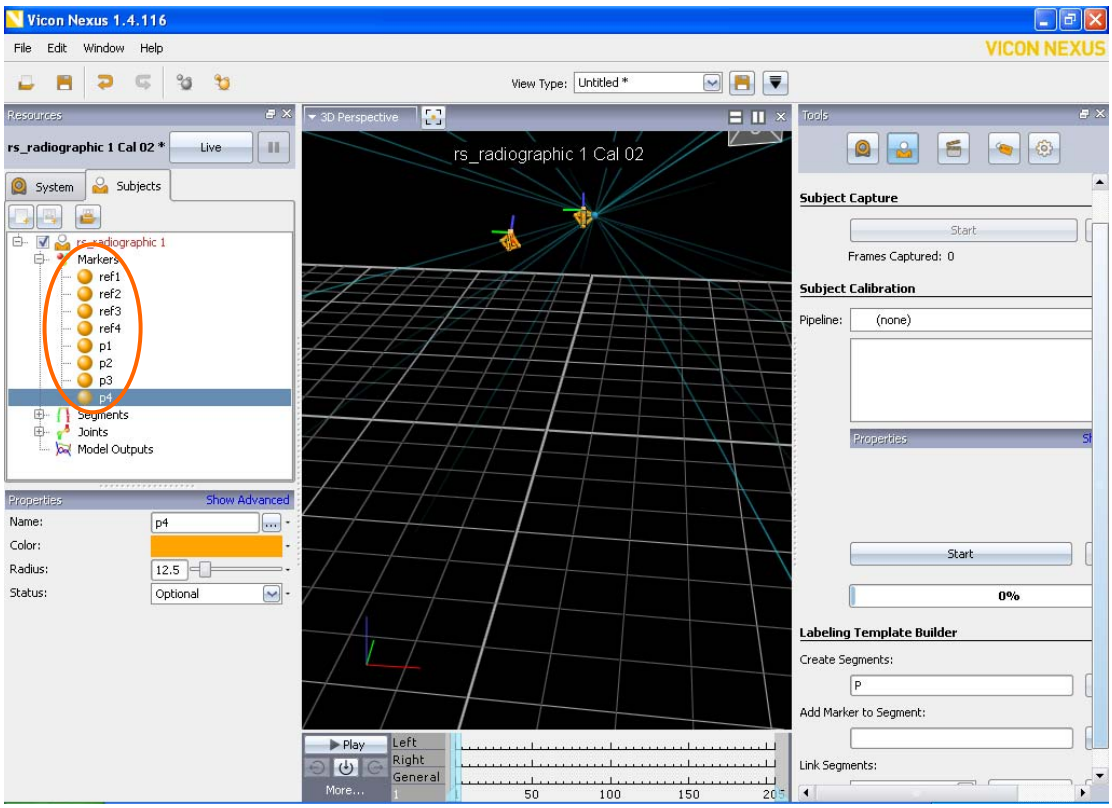

Figure 4.4 Marker labeling

Once finished labeling the markers, they appeared as shown in the Figure 4.4. The Nexus software was switched to *pipe line* again and the processed data were exported to ASCII files, where trial data were stored.

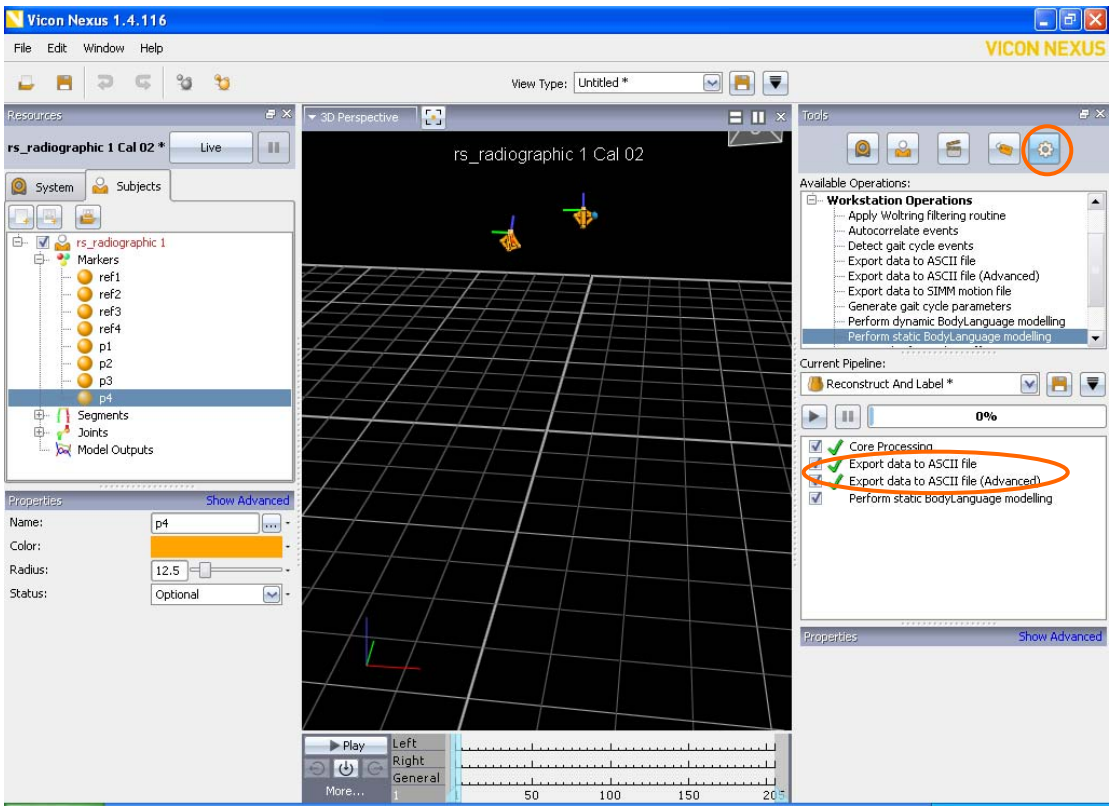

Figure 4.5 Exporting trial data to ASCII files

Data analysis was conducted using VICON BodyBuilder. As an initial step, the BodyBuilder program file was called up in Nexus. This program contained calculations of position coordinates of landmarks. Once executed it, calculated landmark coordinates in the global frame and these were stored in ASCII file format. This BodyBuilder program can be seen in appendix C. Then, those coordinates were exported to Excel. The mathematical expressions derived in Chapter 3 were used to develop the acetabular angle calculation algorithm and implemented in excel to obtain the anteversion and inclination angle values. The angles calculation algorithm is shown in the Figure 4.6. Sample angle calculations using this algorithm are explained in appendix A.

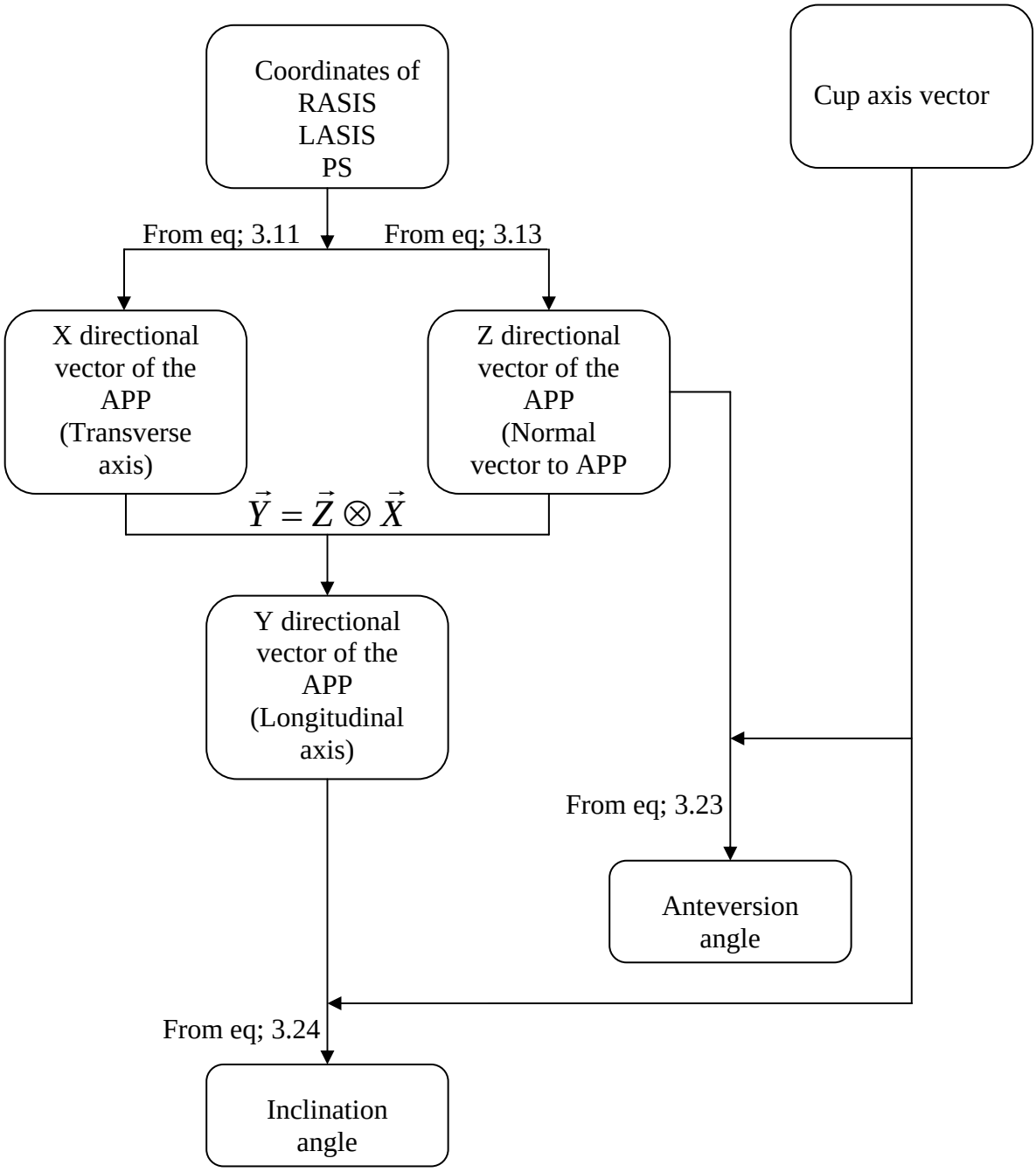

Figure 4.6 Flow chart of angle calculation algorithm (for use with VICON data)

4.3.2 Experimental Set up

The experimental environment can be clearly visualized from the Figure 4.7. Both systems were under the same experimental conditions and capable of capturing the passive transmitters. The author was very careful in arranging both systems without interfering with the each other, specially the VICON cameras. The pelvic phantom was positioned on a table in the supine position of the pelvic. In addition, the reference tracker was attached to a Goniometer and placed at the operated side of the pelvic phantom.

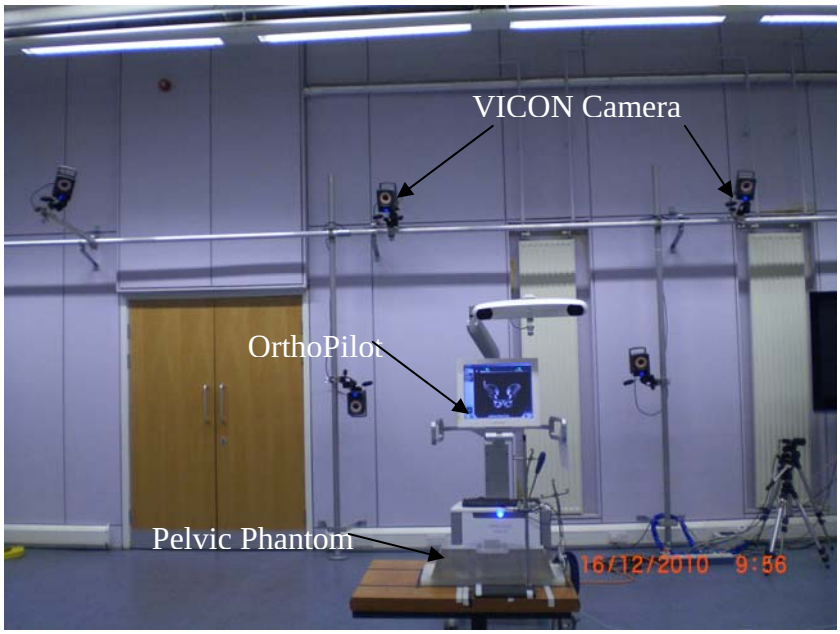

Figure 4.7 Simultaneous data recording from OrthoPilot and VICON systems

Geometrical information of the passive transmitter, which was used during the experiment, is shown from Figure 4.8.

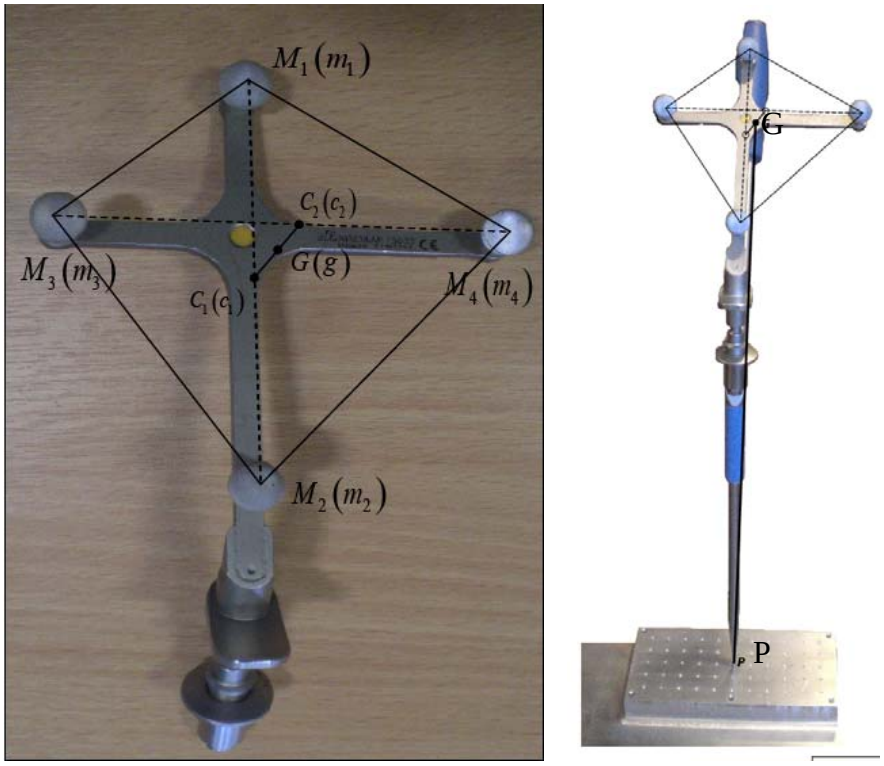

(a) (b)

Figure 4.8 (a) Geometrical information of the passive transmitter; (b) Passive transmitter attached to surgical tool

This passive transmitter has four spheres as shown in the above figure. All these spheres are read as markers by the VICON system. The geometric centre of the four spheres can be seen as *G* and it can be mathematically shown from the following equations

$$c_1 = (m_1 + m_2)/2 \tag{4.1}$$

Where c_1, m_1 and m_2 are the coordinates of the geometric centres of C_1, M_1 and M_2 respectively. C_1 is the geometric centre of $M_1 - M_2$.

$$c_2 = (m_3 + m_4)/2 \tag{4.2}$$

Where c_2, m_3 and m_4 are the coordinates of the geometric centres of C_2, M_3 and M_4 respectively. C_2 is the geometric centre of $M_3 - M_4$.

$$g = (c_1 + c_2)/2 \tag{4.3}$$

Where g is coordinates of the geometric centre of all four spheres, G.

The passive transmitter attached to the surgical tool was captured by VICON. Captured data were used to find the distance between the tool tip and G, which is shown in the Figure 4.8(b).

The trial cup was fixed to the surgical tool as shown in the Figure 4.9 (b) i.e. upside down allowing it to the placed on the flat surface of the phantom. The trial cup registration process is used to record the axis of the native acetabular, which is assumed to be a hemisphere. Therefore, using the surgical tool for the trial cup upside down, the OrthoPilot records same vector, as if it were in the correct position (as shown in Figure 4.9 (a) and (b)). However, the trial cup should not be fixed as shown in Figure 4.9 (b) in the surgical environment.

a-(correct method) b-(upside down)

Figure 4.9 Fixing methods of the trial cup to the surgical tool- but both giving the same position vector

Experiment environment should be kept clear of very shiny objects, to prevent the VICON data being influenced by noise effects. All the shiny objects within the experimental environment were covered with black color tape as well as minimum number of cameras per marker was increased to three to avoid the other noise effects, when capturing the VICON data. Two foot pedal switches were used to achieve simultaneous data capture from both systems.

4.5 Experiment 1- Distance between anatomical landmarks

4.5.1 Introduction

Precise surgical instrument navigation is thought to play a key role in cup navigation. Incorrect landmark palpation may produce a poor output in hip replacement surgery however; the extent of the error causes is unknown. Palpation of the same landmark several times can create deviations. Therefore, the data capturing accuracy of the OrthoPilot system is fundamental to accurate cup placement. Accuracy of the OrthoPilot instrument navigation was examined by comparing the distance between anatomical landmarks, which were palpated to define the APP. The distance data resulted from both OrthoPilot and VICON were compared.

4.5.1 Method

Anatomical landmarks of right anterior superior iliac supine (*RASIS*), left anterior superior iliac supine (*LASIS*) and Pubic Symphasis (*PS*) were palpated to define the APP. In addition, the same palpation procedures were followed for three different sizes of APPs. They were defined as APP1, APP2 and APP3 according to the width and height of the pelvis. They are shown in Figure. 4.10. Each landmark bed was machined with several palpation points as seen in the Figure 4.1. This allowed the definition of different widths and heights of pelvis within the same phantom model. RASIS-LASIS-PS landmarks were palpated 100 times for each APPs.

APP1 : *RASIS-LASIS* 170 mm, *RASIS-PS* 102 mm, *LASIS- PS* 102 mm

APP2 : *RASIS-LASIS* 230 mm, *RASIS-PS* 145 mm, *LASIS- PS* 145 mm

APP3 : *RASIS-LASIS* 290 mm, *RASIS-PS* 190 mm, *LASIS- PS* 190 mm

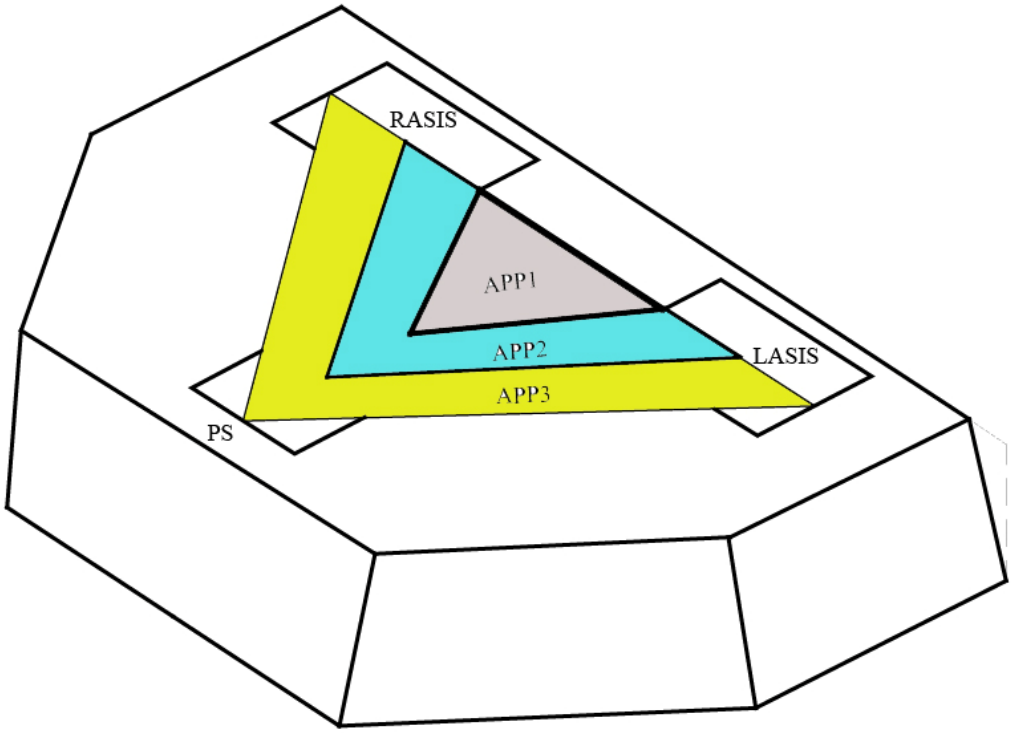

Figure. 4.10 Anterior Pelvic planes on phantom model

Data were captured simultaneously for the supine position of the phantom. OrthoPilot data for the anatomical landmarks were palpated as described in the OrthoPilot surgical navigation process in subsection 3.2. Distance measurements between the anatomical landmarks were calculated by the translation values extracted from the resulted transformation matrices in the OrthoPilot data sheet as explained in subsection 3.7. Distances between each anatomical landmark were obtained according to the equations 4.4, 4.5 and 4.6.

$RASIS = (T_{x\_col}, T_{y\_col}, T_{z\_col},)$,

$LASIS = (T_{x\_con}, T_{y\_con}, T_{z\_con},)$

$PS = (T_{x\_cen}, T_{y\_cen}, T_{z\_cen},)$

$$RASIS - LASIS = \sqrt{\left(T_{x\_col} - T_{x\_con}\right)^2 + \left(T_{y\_col} - T_{y\_con}\right)^2 + \left(T_{z\_col} - T_{z\_con}\right)^2} \quad (4.4)$$

$$RASIS - PS = \sqrt{\left(T_{x\_col} - T_{x\_cen}\right)^2 + \left(T_{y\_col} - T_{y\_cen}\right)^2 + \left(T_{z\_col} - T_{z\_cen}\right)^2} \quad (4.5)$$

$$LASIS - PS = \sqrt{\left(T_{x\_con} - T_{x\_cen}\right)^2 + \left(T_{y\_con} - T_{y\_cen}\right)^2 + \left(T_{z\_con} - T_{z\_cen}\right)^2} \quad (4.6)$$

VICON data were captured for the same anatomical landmarks. Data were captured by 12 VICON cameras and they were exported to static trial modeling. Static trial modeling was performed according to the program run by BodyBuilder software (appendix C). After executing the program position coordinates of each land mark were stored. These data were captured for 1-2s, when the subject was on each anatomical mark. Distances between *RASIS* to *LASIS*, *RASIS* to *PS* and *LASIS* to *PS* were compared as stated earlier and one hundred data sets were utilized for these comparisons.

4.4.3 Results

The distances data from both OrthoPilot and VICON systems were compared with calibrated distances data from the phantom model. Mean value of the distances between pairs of anatomical landmarks and the standard deviation values for APP2 are shown in Table 4.1.

Table 4.1 Distance comparison between anatomical land marks for APP2

APP types	Distance between anatomical land marks	Calibrated Phantom model data (mm)	VICON		OrthoPilot	
			Mean Value (mm) n=100	SD (mm)	Mean Value (mm) n=100	SD (mm)
APP 2	*RASIS-LASIS*	230	231.14	0.11	230.10	0.19
	RASIS-PS	145	143.95	0.17	145.64	0.19
	LASIS-PS	145	144.62	0.09	145.95	0.34

It can be seen that the mean value of the distance between anatomical landmarks obtained from OrthoPilot are within the range of ± 1 mm to the phantom model data. In addition, OrthoPilot distance data are within the range of ± 2 mm to the VICON data. The standard deviations are less than 1% of the measured value.

In addition the distance between anatomical landmarks for APP1 and APP3 were compared from both OrthoPilot and VICON systems. Mean distance data and the standard deviation values for APP1 and APP3 are shown in Table 4.2 and Table 4.3 respectively.

Table 4.2 Distance comparison between anatomical land marks for APP1

APP types	Distance between anatomical land marks	Calibrated Phantom model data (mm)	VICON		OrthoPilot	
			Mean Value (mm) n=100	SD (mm)	Mean Value (mm) n=100	SD (mm)
APP 1	*RASIS-LASIS*	170	170.53	0.08	170.06	0.15
	RASIS-PS	102	102.45	0.09	103.97	0.14
	LASIS-PS	102	101.77	0.10	104.28	0.17

According to the Table 4.2, the mean value of the distance between anatomical landmarks of *RASIS-LASIS* and *RASIS-PS* obtained from OrthoPilot are within the range of ± 2 mm to the phantom model data and VICON data. Distance between *LASIS-PS* is within the range of ± 3 mm to the phantom model data and VICON data. In addition, the standard deviations are less than 1% of the measured value.

Table 4.3 Distance comparison between anatomical land marks for APP3

APP types	Distance between anatomical land marks	Calibrated Phantom model data (mm)	VICON		OrthoPilot	
			Mean Value (mm) n=100	SD (mm)	Mean Value (mm) n=100	SD (mm)
APP3	*RASIS-LASIS*	290	290.46	0.09	290.39	0.42
	RASIS-PS	190	190.12	0.14	188.74	0.98
	LASIS-PS	190	189.36	0.21	188.67	0.54

Table 4.3 represents the mean values of the distance between anatomical landmarks obtained for APP3. The OrthoPilot distance data are within the range of ± 2 mm to the phantom model data and to the VICON data. In addition, the standard deviations are less than 1% of the measured value.

4.4.4 Discussion

Data for the distance between the anatomical landmarks were within the range of ± 2 mm to the exact distance reading. Only, the distance between *LASIS-PS* for the APP1 was larger and in the range of ± 3 mm to the phantom model data and VICON data. This deviation may occur due to a small deviation of the surgical tool positioning, such as bending of the surgical tool, or markers not clearly visible to the camera. All the results were observed to have small standard deviations. Small standard deviations represent the precision of the OrthoPilot results. According to the OrthoPilot manufacture's technical specification distance accuracy is ± 2 mm and was verified with the distance data recorded. The results have clearly answered the

research question raised in subsection 4.2. Therefore, it can be stated here that the OrthoPilot instrument position data are accurate and repeatable enough for the real world surgical operations.

4.5 Experiment 2- Cup navigation algorithm accuracy

4.5.1 Introduction

The cup navigation algorithm's accuracy was examined during this stage. Accuracy of the hip navigation algorithm was tested by applying the calculation methods explained in Chapter 3 to calculate the native anteversion and inclination angles of the acetabulum using the VICON data. Radiographic definition of the acetabular orientation was used to obtain the angle values.

4.5.2 Method

Derivation of APP

APP equation is derived with the *LASIS*, *RASIS* and *PS* as explained in the equations (3.11, 3.12 and 3.13) in Chapter 3.

$$\begin{vmatrix} x - x_{col} & y - y_{col} & z - z_{col} \\ x_{con} - x_{col} & y_{con} - y_{col} & z_{con} - z_{col} \\ x_{cen} - x_{col} & y_{cen} - y_{col} & z_{cen} - z_{col} \end{vmatrix} = 0 \quad (4.7)$$

The normal vector to the APP was derived according to the equations 3.14 to 3.19 explained in Chapter 3 as bellow.

$$n_{x_{app}} = x*\left[\left(y_{con} - y_{col}\right)*\left(z_{cen} - z_{col}\right)\right] - x_{col}*\left[\left(y_{cen} - y_{col}\right)*\left(z_{con} - z_{col}\right)\right] \quad (4.8)$$

$$n_{y_{app}} = y*\left[\left(x_{con} - x_{col}\right)*\left(z_{cen} - z_{col}\right)\right] - y_{col}*\left[\left(x_{cen} - x_{col}\right)*\left(z_{con} - z_{col}\right)\right] \quad (4.9)$$

$$n_{z_{app}} = z*\left[\left(x_{con} - x_{col}\right)*\left(y_{cen} - y_{col}\right)\right] - z_{col}*\left[\left(x_{cen} - x_{col}\right)*\left(y_{con} - y_{col}\right)\right] \quad (4.10)$$

Then the trial cup registration data were captured. The same method explained in subsection 3.2 for the landmark palpation was applied to obtain the cup axis vector. If the resulted cup axis vector is $\left(\vec{a},\vec{b},\vec{c}\right)$, radiographic anteversion and inclination angles were calculated according to the equations (3.17) and (3.18).

Radiographic anteversion and inclination angles were obtained from the phantom model. APP2 was used to obtain the anterior pelvic plane data. Data palpation was achieved exactly on the landmarks defined by APP2. Position vectors for each anatomical landmark from the OrthoPilot system were extracted from relevant transformation matrices, while VICON system position vectors were extracted from the static trial modeling. One hundred data sets were utilized for this comparison. Calculations were done using eq. 3.23 and 3.24.

4.5.3 Results

A comparison was carried out for the anteversion and inclination angles of the acetabulum of the pelvic model. Anteversion and inclination angles resulted from both OrthoPilot and VICON systems are displayed in Table 4.4

Table 4.4 Acetabular angle comparison

Data / Angle	Calibrated phantom model data	VICON		OrthoPilot	
	Value (deg)	Mean Value (deg) n=100	SD (deg)	Mean Value (deg) n=100	SD (deg)
Anteversion angle	14	14.07	0.10	14.54	0.13
Inclination Angle	45	44.87	0.07	45.86	0.15

According to the Table 4.4, the mean angle values of Anteversion and Inclination obtained from OrthoPilot are within the range of $\pm 1^0$ to the phantom model angle values and VICON angle data. The standard deviations (SD) of the angle values are less than 1%.

4.5.4 Discussion

Data for the acetabular angles were within the range of $\pm 1^0$ to the exact angle reading. All the results were observed with small standard deviations. Small standard deviations represent the precision of the OrthoPilot results. According to the OrthoPilot manufacturer's technical specification angular accuracy is $\pm 2^0$ and which is verified by the experimental results. The results have clearly answered the research question raised in subsection 4.2. Therefore, it can be stated here that the Cup navigation algorithm produces accurate and repeatable angle results.

4.6 Experiment 3-Effect of reference tracker tilt during the APP registration

4.6.1 Introduction

Further, there is a possibility to tilt the reference tracker accidentally, during the surgery. A tilt of a few degrees may considerably affect the acetabular angles. During this stage, acetabular angle variation is going to be examined by tilting the reference tracker, while registering the APP. Reference tracker was tilted along four different directions and landmarks for the APP2 were palpated.

4.6.2 Method

Reference tracker was fitted to a vernier Goniometer (Figure 4.11), and this reference tracker was tilted along two different axes; axis along anterior-posterior and axis along medial-lateral. Rotational axis and the orientation of the reference transmitter during the experiment are shown in the Figure 4.12 (b and c); Figure 4.12(b) shows the reference tracker rotating along anterior-posterior axis and Figure 4.12(c) shows the reference tracker rotation along the medial-lateral axis.

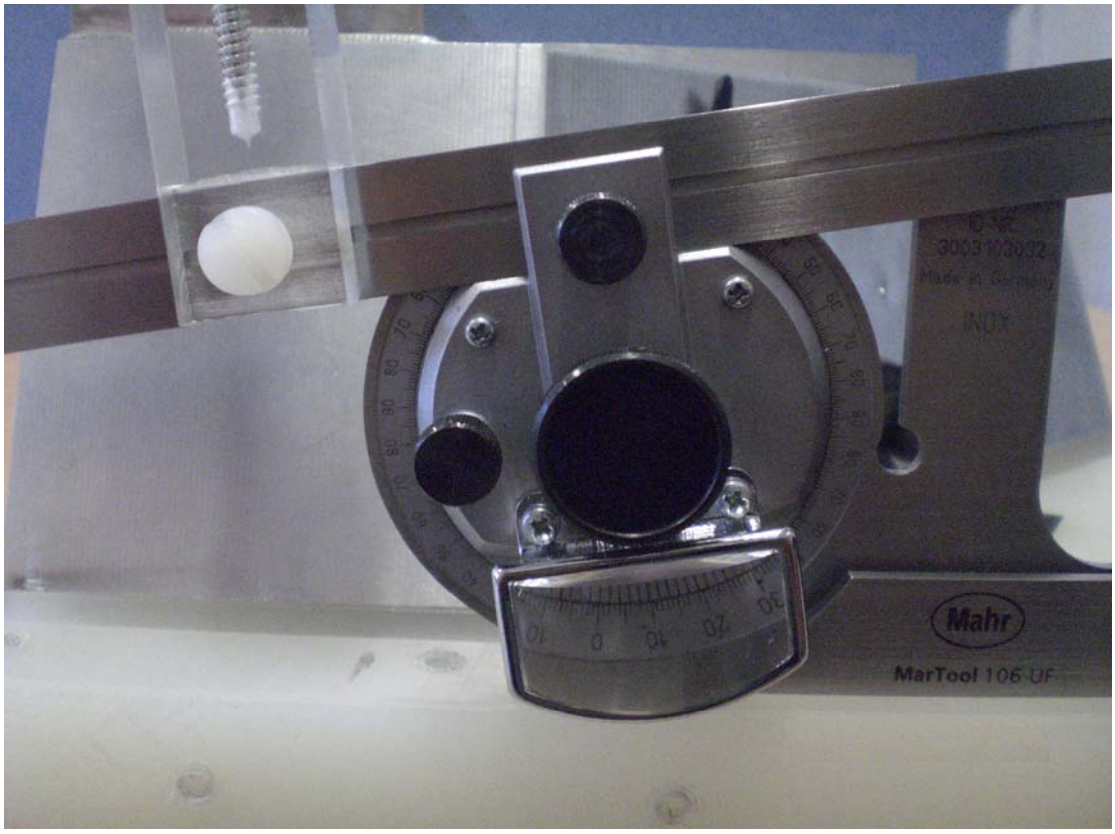

Figure 4.11 Goniometer (least count/ Resolution of 0.5^0)

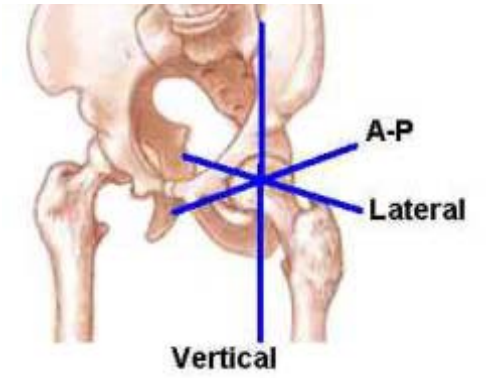

(a)

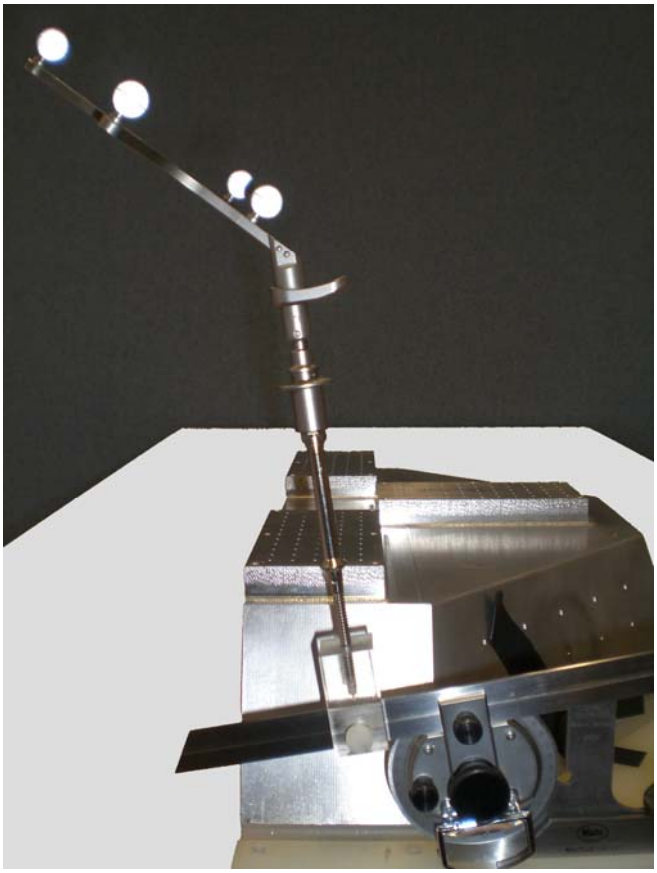

(b)

(c)

Figure 4.12 (a) Pelvic axis system; (b) Rotation of the reference transmitter along anterior-posterior axis; (c) Rotation of the reference transmitter along medial-lateral axis

Similar data palpation method was followed as explained in the previous subsection 4.5 and only reference tracker was tilted. Reference tracker was rotated starting from 3° to 15° by increasing the rotational angle in 2^0 intervals. Once the reference tracker has been rotated, the APP data (*RASIS*, *LASIS* and *PS* with respect to reference tracker) were recorded. The pelvic phantom was in the supine position during this recording. The reference tracker was placed back to its original position (0^0 position of the goniometry reading) to record the medial wall point and trial cup data.

4.6.3 Results

APP was varied by tilting the reference tracker along the anterior-posterior axis and resulted Anteversion and Inclination angles are displayed in Table 4.5. Mean angle values and the standard deviations can be found from this table.

Table 4.5 Acetabular angle comparison for APP variations by tilting the reference tracker in the direction of anterior-posterior axis

		VICON				OrthoPilot			
		Anteversion		Inclination		Anteversion		Inclination	
	Deg	Value (Deg)	SD (Deg)	Value (Deg)	SD (Deg)	Value (Deg)	SD (Deg)	Value (Deg)	SD (Deg)
Anterior	-15	3.04	0.09	44.90	0.16	2.61	0.38	44.11	0.13
	-13	4.39	0.07	44.94	0.45	4.10	0.16	44.55	0.10
	-11	5.75	0.07	44.32	0.44	5.62	0.11	44.78	0.22
	-9	7.12	0.08	44.55	0.38	6.95	0.44	45.10	0.26
	-7	8.51	0.09	44.78	0.52	8.26	0.30	44.91	0.36
	-5	9.92	0.10	45.12	0.25	9.61	0.24	45.00	0.38
	-3	11.33	0.10	45.48	0.52	11.46	0.10	45.37	0.25
Neutral	0	14.07	0.10	44.87	0.07	14.54	0.13	45.86	0.15
Posterior	3	15.55	0.11	46.45	0.36	15.28	0.24	46.46	0.23
	5	16.98	0.12	47.01	0.29	17.26	0.33	47.03	0.22

	7	18.38	0.12	47.62	0.35	17.81	0.34	46.94	0.29
	9	19.77	0.13	48.43	0.44	19.38	0.20	47.72	0.32
	11	21.10	0.16	48.58	0.46	20.58	0.19	48.18	0.49
	13	22.46	0.15	49.20	0.49	22.08	0.23	49.32	0.40
	15	23.80	0.15	49.54	0.50	23.59	0.10	49.68	0.32

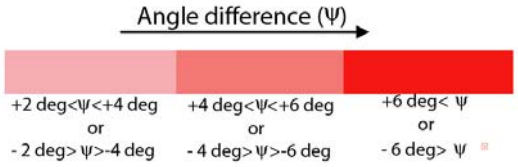

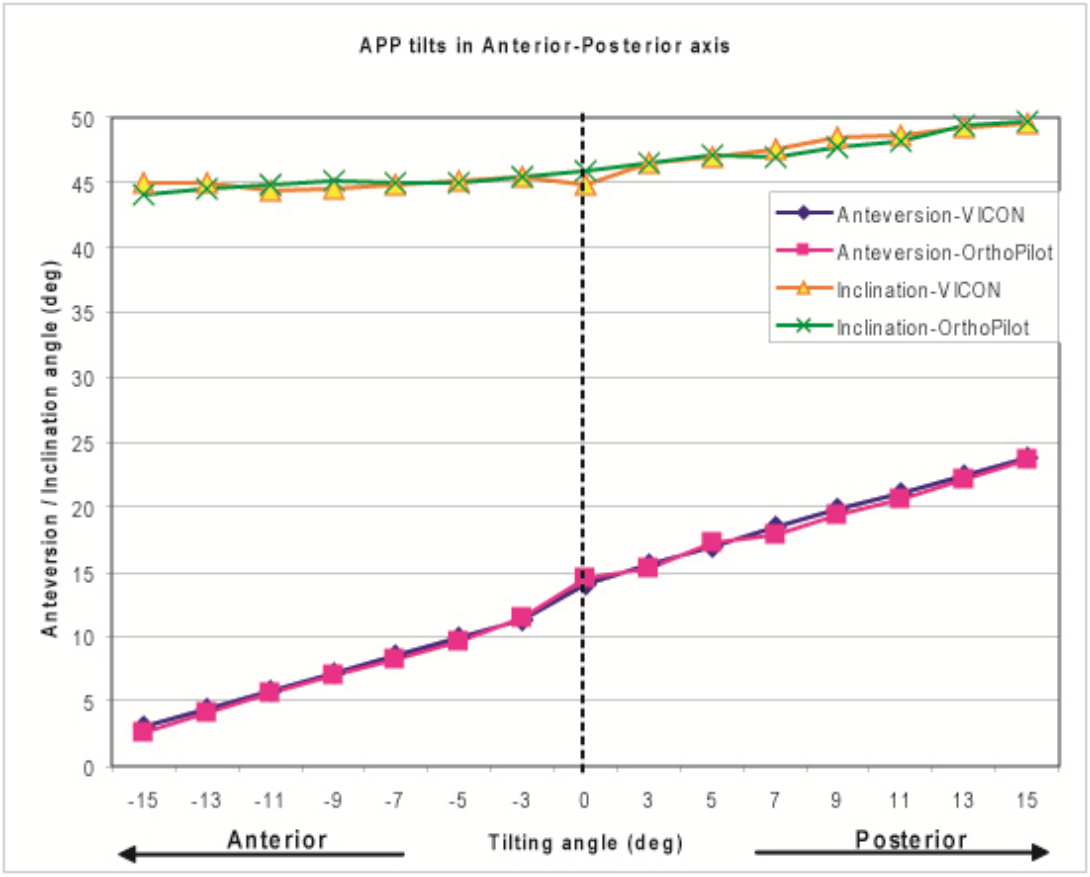

Figure 4.13 Graphical representation of the acetabular angle variation when APP varies by tilting the reference tracker along anterior-posterior axis.

As shown in Figure 4.13, when the APP tilted towards the anterior direction, the anteversion angle decreased significantly, whereas the inclination angle showed only

a slight reduction. When the APP tilted towards the posterior direction, the anteversion angle increased significantly and the inclination angle increased slightly. The end note of the table 4.5, shows the colour range of the highlighted angular values. This colour range was selected according to the angle difference to the normal angular value. If the angles values are with in the range of $+2^0$ to $+4^0$ or -2^0 to -4^0 to the normal angular values, those values are displayed in lightest colored cells. If the values are larger (or smaller) than $+6^0$ (or -6^0) to the normal angular values, those values are displayed in darkest colored cells. Middle color range shows the angels when they are with in the range of $+4^0$ to $+6^0$ or -4^0 to -6^0 to the normal angular values. Uncolored cells represent almost comparable angle values to the neutral angular values (with in the range of $\pm 2^0$ to the normal angular values). Further, according to the Table 4.5, the mean angle values of Anteversion and Inclination obtained from OrthoPilot are within the range of $\pm 2^0$ to VICON angle data. The standard deviations (SD) of the angle values are less than 1%.

Table 4.6 shows the effect of medial-lateral tracker rotation. Similar to Table 4.5, few important observations can be seen in the acetabular angles when varying the APP by tilting the reference tracker along the medial-lateral axis as shown in Table 4.6.

Table 4.6 Acetabular angle comparison for APP variations by tilting the reference tracker in the direction of medial-lateral axis

		VICON data				OrthoPilot			
		Anteversion		Inclination		Anteversion		Inclination	
	Deg	Value (Deg)	SD (Deg)	Value (Deg)	SD (Deg)	Value (Deg)	SD (Deg)	Value (Deg)	SD (Deg)
Lateral	-15	1.32	0.22	46.66	0.31	2.32	0.29	47.55	0.28
	-13	2.61	0.24	46.59	0.19	3.51	0.19	47.18	0.31
	-11	4.51	0.31	46.37	0.29	5.13	0.26	47.13	0.29
	-9	6.25	0.29	46.42	0.29	6.55	0.27	46.72	0.30

	-7	8.29	0.11	46.5	0.30	8.25	0.24	46.75	0.32
	-5	9.48	0.34	46.33	0.29	9.78	0.31	46.89	0.22
	-3	11.20	0.21	46.04	0.21	10.97	0.09	46.18	0.18
Neutral	0	14.07	0.10	44.87	0.07	14.54	0.13	45.86	0.15
Medial	3	15.79	0.20	44.87	0.31	15.86	0.17	45.21	0.36
	5	18.47	0.22	44.76	0.37	17.10	0.16	44.83	0.22
	7	20.20	0.21	44.6	0.34	18.96	0.44	44.54	0.19
	9	21.60	0.30	44.74	0.26	20.33	0.35	44.18	0.28
	11	23.49	0.29	44.64	0.34	21.39	0.27	43.72	0.31
	13	25.13	0.33	44.66	0.34	22.88	0.42	43.09	0.41
	15	26.59	0.25	44.67	0.33	24.69	0.29	42.47	0.19

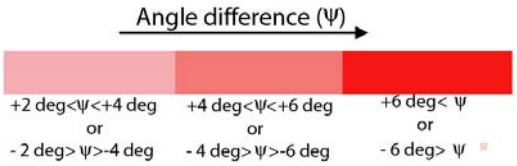

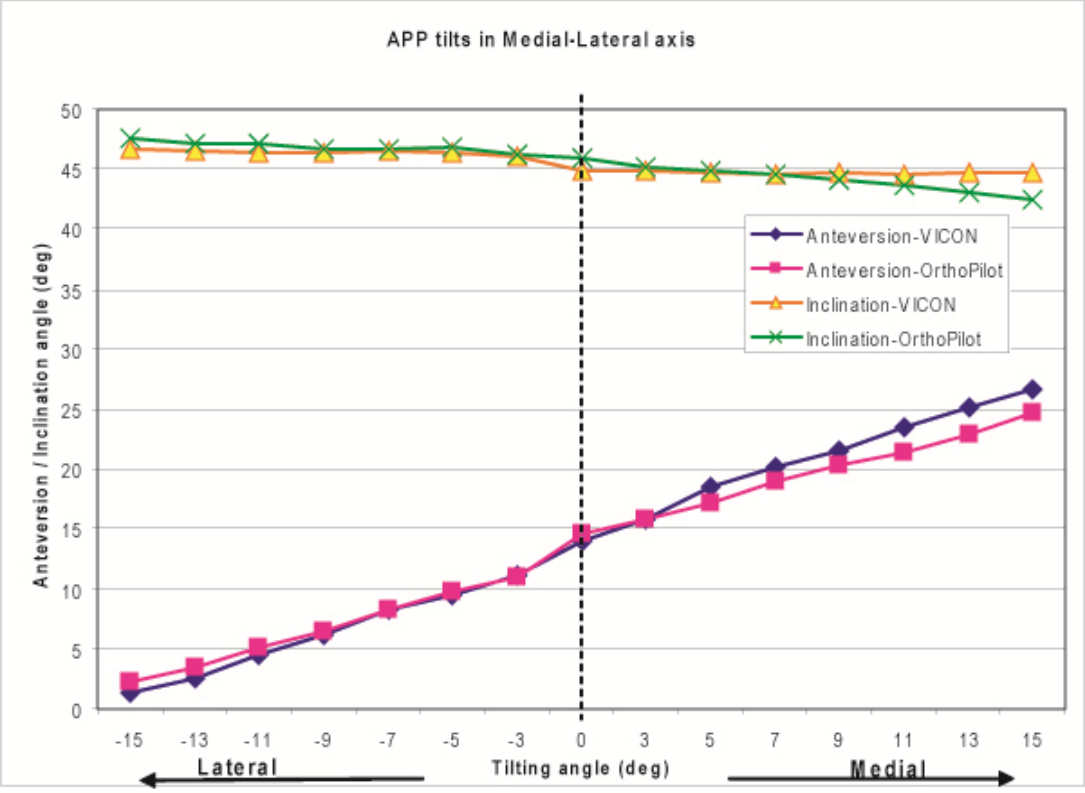

Figure 4.14 Graphical representation of the acetabular angle variation when APP tilts along medial-lateral axis.

In addition, the anteversion angle was significantly decreased, whereas the inclination angle did not show considerable deviation, when the APP tilted towards the lateral direction as shown in Figure 4.14. However, a slight decrement at inclination angle with significant increment in anteversion angle can be observed, when it was tilted towards the medial direction. The end note of the table shows the same colour range of the highlighted angular values used with the Table 4.5. Almost comparable angle values (with in the range of $\pm 2^0$ to the normal angular values) to the neutral position angles are displayed in uncolored cells.

Similar to the anterior-posterior section above, the mean angle values of Anteversion and Inclination obtained from OrthoPilot are within the range of $\pm 1^0$ to VICON angle data, when the reference tracker tilted along lateral direction. The mean angle values obtained from OrthoPilot are within the range of $\pm 2^0$ to VICON angle data,

when the reference tracker tilted along medial direction. The standard deviations (SD) of the angle values are less than 1%.

4.6.4. Discussion

When the reference tracker rotates along anterior-posterior axis, errors were only introduced to the Y and Z coordinates of the palpated anatomical land marks. When it rotates along medial-lateral axis, X and Z coordinates of the landmarks were affected.

When APP tilts towards the anterior direction, landmark position coordinates changes;

$$Y_{new} = Y_{previous} + l * \sin(\theta_{anterior}) \quad (4.11)$$

$$Z_{new} = Z_{previous} - l * \cos(\theta_{anterior}) \quad (4.12)$$

When APP tilts towards the posterior direction, landmark position coordinates changes;

$$Y_{new} = Y_{previous} + l * \sin(\theta_{posterior}) \quad (4.13)$$

$$Z_{new} = Z_{previous} + l * \cos(\theta_{posterior}) \quad (4.14)$$

When APP tilts towards the medial direction, landmark position coordinates changes;

$$X_{new} = X_{previous} + l * \sin(\theta_{medial}) \quad (4.15)$$

$$Z_{new} = Z_{previous} + l * \cos(\theta_{medial}) \quad (4.16)$$

When APP tilts towards the lateral direction, landmark position coordinates changes;

$$X_{new} = X_{previous} + l * \sin(\theta_{lateral}) \quad (4.17)$$

$$Z_{new} = Z_{previous} - l * \cos(\theta_{lateral}) \quad (4.18)$$

These position vectors' variations of the landmarks produced the deviations to the acetabular angles, when the reference tracker tilts during APP registration.

4.7 Experiment 4-Varying the dimensions of the APP

4.7.1 Introduction

Incorrect palpation of the anatomical landmark may result in a poor quality joint replacement. Deviation of the landmark from its exact position, during the APP registration can make a difference to the final cup orientation. Hence, variation of the acetabular orientation due to the deviation of the landmark from its exact point was examined during this stage.

4.7.2 Method

Landmark was moved along the directions of caudal, cranial, medial and lateral. Each landmark bed was machined with a peg point grid of 10mm orthogonal distance (Figure 4.1). In addition, the same algorithm was used to calculate the angle values from OrthoPilot and VICON data.

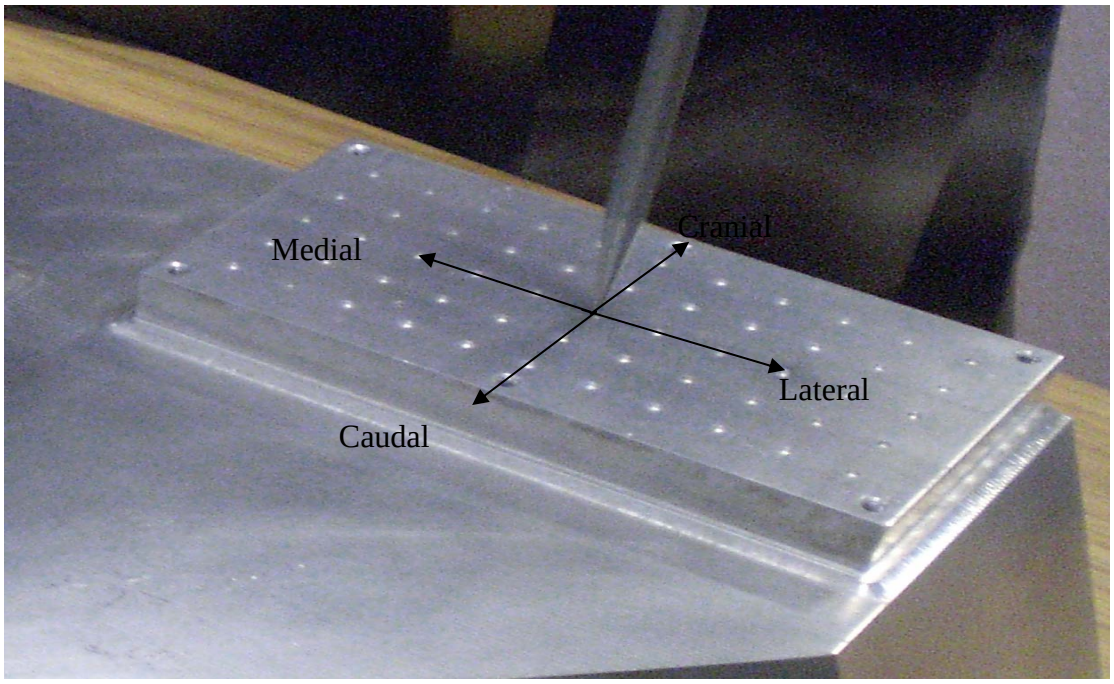

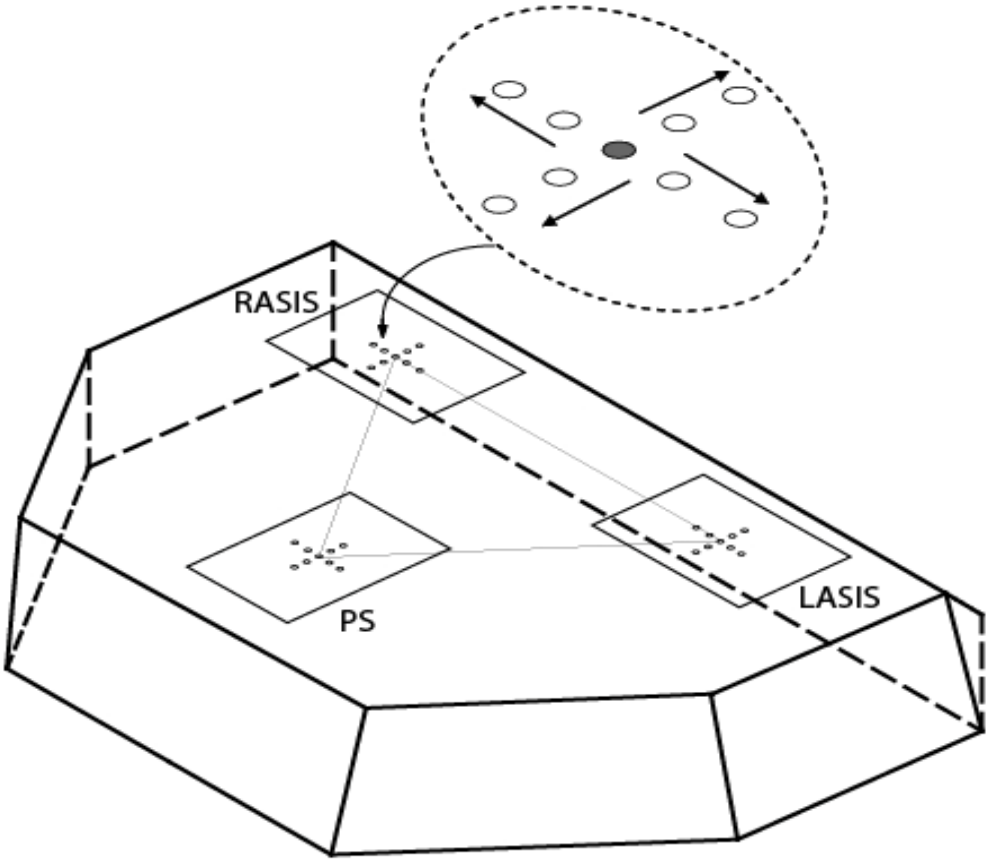

Figure 4.15 Landmark variations in Coronal plane.

The APP was changed by varying the anatomical land marks in coronal plane. One anatomical land mark was changed at a time, while keeping the other two land marks stationary. The surgical tool was moved only in the directions of Caudal-Cranial and Medial-Lateral. There was no vertical movement of the tool. The pointer palpation tool was moved along the caudal-cranial and medial-lateral directions and this can be seen in the Figure 4.15. The *RASIS* was moved from its original position along the lateral direction by 10 mm, while keeping the *LASIS* and *PS* stationary. At the next stage, the *RASIS* was displaced by 20 mm. Subsequently, the same procedure was followed to the *RASIS* in the medial, caudal and cranial directions, while keeping *LASIS* and *PS* stationary. Next, the procedure was repeated for the *LASIS* and *PS* along the four directions, while keeping other two land marks stationary. Data were recorded without rotating the reference tracker during this procedure, which was fixed at the vertical position as indicated by the Goniometer. The Pelvic phantom was in the supine position, while recording the data. During this process, the y coordinate changed, when the marker was moved along the caudal-cranial direction, whereas, the x coordinate changed, when it was displaced along the medial-lateral direction.

4.7.3 Results

The APP was varied by changing the landmark position and resulted mean angle values and the standard deviations for the Anteversion and Inclination angles are displayed in the Table 4.7, 4.8 and 4.9. Table 4.7 represents the angle results, when changing the landmark position at RASIS along caudal, cranial, medial and lateral directions.

Table 4.7: Acetabular angle comparison for APP variations in coronal plane – Changing anatomical landmark position at RASIS

Changing Landmark	Varying direction	Variation from exact position (mm)	VICON				OrthoPilot			
			Anteversion		Inclination		Anteversion		Inclination	
			Value (Deg)	SD (Deg)	Value (Deg)	SD (Deg)	Value (Deg)	SD (Deg)	Value (Deg)	SD (Deg)
RASIS	Caudal	-20	14.10	0.12	40.03	0.33	14.88	0.40	40.65	0.38
		-10	14.31	0.27	43.07	0.24	13.66	0.47	43.57	0.31
		0	14.07	0.1	44.87	0.07	14.54	0.13	45.86	0.15
		10	14.00	0.28	47.80	0.16	13.79	0.41	48.21	0.37
		20	14.00	0.23	49.15	0.26	13.99	0.39	50.54	0.47
	Medial	-20	14.07	0.13	45.16	0.27	13.57	0.14	45.88	0.23
		-10	14.10	0.12	44.90	0.16	13.63	0.31	45.10	0.36
		0	14.07	0.1	44.87	0.07	14.54	0.13	45.86	0.15
		10	14.16	0.26	44.66	0.04	13.71	0.16	45.32	0.25
		20	14.15	0.22	44.98	0.15	13.63	0.40	45.41	0.25

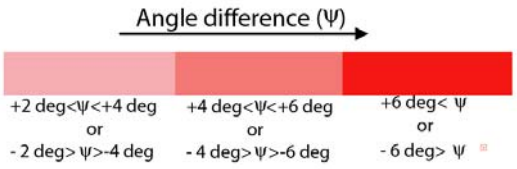

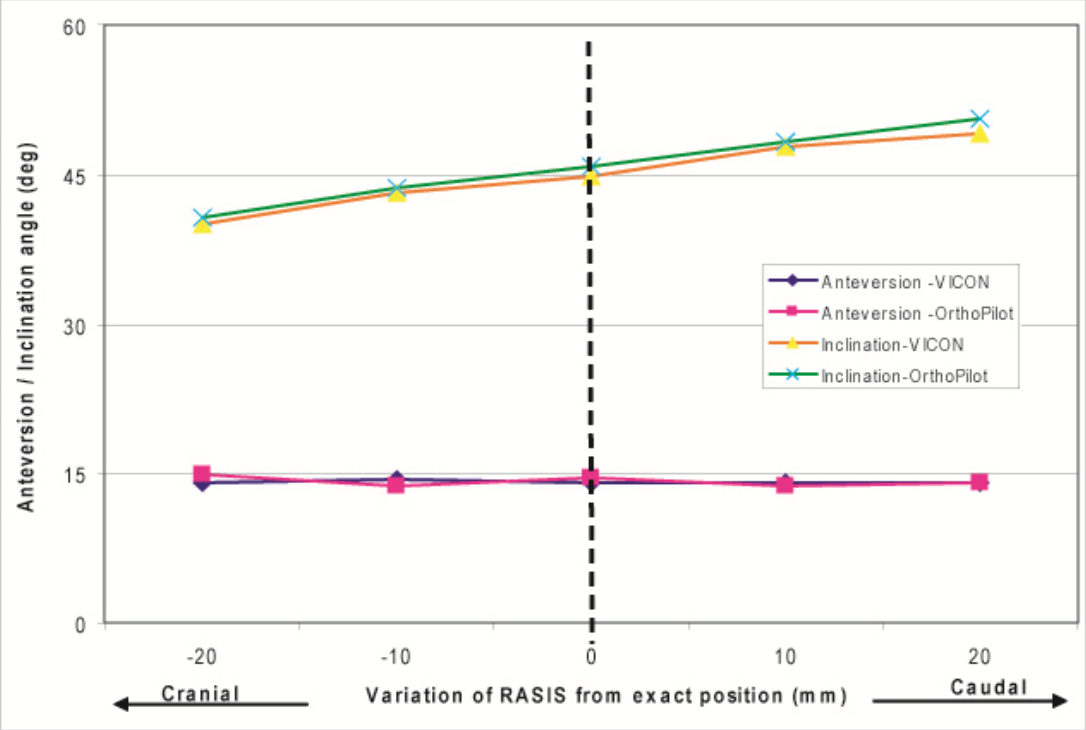

Figure 4.16 Graphical representation of the acetabular angle variation when RASIS changes along Caudal and Cranial directions

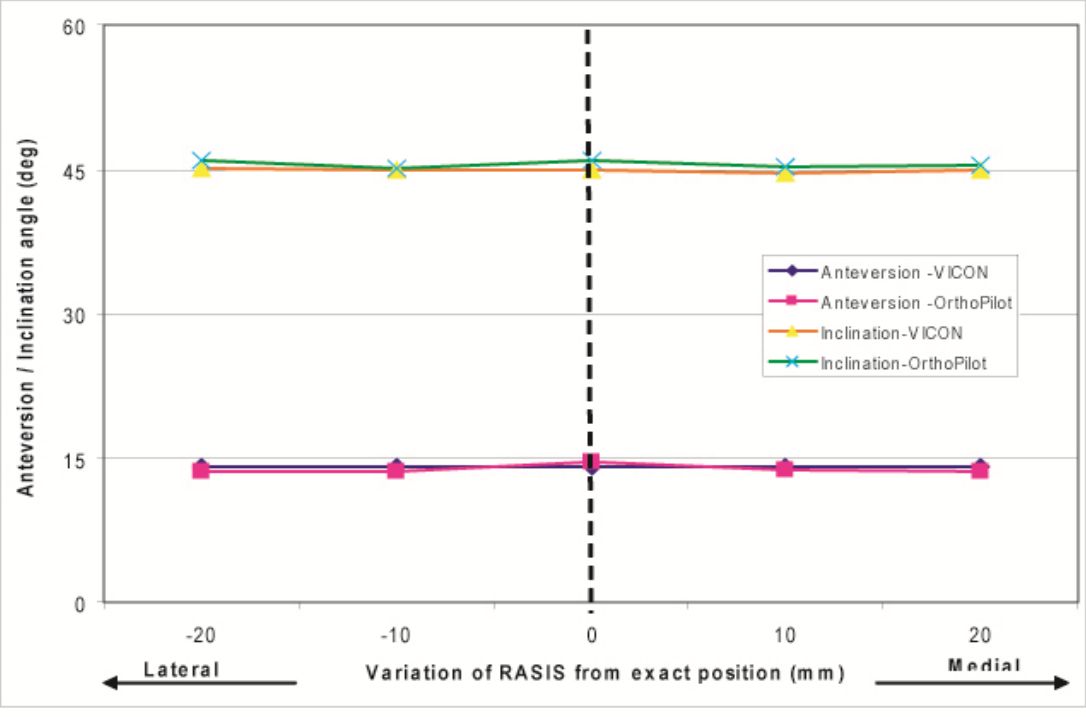

Figure 4.17 Graphical representation of the acetabular angle variation when RASIS changes along Medial and Lateral directions

When the landmark position at *RASIS* varies along caudal and cranial directions by 10 mm and 20 mm, inclination angle changed considerably from its original value, whereas no considerable deviation in anteversion angle was observed (Figure 4.16). Moving the *RASIS* towards the caudal direction acted to increase the inclination angles significantly, while the anteversion angle remains unchanged. When it moved towards the cranial direction, inclination angle was significantly decreased with unchanged anteversion angle. When, the landmark position of *RASIS* moves along medial or lateral directions, both anteversion and inclination angles do not change (Figure 4.17). Same colour range was used as explained in the sub section 4.7, when highlighting the angular difference to the normal angular values as shown in Table 4.7.

The mean angle values of Anteversion and Inclination obtained from OrthoPilot are within the range of $\pm 1^0$ to VICON angle data, when the landmark position of RASIS changes in the coronal plane. The standard deviations (SD) of the angle values are less than 1%.

Table 4.8 represents mean angle values and the standard deviations for Anteversion and Inclination angles, when changing the landmark position at LASIS along caudal, cranial, medial and lateral directions.

Table 4.8: Acetabular angle comparison for APP variations in coronal plane – Changing anatomical landmark position of LASIS

Changing Landmark	Varying direction	Variation from exact position (mm)	VICON				OrthoPilot			
			Anteversion		Inclination		Anteversion		Inclination	
			Value (Deg)	SD(Deg)	Value (Deg)	SD (Deg)	Value (Deg)	SD (Deg)	Value (Deg)	SD (Deg)
LASIS	Caudal	-20	14.16	0.14	50.52	0.25	14.36	0.30	49.54	0.27
		-10	13.77	0.19	48.35	0.31	14.15	0.10	47.95	0.30
		0	14.07	0.1	44.87	0.07	14.54	0.13	45.86	0.15

		10	14.23	0.19	43.45	0.27	14.14	0.33	43.18	0.28
		20	14.11	0.19	41.19	0.27	14.31	0.14	40.64	0.30
	Medial	-20	13.73	0.20	44.77	0.18	14.13	0.25	45.75	0.25
		-10	13.41	0.20	45.06	0.31	14.22	0.24	46.04	0.22
		0	14.07	0.1	44.87	0.07	14.54	0.13	45.86	0.15
		10	13.73	0.23	45.56	0.29	13.62	0.42	45.46	0.21
		20	13.97	0.24	45.81	0.12	14.42	0.17	45.65	0.38

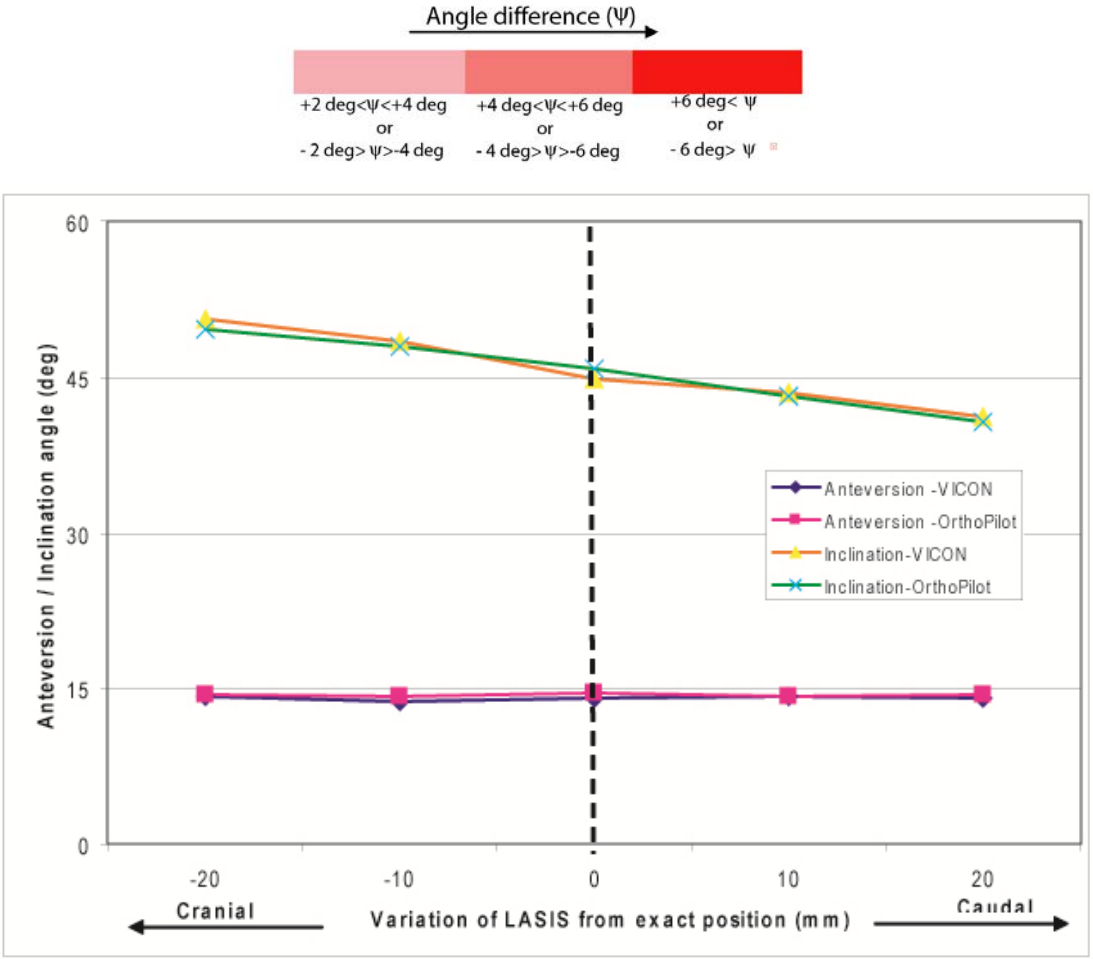

Figure 4.18 Graphical representation of the acetabular angle variation when LASIS changes along Caudal and Cranial directions

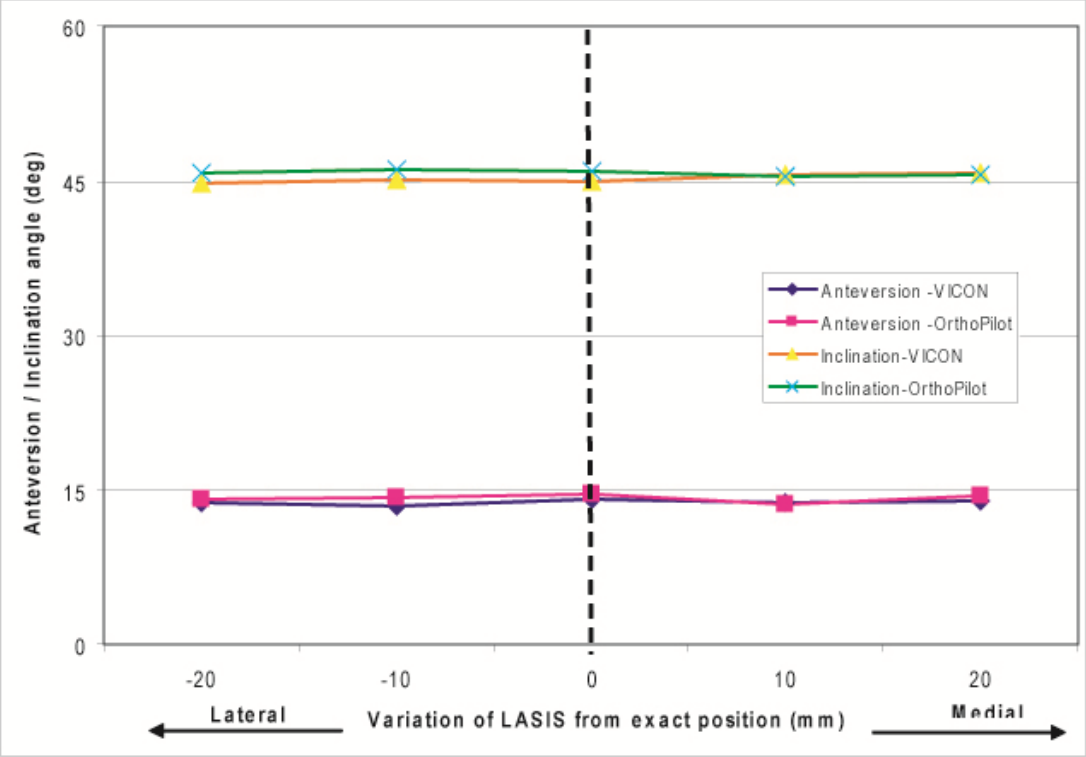

Figure 4.19 Graphical representation of the acetabular angle variation when LASIS changes along Medial and Lateral directions

The Inclination angle deviated considerably from its original value, whereas no deviation in anteversion angle was observed, when the APP was changed by varying the anatomical landmark of *LASIS* in the coronal plane along the caudal and cranial directions (Figure 4.18). Moving the *LASIS* towards the caudal direction caused a decrease in the inclination angles, while the anteversion angle remains unchanged. When the *LASIS* was moved towards the cranial direction, inclination angle was significantly increased with unchanged anteversion angle. In addition, no significant changes occur in anteversion or inclination angles when the *LASIS* moved towards the medial and lateral axes (Figure 4.19). Same colour range was used as explained in the sub section 4.7, when highlighting the angular difference to the normal angular values as shown in Table 4.8.

The mean angle values of Anteversion and Inclination obtained from OrthoPilot are within the range of $\pm 1^0$ to VICON angle data, when the landmark position of LASIS

changes in the coronal plane. The standard deviations (SD) of the angle values are less than 1%.

Table 4.9 represents mean angle values and the standard deviations for Anteversion and Inclination angles, when changing landmark position at PS along caudal, cranial, medial and lateral directions.

Table 4.9: Acetabular angle comparison for APP variations in coronal plane – Changing anatomical landmark position of PS

Changing Landmark	Varying direction	Variation from exact position (mm)	VICON				OrthoPilot			
			Anteversion		Inclination		Anteversion		Inclination	
			Value (Deg)	SD (Deg)	Value (Deg)	SD (Deg)	Value (Deg)	SD (Deg)	Value (Deg)	SD (Deg)
PS	Caudal	-20	14.15	0.17	46.19	0.35	13.68	0.37	45.97	0.30
		-10	13.32	0.21	45.55	0.27	13.55	0.14	46.26	0.21
		0	14.07	0.1	44.87	0.07	14.54	0.13	45.86	0.15
		10	13.66	0.14	45.52	0.12	13.45	0.22	46.00	0.30
		20	13.44	0.17	45.79	0.23	13.07	0.12	45.95	0.20
	Medial	-20	14.13	0.18	45.58	0.17	14.17	0.16	45.25	0.16
		-10	13.84	0.28	44.71	0.12	14.46	0.24	45.07	0.43
		0	14.07	0.1	44.87	0.07	14.54	0.13	45.86	0.15
		10	14.00	0.21	44.90	0.18	13.43	0.41	45.66	0.26
		20	14.13	0.18	45.58	0.17	14.47	0.16	45.25	0.16

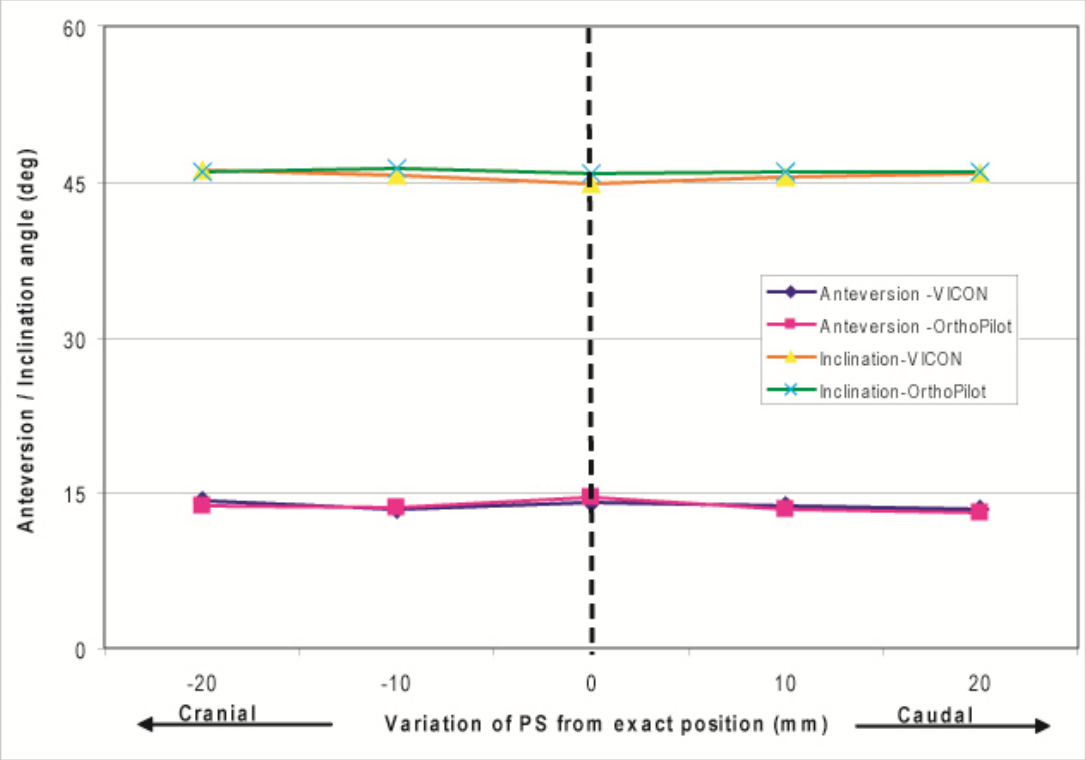

Figure 4.20 Graphical representation of the acetabular angle variation when PS changes along Caudal and Cranial directions

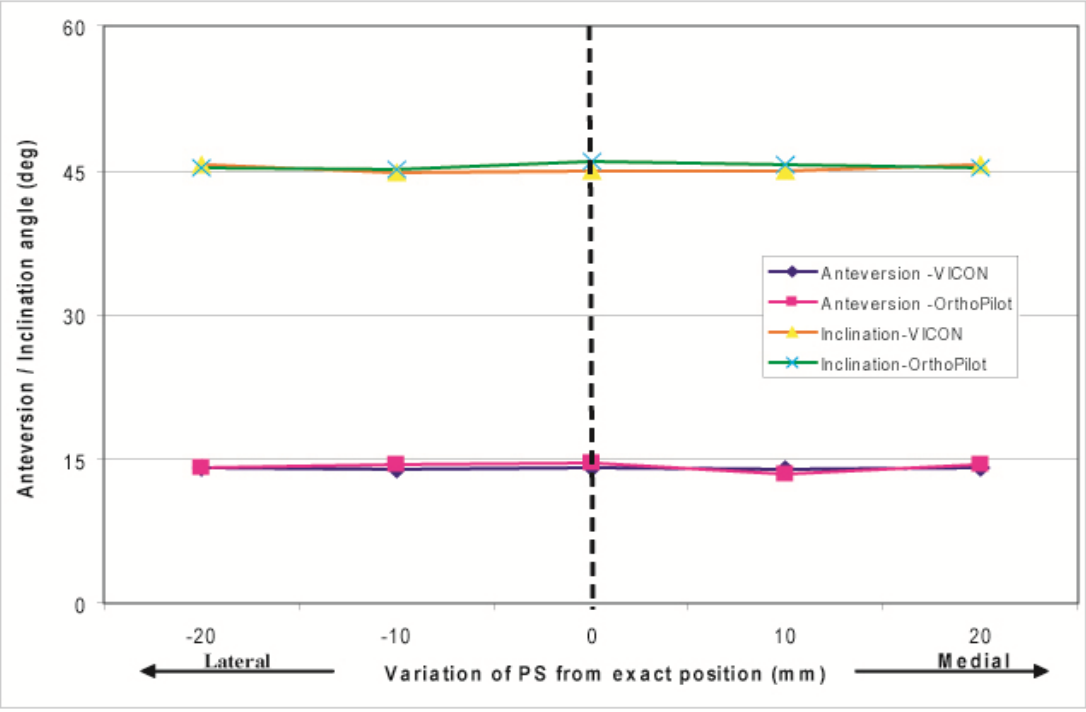

Figure 4.21 Graphical representation of the acetabular angle variation when PS changes along Medial and Lateral directions

When the landmark position of PS changes along caudal and cranial directions (Figure 4.20) as well as medial and lateral directions (Figure 4.21), almost the same inclination and anteversion angle values were observed.

The mean angle values of Anteversion and Inclination obtained from OrthoPilot are within the range of $\pm 1^0$ to VICON angle data, when the landmark position of PS changes in the coronal plane. The standard deviations (SD) of the angle values are less than 1%.

Chapter 5

DISCUSSION

5.1 Introduction

Computer-assisted navigation is thought to improve the outcome of joint replacement surgery. However, some surgeons still hesitate to apply navigational techniques. This is partly due to the uncertainty related to the accuracy of these navigational techniques. As a result, it is highly important to validate the navigational system for its accuracy and precision if such systems are to be widely adopted.

This research study was conducted to validate the accuracy of OrthoPilot hip navigation process from an engineering point of view. According to the OrthoPilot manufacturer's technical specification (user manual), the system precision with regard to the computed angles and distances is $\pm 2^0$ and $\pm$ 2 mm respectively. The accuracy of the computed angles and distances of this system required to be determined independently of the manufacturer. The clinical validation contains many sources of error or deviation from an ideal outcome in terms of the surgeons' use of the system, inaccurate palpation of landmarks, variation in actual cup position from that given by the navigation system and measurement of the final cup position. It is therefore not possible to validate the claims of the OrthoPilot manufacturer about the accuracy of the system easily from clinical data. Therefore, it is important to evaluate the technical accuracy of the system i.e. the ability of the system to measure known inputs.

5.2 Discussion of the experiment process

During this study, cup only navigation process was considered. All the experiments were conducted for the surgical navigation processes of APP registration to trial cup registration. APP is considered as the reference to place the cup implant precisely in the acetabulum. Therefore, the APP registration plays the key role in cup navigation. The effect of accurate APP registration for the native acetabular registration was examined during the experiments. The accuracy of the anatomical landmark palpation for the APP registration was experimented. Data were captured from a calibrated pelvic phantom model made from Aluminium. The reason for selecting Aluminium was to overcome the enlargement of a peg point hole due to wear, when repeating the tests. This phantom had three peg point grids for each anatomical landmarks of RASIS, LASIS and PS. These grids were machined to achieve different sizes of APP. In addition, surface of the acetabular face had a grid of peg points. Same peg point was used during all the experiments, when palpating the deepest point of the acetabular (medial wall point). All the experiments were carried out for the radiographic definition of the acetabular anteversion and inclination angles using the calibrated pelvic phantom model and used passive trackers only for the data palpation process.

The native acetabular orientation reading can be varied due to two main reasons. One is varying the APP registration and the other one is varying the registration of the trial cup axis. The APP was varied throughout all the experiments, without varying the trial cup registration. For that, the surgical tool was kept in the same orientation when registering the trial cup throughout the entire experimental procedure. Retort stands were used all the time when registering medial wall point and the trial cup to hold the surgical tool.

Another challenging problem with the experimental environment was, positioning of the Polaris camera. It should be placed without disturbing the VICON cameras. After several trials, optimum camera place was determined. Reference tracker was fixed close to the assumed operated side of the phantom. When tilting the reference

tracker, it was attached to the Goniometer. Goniometer attached reference tracker was then fixed on the assigned place.

5.3 Discussion of the results with literature and their clinical implication

Kalteis et. al (2006), have concluded that, the accuracy of acetabular component positioning using free hand, CT-based and imageless navigation as follows; with conventional method, 53% of the components were outside the Lewinneck's safe zone and 7% when using imageless navigation. These results show the accuracy and repeatability of image-free navigation such as the OrthoPilot system. OrthoPilot accuracy and repeatability were observed during this study. Results for the distance between the anatomical landmarks were within the range of ± 2 mm to the exact distance reading. In addition, results for the acetabular angle were within the range of $\pm 2^0$ to the exact angle values with small standard deviations (Table 4.4). Small standard deviations show the precision of the OrthoPilot results.

However, errors introduced during landmark palpation have a substantial effect on the final cup orientation and hence potentially on impingement, dislocation, wear and loosening (Wolf. et al. 2005). Lee et al (2008) discussed the acetabular angle errors introduced due to the fat tissue thickness. Fat tissue thickness introduces coordinates errors mainly in the anterior axis. However, except for the fat tissue thickness, errors can be introduced with the incorrect landmark registration due to the deviation of the exact point in the coronal plane. These factors result to position the implant incorrectly. The above fact can be clearly seen from the resultant acetabular angles in this study, when varying the anterior pelvic plane in coronal plane.

According to the Figure 4.16, landmark palpation of 10 mm away from the exact RASIS, along caudal or cranial directions, deviate the inclination angle by $\pm 3^0$. Similarly, palpation of 20 mm away from exact landmark point deviate inclination angle by $\pm 5^0$. Furthermore, similar inclination angle deviation can be observed when changing the exact landmark position of LASIS along caudal and cranial directions

by 10 mm and 20 mm (Figure 4.18). This inclination angle deviation can be explained as bellow,

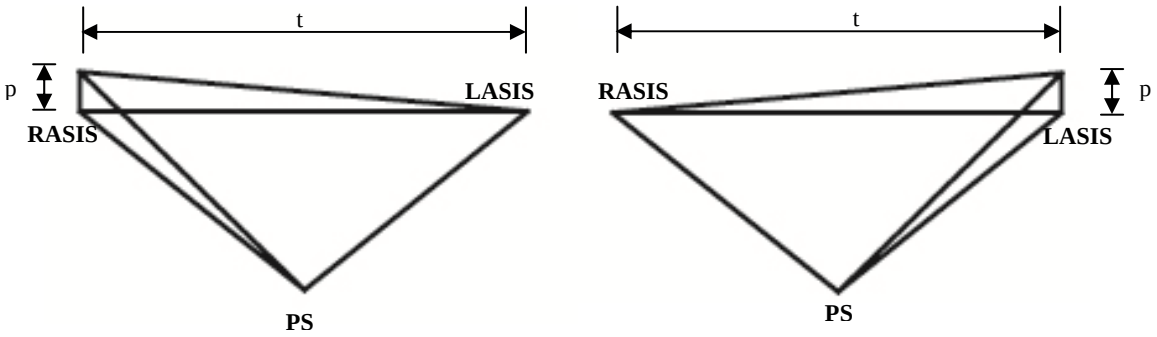

Figure 5.1 APP variations, (a) when changing the landmark of RASIS along caudal and cranial direction, (b) when changing the landmark of LASIS along caudal and cranial direction.

The APP changes with an angle (θ_{APP}) of $\tan^{-1}(\frac{p}{t})$, when the RASIS changes by p along caudal-cranial axis. When p = 10 mm and t = 230 mm, $\theta_{APP} = 3^0$. This means, inclination angle also changes by ± 3^0 when either LASIS or RASIS position changes along above-mentioned axis. Similarly, when p = 20mm $\theta_{APP} = 5^0$ and inclination angle changes by ± 5^0. Above-observed relationship can be expressed as; the APP changing angle equals to the amount of deviation of the inclination angle.

If, the small size APP (APP1) is taken for the above condition, when t = 170 mm and p = 10 mm and 20 mm, then $\theta_{APP} = 4^0$ and 7^0 respectively. With the above-observed relationship, it is recommended to expect that the inclination angle deviates by ± 4^0 and ± 7^0, when the landmark positions of either RASIS or LASIS changes along caudal-cranial axis by 10 mm and 20 mm respectively. So the error will be larger if it occurs on a small pelvis.

In addition, for the large size APP (APP3), t = 290 mm, and p = 10 mm and 20 mm, then θ_{APP} = 2^0 and 4^0 respectively, resulting deviations of ± 2^0 and ± 4^0 of the inclination angles respectively. Hence, error will be smaller if it occurs on larger pelvis.

Therefore, it is recommended that, changing the landmark positions of RASIS and LASIS along caudal-cranial axis, deviates APP resulting deviations on inclination angle. However, above landmarks' change along medial-lateral axis do not affect to deviate either anteversion or inclination angles. When similar changes occur at the landmark position of PS do not change anteversion or inclination angles. Therefore, care should be taken when registering the anatomical landmarks at ASIS to avoid the deviations along caudal- cranial axis.

During the surgical navigation process, orientation of the reference tracker can be changed accidentally. This changes the cup position reference (APP), resulting in incorrect anteversion and inclination angles. Reference tracker was tilted during APP registration only and then it was taken back to the neutral position to register other data. Then, new acetabular angles were observed. Reference tracker was tilted in anterior-posterior and medial-lateral axes until it reaches to ± 15^0. If the reference tracker tilts more than ± 15^0, it is no longer within the camera visible region. Tilting of ± 3^0 of the reference tracker deviate the anteversion angle by ± 3^0, and tilting of ± 15^0 of the reference tracker deviate the anteversion angle by up to ± 12^0. This reference tracker tilt causes to vary the anatomical landmark coordinates in the Z axis (which is defined by the cross product of longitudinal axis and transverse axis) compare to their initial coordinates at neutral position. Anteversion angle calculation depends more on the Z axis variation compare to the inclination angle.

At the same time inclination angle deviates slightly, when reference tracker tilts along anterior, medial and lateral directions, and when it tilts only in the posterior direction, inclination angle deviates considerably. A possible reason behind this observation is, when the reference tracker tilts along posterior direction, reference tracker stays away from effective camera visible region.

It is clearly seen that, acetabular angle results can be significantly changed, if, the reference tracker moved accidentally during the navigation procedure. In such condition, APP should be re-registered from the beginning or tracker should be placed back where it was at the beginning. In this instance, inclination angle can be trust, but be sceptical of the anteversion angle.

All the experiments were conducted with a calibrated pelvic phantom model. OrthoPilot data were compared against the gold standards of the VICON system. All the OrthoPilot data produce comparable results to the VICON data and calibrated pelvic phantom model data. This shows that OrthoPilot data capturing process is highly accurate and repeatable in engineering point of view.

5.4 Future Work

This study was carried out to check the accuracy of the APP registration during cup only navigation. However, registration of the trial cup axis is another main factor to be concerned during the cup navigation process. The accuracy of trial cup registration can be achieved by introducing known errors to cup axis and keeping APP unchanged. The clinical importance of this work is anteversion and inclination angles resulted at the end of the trial cup registration going to be used in the reamer navigation and final cup navigation processes. Therefore, precise trial cup registration is essential. For this work, same pelvic phantom model can be used with a grid of peg points at the surface of the acetabular face. Difference peg points can be selected with known error inputs from the grid and deviation of the acetabular angles can be observed.

During this study, radiographic definition of the acetabular orientation was examined. However, OrthoPilot is used to measure acetabular angles for anatomical and operative definitions. Same experimental procedure used above can be applied to check accuracy of the acetabular orientation for anatomical and operative definitions. In this situation, angle calculation algorithm used for VICON data should be changed

according to the anatomical and operative definitions. Angles should only be measured for the neutral position of the APP. It is expected to observe similar acetabular angle deviations due to the APP variation, as observed for the radiographic definition of the angle calculation.

This study was carried out for the cup only navigation. Similar procedure can be applied to validate the OrthoPilot based femoral navigation process in engineering point of view. For that, modification should be introduced to the pelvic phantom which was used during this study. In addition, calibrated femoral phantom should be made to attach to the pelvic phantom. Experiments can be organized to measure some femoral parameters like leg length and femoral diameter.

Chapter 6

CONCLUSIONS

The final chapter is dedicated to discuss the conclusion of the research. Data from both OrthoPilot and VICON systems were captured under the same laboratory conditions using the calibrated pelvic phantom model with passive trackers to perform this research. According to the tabulated results shown in the chapter 4, several conclusions can be highlighted as follows.

- From the results obtained by tilting the APP, it is clearly seen that, the acetabular angles results can be significantly affected, if, the reference tracker was moved accidentally during the navigation procedure (anterior-posterior or medial-lateral). In such condition, APP should be reregistered from the beginning. In this instance, the inclination angle can be trusted, but it could be in error in the anteversion angle.

- An error in ASIS landmark palpation in excess of 10mm along caudal / cranial direction leads to considerable deviations of the acetabular orientation. Therefore, it is advisable to avoid possible errors in pointer palpations along caudal-cranial directions and care should be taken to palpate the exact anatomical landmark, especially with a small size pelvis.

- It is clear that the distances obtained from the OrthoPilot are within ±1mm to those obtained from the gold standard VICON system and the accurately measured distances of the phantom. Also, small standard deviations of less than 1% of actual value illustrate the precision of data capturing. This concludes that, the OrthoPilot data capturing is accurate and repeatable.

- Acetabular angles obtained from the OrthoPilot are within the $\pm 1^0$ to those obtained from the VICON and the accurately measured phantom angles, when the APP was exactly on *RASIS*, *LASIS* and *PS*. Also, with small standard deviations of less than 1% of actual value. These findings conclude that, the OrthoPilot cup navigation algorithm produces accurate and repeatable results under non- clinical laboratory conditions on a pelvic phantom.

From the above-mentioned concluding remarks, it can be ultimately concluded that data palpation from OrthoPilot system and acetabular angle calculation algorithm, if used correctly, for the radiographic definition of the acetabular alignment using passive trackers, are sufficiently accurate enough for the real world clinical applications.

BIBLIOGRAPHY

1. Crowe J.F, Mani V. J, Ranawat C S, (1979), Total hip replacement in congenital dislocation and dysplasia of the hip, J Bone Joint Surg, pp. 61:15-23.
2. Dandy D. J and Edwards D. J., (2003), Essential Orthopaedics and Trauma. 3rd ed. Churchill Livingston, Oxford, UK. ISBN 0443072132
3. DiGioia A.M, Simon D.A, Jaramaz B, Blackwell M, Morgan F.M, Colgan R.D, (1998), Intraoperative measurement of pelvic and acetabular component alignment using an image guided navigational tool. Trans Orthop Res Soc. 23:198
4. DiGioia III A.M, , Jaramaz B, Plakseychuk A. Y, Moody J. E, Nikou C, LaBarca R. S, Levison T. J, and Picard F, (2002), Comparison of a Mechanical Acetabular Alignment Guide With Computer Placement of the Socket. The Journal of Arthroplasty, Vol. 17 No. 3
5. Ecker T. M, Tannast M, Murphy S.B, (2007), Computed Tomography-based Surgical Navigation for Hip Arthroplasty, Clinical Orthopaedics And Related Research Number, pp. 100–105
6. Erhardt K (1995), Osteoarthritis in old age, Report of joint meeting of the sections of Geriatrics & Gerentology and Rheumatology & Rehabilitation. J. Rheumatology. Soc. Med. 88: 539 - 542.
7. Fender D, Harper W. M, Gregg P. J, (1999), Outcome of Charnley total hip replacement across a single health region in England, Journal of bone and joint surgery, 81-B(4): 577 - 581.
8. Frankel S, Eachus J, Pearson N, Greenwood R, Chan P, Peters T.J, Donovan J, Smith G. D, Dieppe P, (1999), Population requirements for primary hip replacement surgery: a cross sectional study, The Lancet, 353(9161): 1304 - 1309.
9. Herberts P and Malchau H, (2000), Long-term registration has improved the quality of hip replacement. A review of the Swedish Total Hip Replacement registers comparing 160,000 cases. Acta. Orthop. Scan. 71(2): 111 - 121.

10. Jaramaz B, DiGioia III A.M., Blackwell M, Nikou C, (1998), Computer assisted measurement of cup placement in total hip replacement. Clinical Orthopaedics Relatated Research, 354:70–81
11. Kalteis T, Handel M, Bäthis H, Perlick L, Tingart M, Grifka J, (2006), Imageless navigation for insertion of the acetabular component in total hip arthroplasty, J Bone Joint Surg Brit Med;88-B:163-167
12. Kelley T.C and Swank M. L, (2009), Role of Navigation in Total Hip Arthroplasty, J Bone Joint Surg, volume 91-A
13. Kennedy J.G, Rogers W.B, Soffe K.E, Sullivan R.J, Griffen D.G, Sheehan L.J. (1998), Effect of acetabular component orientation on recurrent dislocation, pelvic osteolysis, polyethylene wear, and component migration. Journal of Arthroplasty. 13:530-4
14. Kiefer H, (2003), OrthoPilot cup navigation – How to optimize cup positioning, International Orthopaedics (SICOT) , 27 (Suppl.1):S37–S42
15. Langlotz U, Gru¨tzner P A, Bernsmann K, Kowa J H, Tannast M, Caversaccio M, Nolte4 L-P, (2007), Accuracy considerations in navigated cup placement for total hip arthroplasty, Proc. IMechE Vol. 221 Part H: J. Engineering in Medicine, pp 739-753
16. Lee Y. S and Yoon T. R, (2008), Error in acetabular socket alignment due to the thick anterior pelvic soft tissues, The Journal of Arthroplasty Vol. 23 No. 5, pp 699-705
17. Lewinnek G.E, Lewis J.L, Tarr R, Compere C.L, Zimmerman J.R, (1978), Dislocations after total hip-replacement arthroplasties. J Bone Joint Surg Am 60:217–220.
18. Liaw C. K, Yang R. S, Hou S.M, Wu T.Y, Fuh C. S, (2008), A simple mathematical standardized measurement of acetabulum anteversion after total hip arthroplasty. Computational and Mathematical Methods in Medicine Vol. 9, No. 2,105–119.
19. Lin F, Lim D, Wixson R. L, Milos S., Hendrix R. W, Makhsous M, (2008), Validation of a computer navigation system and a CT method for determination of the orientation of implanted acetabular cup in total hip arthroplasty: A cadaver study, Clinical Biomechanics 23, pp1004–1011

20. Logishetty K, Bedi A, Ranawat A. S, (2010), The Role of Navigation and Robotic Surgery in Hip Arthroscopy, Operative Techniques in Orthopaedics, 20:255-263
21. Murray D.W (1993), The Definition and Measurement of Acetabular Orientation. J Bone Joint Surg, 75-B: 228-32.
22. Numair J, Joshi A. B, Murphy J. C, Porter M. L, Hardinge K, (1999), Total hip arthroplasty for congenital dysplasia or dislocation of the hip, Survivorship analysis and long-term results. J Bone Joint Surg Am, 79:1352–1360
23. RADIN E. L. (1980), Biomechanics of the Human Hip, Clinical Orthopedics and Research
24. Sugano N, (2003), Computer-assisted orthopedic surgery, Journal of Orthopaedic Science , The Japanese Orthopaedic association 8:442–448
25. Świątek-Najwer E, Będziński R, Krowicki P, Krysztoforski K, Keppler P, Kozak J, Improving surgical precision-application of navigation system in orthopedic surgery. Acta of Bioengineering and Biomechanics 2008; Vol. 10, No. 4.
26. Tran H. H, Matsumiya K, Masamune K, Sakuma I, Dohi1 T., Liao H, (2009), Interactive 3D Navigation System for Image-guided Surgery, The International Journal of Virtual Reality, 8(1): 9-16
27. Wolf A, DiGioia III A M, Mor A. B, Jaramaz B, (2005), Cup alignment error model for THA, Clinical orthopaedic and related research, Number 437, pp 132-137
28. www.brainlab.com/ hip-navigation-application
29. www.orthopilot.com
30. www.robodoc.com/pro_about_history.html
31. www.stryker.com
32. www.vicon.com
33. Ybinger T and Kumpan W, (2007), Enhanced acetabular component positioning through computer-assisted navigation, International Orthopaedics (SICOT), 31 (Suppl 1):S35–S38

PUBLICATIONS FROM THIS STUDY

11th Annual Meeting of the International Society for Computer Assisted Orthopaedic Surgery London, UK, June 15th to 19th 2011, Conference proceedings

Abstract ID 120
Accepted on 15th March 2011
Presented on 17th June 2011

Technical validation of the accuracy of measurement of pelvic planes and angles with a navigation system

ARACHCHI SMA[1], AUGUSTINE A[1], DEAKIN A[2], PICARD F[2], ROWE P[1]

[1]*Department of Bioengineering, University of Strathclyde, Glasgow, United Kingdom*
[2]*Golden Jubilee National Hospital, Clydebank, United Kingdom*

shanika.arumapperuma-arachchi@strath.ac.uk

Introduction: Computer assisted surgery is becoming more frequently used in the medical world. Navigation of surgical instruments and implants plays an important role in this surgery. OrthoPilot™ Hip Suite (BBraun Aesculap) is one such system used for hip navigation in orthopaedic surgery. However the accuracy of this system remains to be determined Independently of the manufactures. The manufacturers supply a technical specification for the accuracy of the system (+/- 2mm and +/- 2 deg) and previous research has been undertaken to compare its clinical accuracy against conventional hip replacements by X-ray. This clinical validation is important but contains many sources of error or deviation from an ideal outcome in terms of the surgeons' use of the system, inaccurate palpation of landmarks, variation in actual cup position from that given by the navigation system and measurement of the final cup position. It is therefore not possible to validate the claims of the manufacturer from this data. There is no literature evaluating the technical accuracy of the software i.e. the accuracy of the system given known inputs. This study had two main aims validating the accuracy of the OrthoPilot data while navigating the surgical instruments and validating the accuracy of navigation algorithm inside the OrthoPilot system which determines cup implant placement. The OrthoPilot validation was performed and compared against the gold standard of a VICON movement analysis system.

Data capturing accuracy: The system used was OrthoPilot™ with spectra camera from Northern Digital Inc. (Ontario, Canada). Software investigated was the Hip Suite THA cup only navigation software Version 3.1. The validation was performed and compared against the VICON Nexus version 1.4.116 with Bodybuilder software version 3.55. An aluminium phantom of a pelvis was machined with high accuracy. The OrthoPilot system has three types of instruments sets; passive, active and hybrid. This study was carried out with the passive instruments set. Data were captured simultaneously from both the OrthoPilot and VICON systems for the supine position of the phantom. Distances between the anatomical land marks on the phantom were compared to test the data capturing accuracy of the OrthoPilot system. Anatomical land marks of right anterior superior iliac supine (RASIS), left anterior superior iliac supine (LASIS) and Pubic Symphasis (PS) were palpated to define the Anterior Pelvic Plane (APP). Distances between the anatomical landmarks of RASIS to LASIS, RASIS to PS and LASIS to PS were considered for comparison. Using the phantom model three different APPs were considered with varying width and height (APP1, APP2, and APP3) and as shown in Figure 1. One hundred APP data sets were captured at each instance.

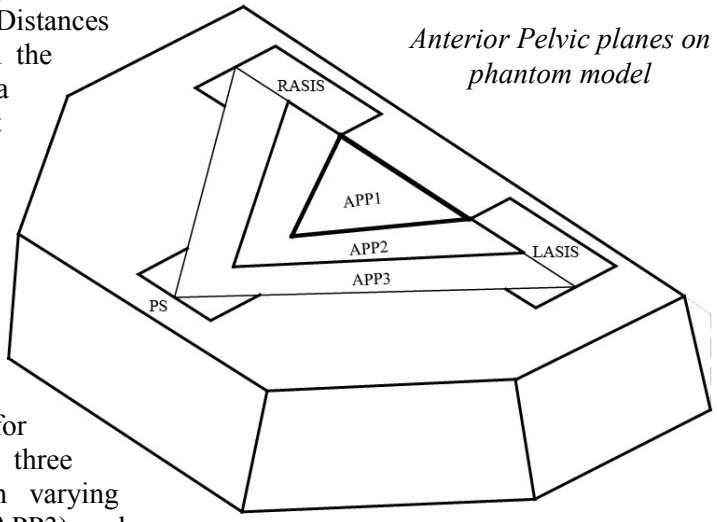

Anterior Pelvic planes on phantom model

Algorithm accuracy: The accuracy of the hip navigation algorithm was tested by applying similar algorithm to calculate the native anteversion and inclination angles of the acetabulum using the VICON system. Data were captured simultaneously from both OrthoPilot and VICON systems.

Radiographic anteversion and inclination angles were obtained with phantom model, which is built with 14 degrees of anteversion angle and 45 degrees of inclination angle. APP2 was used to obtain anterior pelvic plane data. Position vectors for each anatomical land mark from the OrthoPilot system were extracted from relevant transformation matrices, while position vectors from the VICON system were extracted from static trial modelling.

Results: The distance data from both systems were compared with calibrated distance data from the phantom model. Mean value of the distance between pairs of anatomical landmarks and the standard deviation values are shown in Table 1. It can be seen that the mean value of the distance between landmarks are almost identical and the standard deviations are less than 1% of the measured value.

APP types	Distance between anatomical land marks	Calibrated Phantom model data (mm)	VICON		OrthoPilot	
			Value (mm)	SD	Value (mm)	SD
APP 1	RASIS-LASIS	170	170.53	0.08	170.06	0.15
	RASIS-PS	102	102.45	0.09	103.97	0.14
	LASIS-PS	102	101.77	0.10	104.28	0.17
APP 2	RASIS-LASIS	230	231.14	0.11	230.10	0.19
	RASIS-PS	145	143.95	0.17	145.64	0.19
	LASIS-PS	145	144.62	0.09	145.95	0.34
APP3	RASIS-LASIS	290	290.46	0.09	290.39	0.42
	RASIS-PS	190	190.12	0.14	188.74	0.98
	LASIS-PS	190	189.36	0.21	188.67	0.54

Table 1: Distance comparison between anatomical land marks

Comparison was also made for the anteversion and inclination angles of the acetabulum of the pelvic model with OrthoPilot and VICON data. Results are presented in Table 2.

Data / Angle	Calibrated phantom model data	VICON Data		OrthoPilot	
	Value in deg	Value in deg	SD	Value in deg	SD
Anteversion angle	14	14.07	0.10	14.54	0.13
Inclination Angle	45	44.87	0.07	45.86	0.15

Table 2: Acetabular angle comparison

Again the mean value is close to the true value and the SD of the measures is less than 1%.

Conclusions: All the data were captured simultaneously from both OrthoPilot and VICON systems under the same laboratory conditions. According to the above results (Table1) it is cleared that the distance readings obtained from the OrthoPilot are almost comparable to the results obtained from the gold standard VICON system and the calibrated distance readings of the phantom. In addition, acetabular angle results obtained from OrthoPilot are almost equivalent to results obtained from VICON and the calibrated phantom angles. Finally it is can be concluded that, both the data palpation with OrthoPilot system and acetabular angle calculation algorithm of the OrthoPilot system are accurate enough for the real world clinical tasks they are expected to perform.

Acknowledgement: We would like to give our special thanks to Dr. Bruce Carse and the Golden Jubilee National Hospital for their kind support on this research.

References

1. E. Świątek-Najwer et al. Improving surgical precision-application of navigation system in orthopedic surgery. Acta of Bioengineering and Biomechanics Vol. 10, No. 4, 2008.
2. C. K. Liaw et al. A simple mathematical standardized measurement of acetabulum anteversion after total hip arthroplasty. Computational and Mathematical Methods in Medicine Vol. 9, No. 2, June 2008, 105–119.
3. D.W. Murray. The Definition and Measurement of Acetabular Orientation. The Journal of Bone and Joint Surgery 1993, 75-B: 228-32.

Engineers and Surgeons: Joined at the Hip III IMechE 1-3 November 2011-London, Event proceedings pp 75-78

Accepted on 10th August 2011
Presented on 2nd November 2011

Technical validation of the accuracy of the OrthoPilot cup navigation software- measurement of native acetabular alignment

S.M.A. Arachchi[1*], A. Augustine[1,2], A.H. Deakin[1,2], F. Picard[2], Philip Rowe[1]

[1]Bioengineering Unit, University of Strathclyde, Glasgow, United Kingdom
[2]Golden Jubilee National Hospital, Clydebank, United Kingdom

*shanika.arumapperuma-arachchi@strath.ac.uk

Keywords: Validation, APP, Anteversion angle, Inclination angle

Introduction: Computer assisted surgery is becoming more frequently used in the medical world. In arthroplasty navigation the instruments and implants play an important role in this surgery. OrthoPilot™ Hip Suite (BBraun Aesculap) is one such system used for hip navigation in orthopaedic surgery. However, the accuracy of this system remains to be determined independently of the manufacturers. According to the manufacturer's technical specification, the accuracy of the system is +/- 2mm and +/- 2 deg. Previous research has been undertaken to compare its clinical accuracy against conventional hip replacements by x-ray. This clinical validation is important; however, it contains many sources of error or deviation from an ideal outcome in terms of the surgeons' use of the system, inaccurate palpation of landmarks, variation in actual cup position from that given by the navigation system and measurement of the final cup position. It is, therefore, not possible to validate the claims of the manufacturer from this data. There is no literature evaluating the technical accuracy of the software, i.e. the accuracy of the system given known inputs. The main aims of this study were to validate the accuracy of the OrthoPilot data while navigating the surgical instruments and to validate the accuracy of navigation algorithm inside the OrthoPilot system which determines positioning of the implant cup. The OrthoPilot validation was performed and compared against the gold standard of a VICON motion analysis system.

Methodology: The system used for navigation was OrthoPilot™ with spectra camera from Northern Digital Inc. (Ontario, Canada). Software was the Hip Suite THA cup only navigation software Version 3.1. The validation was performed and compared against the VICON Nexus version 1.4.116 with Bodybuilder software version 3.55. An aluminium phantom of a pelvis was machined with high accuracy. The OrthoPilot system has three types of instruments sets; passive, active and hybrid and this study was carried out with the passive instruments set. Data were captured simultaneously from both the OrthoPilot and VICON systems for the supine position

of the phantom. Distances between the anatomical landmarks on the phantom were compared to test the data capturing accuracy of the OrthoPilot system. Anatomical landmarks of right anterior superior iliac supine (RASIS), left anterior superior iliac supine (LASIS) and Pubic Symphasis (PS) were palpated to define the Anterior Pelvic Plane (APP). Position vectors for each anatomical landmark from the OrthoPilot system were extracted from relevant transformation matrices, while position vectors from the VICON system were extracted from static trial modelling. The hip navigation algorithm accuracy was tested by applying similar algorithm to calculate the native anteversion and inclination angles of the acetabulum using the VICON system. Radiographic anteversion and inclination angles were obtained with phantom model, which is built with 14 degrees of anteversion angle and 45 degrees of inclination angle. Anteversion and inclination angles were obtained for different set ups, where the APP was changed from 3 degrees to 15 degrees by 2 degrees intervals in Medial-Lateral and Anterior-Posterior directions by the movement of the reference tracker as shown in Figure 01.

(a) (b)

Figure 01. Reference tracker variation in (a) anterior-posterior (b) medial-lateral directions

In addition, APP was changed in another way by varying the anatomical landmarks. One anatomical landmark was changed at a time, while keeping other two landmarks stationary. Each anatomical landmark was varied in the directions of Caudal-Cranial and Medial-Lateral as shown in the Figure 02. This method was performed with LASIS, RASIS and PS. Resulted angles were compared from both systems.

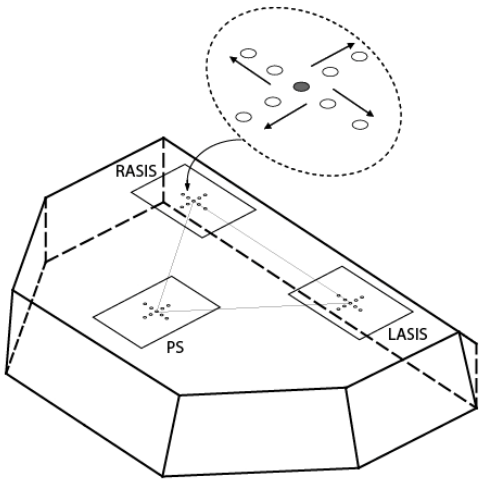

Figure 02. APP variation by changing the anatomical landmarks

Results and discussion: Acetabular angle results obtained from OrthoPilot are almost equivalent to the results obtained from gold standard VICON and the calibrated phantom angles when the APP was on the coronal plane without any inclinations. However, when the APP was changed in the directions of Medial-Lateral and Anterior-Posterior, OrthoPilot based acetabular angles have shown the deviation of 1-2 degrees compare to angle results obtained with VICON. Results for the mean angle values and standard deviation values are displayed in Table 01 and Table 02.

Table 01: Acetabular angle comparison for APP variations along Anterior-Posterior direction

		VICON data				OrthoPilot			
		Anteversion		Inclination		Anteversion		Inclination	
	Deg	Value (Deg)	SD	Value (Deg)	SD	Value (Deg)	SD	Value (Deg)	SD
Anterior	-15	3.04	0.09	44.90	0.16	2.61	0.38	44.11	0.13
	-13	4.39	0.07	44.94	0.45	4.10	0.16	44.55	0.10
	-11	5.75	0.07	44.32	0.44	5.62	0.11	44.78	0.22
	-9	7.12	0.08	44.55	0.38	6.95	0.44	45.10	0.26
	-7	8.51	0.09	44.78	0.52	8.26	0.30	44.91	0.36
	-5	9.92	0.10	45.12	0.25	9.61	0.24	45.00	0.38
	-3	11.33	0.10	45.48	0.52	11.46	0.10	45.37	0.25
Neutral	0	14.07	0.10	44.87	0.07	14.54	0.13	45.86	0.15
Posterior	3	15.55	0.11	46.45	0.36	15.28	0.24	46.46	0.23
	5	16.98	0.12	47.01	0.29	17.26	0.33	47.03	0.22
	7	18.38	0.12	47.62	0.35	17.81	0.34	46.94	0.29
	9	19.77	0.13	48.43	0.44	19.38	0.20	47.72	0.32
	11	21.10	0.16	48.58	0.46	20.58	0.19	48.18	0.49
	13	22.46	0.15	49.20	0.49	22.08	0.23	49.32	0.40
	15	23.80	0.15	49.54	0.50	23.59	0.10	49.68	0.32

Table 02: Acetabular angle comparison for APP variations along Medial-Lateral directions

		VICON data				OrthoPilot			
		Anteversion		Inclination		Anteversion		Inclination	
	Deg	Value (Deg)	SD	Value (Deg)	SD	Value (Deg)	SD	Value (Deg)	SD
Lateral	-15	1.32	0.22	46.66	0.31	2.32	0.29	47.55	0.28
	-13	2.61	0.24	46.59	0.19	3.51	0.19	47.18	0.31
	-11	4.51	0.31	46.37	0.29	5.13	0.26	47.13	0.29
	-9	6.25	0.29	46.42	0.29	6.55	0.27	46.72	0.30
	-7	8.29	0.11	46.5	0.30	8.25	0.24	46.75	0.32
	-5	9.48	0.34	46.33	0.29	9.78	0.31	46.89	0.22
	-3	11.20	0.21	46.04	0.21	10.97	0.09	46.18	0.18
Neutral	0	14.07	0.10	44.87	0.07	14.54	0.13	45.86	0.15
Medial	3	15.79	0.20	44.87	0.31	15.86	0.17	45.21	0.36
	5	18.47	0.22	44.76	0.37	17.10	0.16	44.83	0.22
	7	20.20	0.21	44.6	0.34	18.96	0.44	44.54	0.19
	9	21.60	0.30	44.74	0.26	20.33	0.35	44.18	0.28
	11	23.49	0.29	44.64	0.34	21.39	0.27	43.72	0.31
	13	25.13	0.33	44.66	0.34	22.88	0.42	43.09	0.41
	15	26.59	0.25	44.67	0.33	24.69	0.29	42.47	0.19

When changing the anatomical landmarks in the directions of Caudal-Cranial and Medial-Lateral have shown the deviation of 1-2 degrees compare to the VICON angles. Mean values and standard deviation values of the resulted angles are displayed in Table 03.

Table 03: Acetabular angle comparison for APP variations –Changing anatomical landmark position

Changing Landmark	Varing direction	Variation from exact position (mm)	VICON				OrthoPilot			
			Anteversion		Inclination		Anteversion		Inclination	
			Value (deg)	SD	Value (deg)	SD	Value (deg)	SD	Value (deg)	SD
RASIS	Caudal	-20	14.10	0.12	40.03	0.33	14.88	0.40	40.65	0.38
		-10	14.31	0.27	43.07	0.24	13.66	0.47	43.57	0.31
		0	14.07	0.1	44.87	0.07	14.54	0.13	45.86	0.15
		10	14.00	0.28	47.80	0.16	13.79	0.41	48.21	0.37
		20	14.00	0.23	49.15	0.26	13.99	0.39	50.54	0.47
	Medial	-20	14.07	0.13	45.16	0.27	13.57	0.14	45.88	0.23
		-10	14.10	0.12	44.90	0.16	13.63	0.31	45.10	0.36
		0	14.07	0.1	44.87	0.07	14.54	0.13	45.86	0.15
		10	14.16	0.26	44.66	0.04	13.71	0.16	45.32	0.25
		20	14.15	0.22	44.98	0.15	13.63	0.40	45.41	0.25
LASIS	Caudal	-20	14.16	0.14	50.52	0.25	14.36	0.30	49.54	0.27
		-10	13.77	0.19	48.35	0.31	14.15	0.10	47.95	0.30

		0	14.07	0.1	44.87	0.07	14.54	0.13	45.86	0.15
		10	14.23	0.19	43.45	0.27	14.14	0.33	43.18	0.28
		20	14.11	0.19	41.19	0.27	14.31	0.14	40.64	0.30
	Medial	-20	13.73	0.20	44.77	0.18	14.13	0.25	45.75	0.25
		-10	13.41	0.20	45.06	0.31	14.22	0.24	46.04	0.22
		0	14.07	0.1	44.87	0.07	14.54	0.13	45.86	0.15
		10	13.73	0.23	45.56	0.29	13.62	0.42	45.46	0.21
		20	13.97	0.24	45.81	0.12	14.42	0.17	45.65	0.38
PS	Caudal	-20	14.15	0.17	46.19	0.35	13.68	0.37	45.97	0.30
		-10	13.32	0.21	45.55	0.27	13.55	0.14	46.26	0.21
		0	14.07	0.1	44.87	0.07	14.54	0.13	45.86	0.15
		10	13.66	0.14	45.52	0.12	13.45	0.22	46.00	0.30
		20	13.44	0.17	45.79	0.23	13.07	0.12	45.95	0.20
	Medial	-20	14.13	0.18	45.58	0.17	14.17	0.16	45.25	0.16
		-10	13.84	0.28	44.71	0.12	14.46	0.24	45.07	0.43
		0	14.07	0.1	44.87	0.07	14.54	0.13	45.86	0.15
		10	14.00	0.21	44.90	0.18	13.43	0.41	45.66	0.26
		20	14.13	0.18	45.58	0.17	14.47	0.16	45.25	0.16

Conclusions: Acetabular angle results obtained from OrthoPilot are almost equivalent to the results obtained from VICON and the calibrated phantom angles when APP lies on the exact RASIS, LASIS and PS. However, when APP changes in anterior-posterior or medial-lateral or caudal-cranial directions, resulted acetabular angle values from OrthoPilot deviates 1-2 degrees from VICON angle values. Finally, it can be concluded that, both the data palpation with OrthoPilot system and acetabular angle calculation algorithm of the OrthoPilot system are accurate enough for the real world clinical tasks they are expected to perform.

Abstract for British Journal of Bone and Joint Surgery, JBJS (in press)

Accepted on 24th May 2011

Technical Validation Of The Accuracy Of Measurement Of Pelvic Planes And Angles With A Navigation System

S.M.A. Arachchi, A. Augustine, A.H. Deakin, F. Picard, P.J. Rowe
Department of Bioengineering, University of Strathclyde, 106, Rottenrow, Glasgow, G4 0NW, UK

Computer assisted surgery is becoming more frequently used in the medical world. Navigation of surgical instruments and implants plays an important role in this surgery. OrthoPilot™ Hip Suite (BBraun Aesculap) is one such system used for hip navigation in orthopedic surgery. However the accuracy of this system remains to be determined independently of the manufacturer. The manufacturer supplies a technical specification for the accuracy of the system (± 2 mm and ± 2°) and previous research has been undertaken to compare its clinical accuracy against conventional hip replacements by x-ray. This clinical validation is important but contains many sources of error or deviation from an ideal outcome in terms of the surgeons' use of the system, inaccurate palpation of landmarks, variation in actual cup position from that given by the navigation system and measurement of the final cup position. It is therefore not possible to validate the claims of the manufacturer from this data. There is no literature evaluating the technical accuracy of the software i.e. the accuracy of the system given known inputs. This study had two main aims 1) validating the accuracy of the OrthoPilot data while navigating the surgical instruments and 2) validating the accuracy of navigation algorithm inside the OrthoPilot system which determines cup implant placement. The OrthoPilot validation was performed and compared against the gold standard of a VICON movement analysis system.

The system used was OrthoPilot™ with a Spectra camera from Northern Digital Inc. (Ontario, Canada). Software investigated was the Hip Suite THA cup only navigation software Version 3.1. The validation was performed and compared against the VICON Nexus version 1.4.116 with Bodybuilder software version 3.55. An aluminium pelvis phantom was used for measurement allowing accurate and repeatable inputs. The OrthoPilot system has three types of instruments sets; passive, active and hybrid. This study was carried out with the passive instruments set. Data were captured simultaneously from both the OrthoPilot and VICON systems for the supine position of the phantom. Distances between the anatomical land marks on the phantom were compared to test the data capturing accuracy of the OrthoPilot system. Anatomical land marks of right anterior superior iliac supine (RASIS), left anterior superior iliac supine (LASIS) and Pubic Symphasis (PS) were palpated to define the Anterior Pelvic Plane (APP). Distances between the anatomical landmarks of RASIS to LASIS, RASIS to PS and LASIS to PS were considered for comparison. Width and height of the pelvis was varied to examine different APPs. The width and height used were 170 mm and 53 mm, 230 mm and 88 mm, and 290 mm and 123 mm respectively. One hundred APP data sets were captured at each instance.

The accuracy of the hip navigation algorithm was tested by applying similar algorithm to calculate the native anteversion and inclination angles of the acetabulum using the VICON system. Data were captured simultaneously from both OrthoPilot and VICON systems. Radiographic anteversion and inclination angles were obtained with phantom model, which had 14° of anteversion angle and 45° of inclination angle. APP of 230 mm in width and 88 mm in height was used to obtain anterior pelvic plane data. Position vectors for each anatomical land mark from the OrthoPilot system were extracted from relevant transformation matrices, while position vectors from the VICON system were extracted from static trial modeling.

The distance data from both systems were compared with calibrated distance data from the phantom model. Mean values of the distances between anatomical landmarks were found to be similar for both OrthoPilot and VICON systems. In addition, these distances were comparable with the pelvic phantom model data, within 1 mm for all measured distances for the VICON and 2 mm for the OrthoPilot. Furthermore, the standard deviations were less than 1% of the measured value. Comparison was also made for the anteversion and inclination angles of the acetabulum of the pelvic model with OrthoPilot and VICON data. Both systems produced similar results for the mean angle values, within 0.5° of the known angles for the VICON and 1° for the OrthoPilot and with standard deviations of the measured values of less than 1%.

All the data were captured simultaneously from both OrthoPilot and VICON systems under the same laboratory conditions. According to the above results it is clear that the distance readings obtained from the OrthoPilot are comparable to the results obtained from the gold standard VICON system and the calibrated distance readings of the phantom. In addition, acetabular angle results obtained from OrthoPilot are almost equivalent to results obtained from VICON and the calibrated phantom angles. Finally it is can be concluded that, both the data palpation with OrthoPilot system and acetabular angle calculation algorithm of the OrthoPilot system are accurate enough for the real world clinical tasks they are expected to perform.

Journal paper for The Journal of Orthopaedic Surgery, (in the process of submission)

Validation of a CT free navigation system for the measurement of native acetabular alignment

S.M.A. Arachchi[1], A. Augustine[1,2], A.H. Deakin[1,2], F. Picard[2], Philip Rowe[1]

[1]Bioengineering Unit, University of Strathclyde, Glasgow, United Kingdom
[2]Golden Jubilee National Hospital, Clydebank, United Kingdom

Abstract:

Computer assisted surgery is becoming more frequently used in the medical world. The OrthoPilot™ Hip Suite CT-free navigation system (BBraun Aesculap) is one such computer assisted navigation system used for total hip replacement and total knee replacement surgery. The validity of the OrthoPilot system remains to be determined independent of the manufacturer. The main aims of this study were to validate the OrthoPilot data, while using the surgical instruments and to validate the cup navigation algorithm. The OrthoPilot was compared with the gold standard of a VICON movement analysis system. An aluminium pelvic phantom was machined with high accuracy to perform the experiments. Data were captured simultaneously from both OrthoPilot and VICON systems and acetabular angles were compared. Both systems produce comparable results for the distance between anatomical landmarks and acetabular angles. It can be concluded that data from the OrthoPilot system, if used correctly, are sufficiently accurate for orthopaedic applications.

Key words: navigation, validation, anteversion angle, inclination angle, Anterior Pelvic Plane

Main text

Introduction:

In the UK, approximately 15% of the female and 10% of the male population over the age of 65 have radiographic evidence of moderate to severe osteoarthritis of the hip joint **(1)**. According to Frankel et al **(2)**, 13-18 people per 1000 aged 35-85 years suffer from hip diseases which require surgery. Navigational techniques have been beginning used in hip implant surgery for a number of years **((3), (4), (5))**. Computer assisted navigation has the ability to measure implant alignment precisely during arthroplasty. Acetabular surface and bone preparation can be more precise, resulting in optimal acetabular cup alignment of 45^{o} of inclination and 20^{o} anteversion **(6)**. Computer assisted surgery systems claim to provide optimal implant positioning and minimize the risk of dislocation impingement and implant wear; hence increasing longevity **(5)**. In image-free navigation, implant alignment is based only on anatomical landmarks, palpated intra-operatively by the surgeon using a reference pointer **(7)**. This is also known as landmark based navigation.

OrthoPilot™ Hip Suite (BBraun Aesculap, Tuttlingen, Germany) is an image free kinematic navigation system used for hip navigation in orthopaedic surgery. The Orthopilot™ system is a leader in the field of computer assisted orthopaedic surgery (CAOS). According to the manufacturer's technical specification, the accuracy of the system is ±2mm and ±2°. However the accuracy of this system remains to be determined independently of the manufacturer. Previous research has been undertaken to compare its clinical accuracy against conventional hip replacements by x-ray and the OrthoPilot based hip replacements produce more accurate results compare to the conventional hip replacements (**(7), (8)**). This clinical validation is important; however it contains many possible sources of error or deviation from an ideal outcome in terms of the surgeons' use of the system, inaccurate palpation of landmarks, variation in actual cup position from that given by the navigation system and measurement of the final cup position. It is therefore not possible to validate the claims of the manufacturer regarding the accuracy of the system itself from this data. There is no literature evaluating the technical accuracy of the software i.e. the accuracy of the system given known inputs. The main aims of this study were to validate the accuracy of the OrthoPilot data while repeatedly identifying the anterior pelvic plane (APP) of a phantom and to validate the accuracy of the navigation algorithm inside this CT free system (OrthoPilot system) which determines the position of the native acetabulum and hence the implanted cup. The OrthoPilot validation was performed and compared against the gold standard of a VICON motion analysis system (Oxford metrics Ltd, Oxford, UK).

Materials and Methods:

The system assessed was the OrthoPilot™ navigation system with a Spectra camera from Northern Digital Inc. (Ontario, Canada). The software used was the Hip Suite THA cup only navigation software Version 3.1. The validation was performed and compared against the VICON Nexus version 1.4.116 with Bodybuilder software version 3.55 (Oxford metrics Ltd, Oxford, UK). Concurrent validity between the OrthoPilot and VICON was performed with a calibrated pelvic phantom model (Figure 1). This phantom model was made to imitate the average size of the human pelvis with the 14 degrees of anteversion and 45 degrees of anteversion (as determined by local analysis of pelvic CTs). These angle values were verified by the engineering measuring techniques after the block had been machined. The physical dimension of the phantom is explained as follows. The average distance between left and right anterior superior iliac supine was 230 mm. The distance between the mid point of anterior superior iliac spines and mid point of the pubic Symphysis was 90 mm. This phantom was machined with a lot of "peg" points around the exact landmark points of RASIS (Right Anterior Superior Iliac Spine), LASIS (Left Anterior Superior Iliac Spine) and PS Pubic Symphysis). The surrounded peg points were used when changing the landmarks points in different directions.

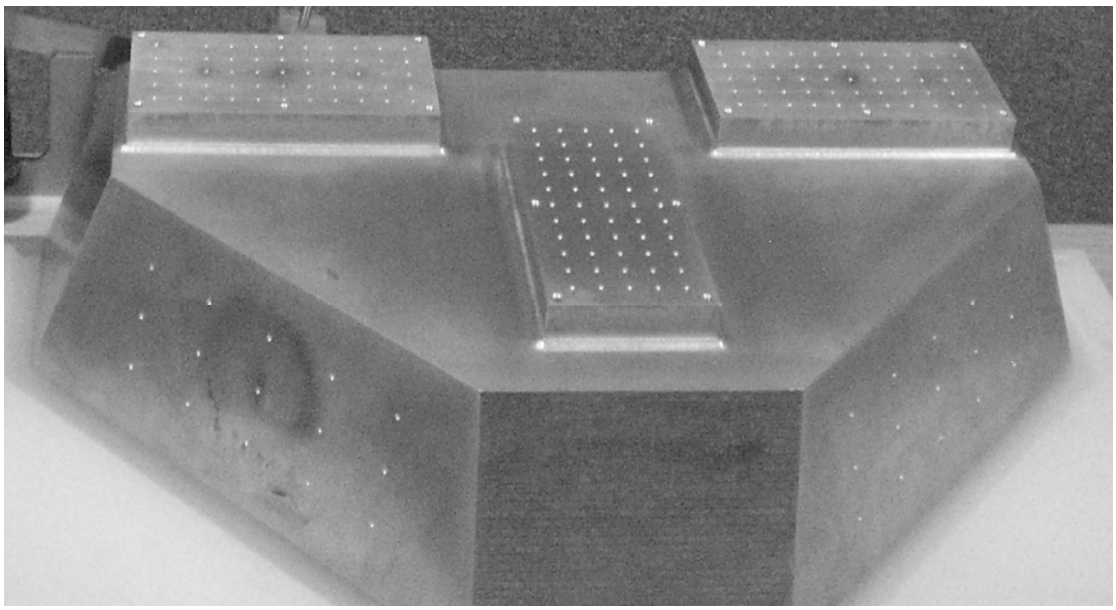

Figure 1 Pelvic Phantom model

This study was carried out with the passive instruments set consisting of two rigid bodies, each having 4 retro-reflective spheres on them in a unique arrangement that enabled the tracking and identification of each rigid body (tracker). One rigid body was used as a reference marker and the other attached to a pointer that was used to identify points in space. Pretended patient details, position during surgery, surgical approach and implant type were inputted at the beginning of the OrthoPilot navigation process to initiate the software. All the anatomical landmark data were captured by keeping the five conditions below unchanged through out the experiment; Patient's sex – female, Patient's position during the surgery – supine ,Surgical approach - right hand side anterior approach, Implant cup type - plasma cup, Diameter of the trial cup - 48 mm.

Anatomical landmarks of right anterior superior iliac spine, left anterior superior iliac spine and Pubic Symphysis were palpated to define the APP by following the OrthoPilot surgical navigation procedure. VICON data were captured for the same anatomical landmarks simultaneously. Data were captured by 12 VICON cameras and they were exported to static trial modeling. Static trial modeling was performed according to the program run by BodyBuilder software. After executing the program position coordinates of each landmark were stored. Distance data between the anatomical landmarks were captured simultaneously from both OrthoPilot and VICON systems for the "supine" position of the phantom (APP horizontal). Figure 11 in the appendix shows the experimental set up in detail. Each landmark bed was machined with several palpation points as seen in the Figure 1. This allowed the definition of different widths and heights of pelvis within the same phantom model. In addition, above-mentioned palpation procedures were followed for three different sizes of APPs. They were defined as APP1, APP2 and APP3 according to the width and height of the pelvis. They are shown in Figure. 2. RASIS-LASIS-PS landmarks were palpated 100 times for each APPs.

Distances between the landmarks on the phantom were compared to test the data capturing accuracy of the OrthoPilot system. Position vectors for each anatomical landmark from the OrthoPilot system were extracted from relevant transformation matrices, while position vectors from the VICON system were extracted from the data using BodyBuilder. The BodyBuilder program contained calculations of position coordinates of landmarks. Once executed it, calculated landmark coordinates in the global frame and these were stored in ASCII file format. Then, those coordinates were exported to Excel for the final calculations. For a single APP measurement each anatomical landmark was palpated once.

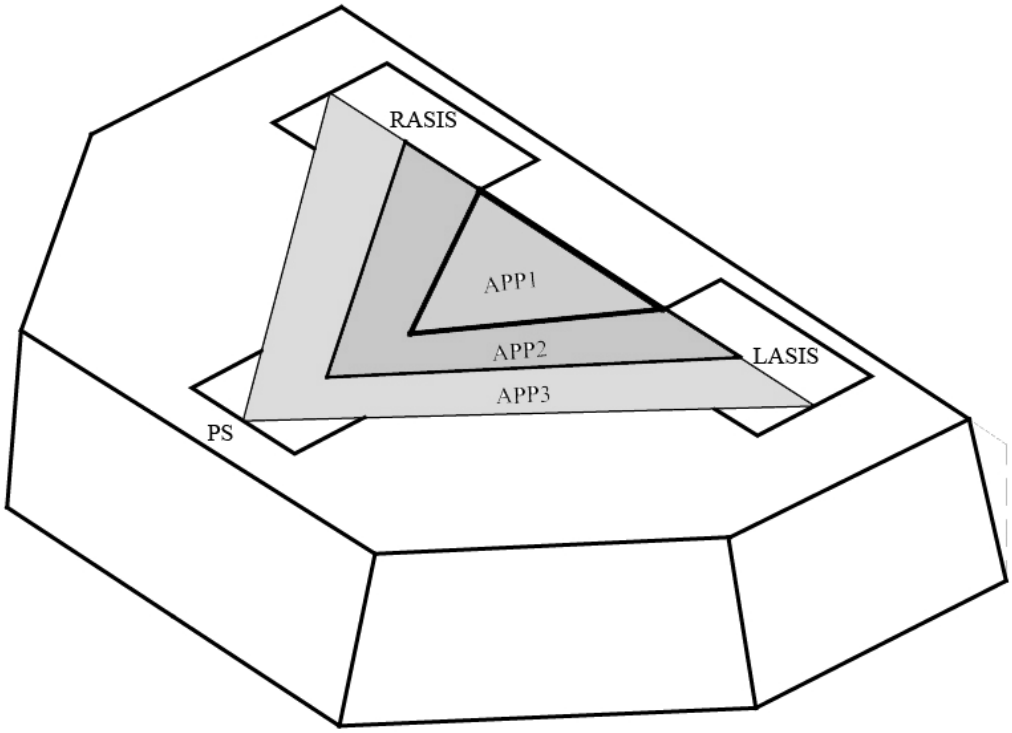

APP1 : *RASIS-LASIS* 170 mm, *RASIS-PS* 102 mm, *LASIS- PS* 102 mm
APP2 : *RASIS-LASIS* 230 mm, *RASIS-PS* 145 mm, *LASIS- PS* 145 mm
APP3 : *RASIS-LASIS* 290 mm, *RASIS-PS* 190 mm, *LASIS- PS* 190 mm
Figure 2 Anterior Pelvic Planes on Phantom model

The cup navigation algorithm accuracy was tested by unpicking the OrthoPilot algorithm and applying a similar algorithm to calculate the native anteversion and inclination angles of the acetabulum using the VICON system. In OrthoPilot surgical navigation procedure, initial step was the anatomical landmark palpation of the APP (RASIS, LASIS and PS), then, system records the deepest point of the acetabular. Next step was the trial cup registration, where, it recorded the acetabular cup axis. With this acetabular cup axis data and the APP data, acetabular angles were calculated for the native acetabulum. Angle calculation algorithm is as shown in the Appendix. Initially, orientation of the native acetabulum was obtained on multiple occasions without varying the APP, by using APP2 shown in the Figure 2 (the mid size APP).
Then, the APP was changed by varying the anatomical landmarks in the coronal plane. One anatomical landmark was changed at a time, while keeping the other two

landmarks the same. To do this the surgical tool was moved in the Caudal / Cranial, and Medial / Lateral directions to the adjacent machined hole (Figure 3). There was no vertical movement (anterior -posterior) of the tool. First the *RASIS* was moved from its original position along the lateral direction by 10 mm, while leaving *LASIS* and *PS* stationary. At the next stage, *RASIS* was moved by 20 mm. Subsequently, the same procedure was followed for the *RASIS* in the medial direction. Then caudal and cranial displacements of 10 mm and 20 mm were applied again, while keeping the *LASIS* and the *PS* stationary. This procedure was repeated for the *LASIS* and *PS* while again keeping the other two landmarks stationary.

Figure 3 Landmark variations

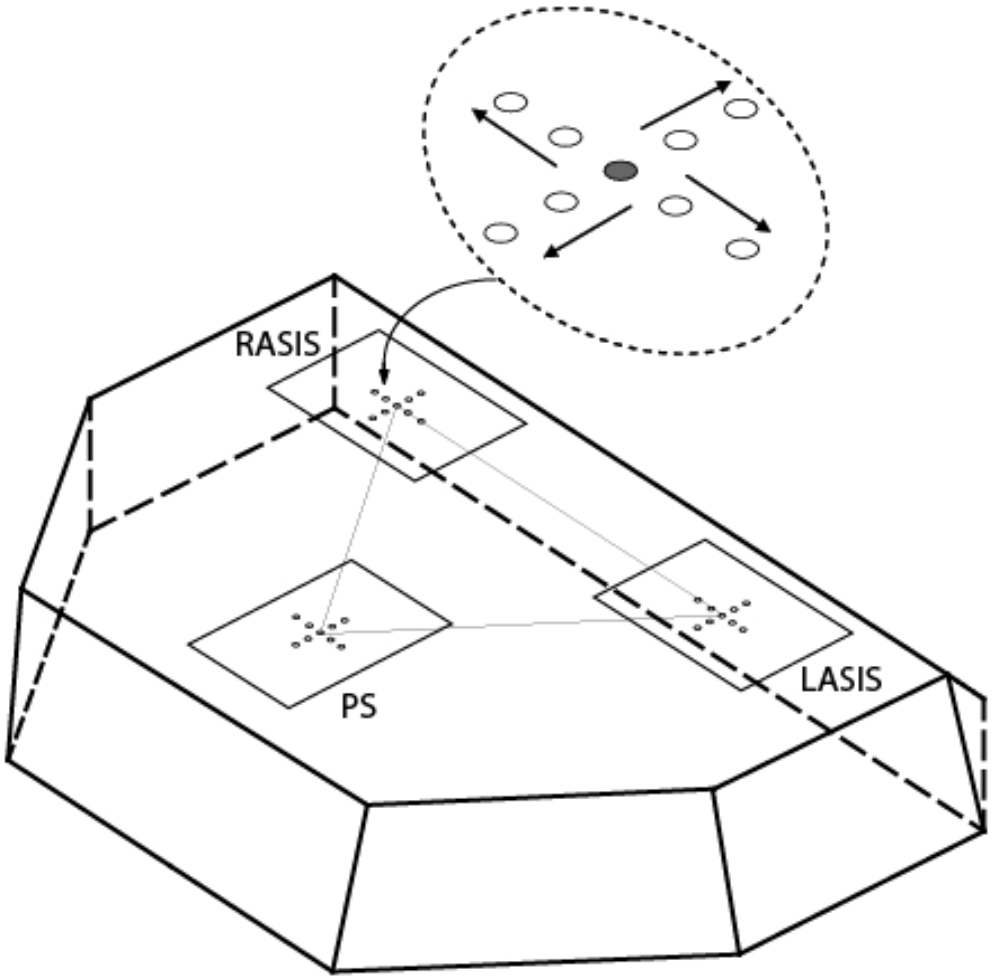

Results

Table 1 Distance comparison between anatomical landmarks of RASIS-LASIS, RASIS-PS and LASIS-PS

APP types	Distance between anatomical landmarks	Phantom model data (mm)	VICON		OrthoPilot	
			Mean Value (mm) n=100	SD	Mean Value (mm) n=100	SD
APP 1	*RASIS-LASIS*	170	171	0.08	170	0.15
	RASIS-PS	102	102	0.09	104	0.14
	LASIS-PS	102	102	0.10	104	0.17
APP 2	*RASIS-LASIS*	230	231	0.11	230	0.19
	RASIS-PS	145	144	0.17	146	0.19
	LASIS-PS	145	145	0.09	146	0.34
APP3	*RASIS-LASIS*	290	290	0.09	290	0.42
	RASIS-PS	190	190	0.14	189	0.98
	LASIS-PS	190	189	0.21	189	0.54

The distances between landmarks from both OrthoPilot and VICON systems were compared with the calibrated distances from the phantom model. Mean value of the distances between pairs of anatomical landmarks and their standard deviations are shown in Table 1. It can be seen that the mean value of the distance between landmarks were almost identical between systems and when compared to the phantom. The standard deviations are less than 1% of the measured value and less than 1 mm in all cases.

Table 2 Acetabular angle comparison

Data / Angle	Phantom model data	VICON system		OrthoPilot system	
	Value (deg)	Mean Value (deg) n=100	SD	Mean Value (deg) n=100	SD
Anteversion angle	14	14.07	0.10	14.54	0.13
Inclination Angle	45	44.87	0.07	45.86	0.15

Comparison was also made for the anteversion and inclination angles of the acetabulum of the pelvic model. Measurements of the anteversion and inclination angles produced by both systems are very similar to the calibrated values (Table 2). More importantly the standard deviations (SD) of the angle values are less than 1% of the phantom values.

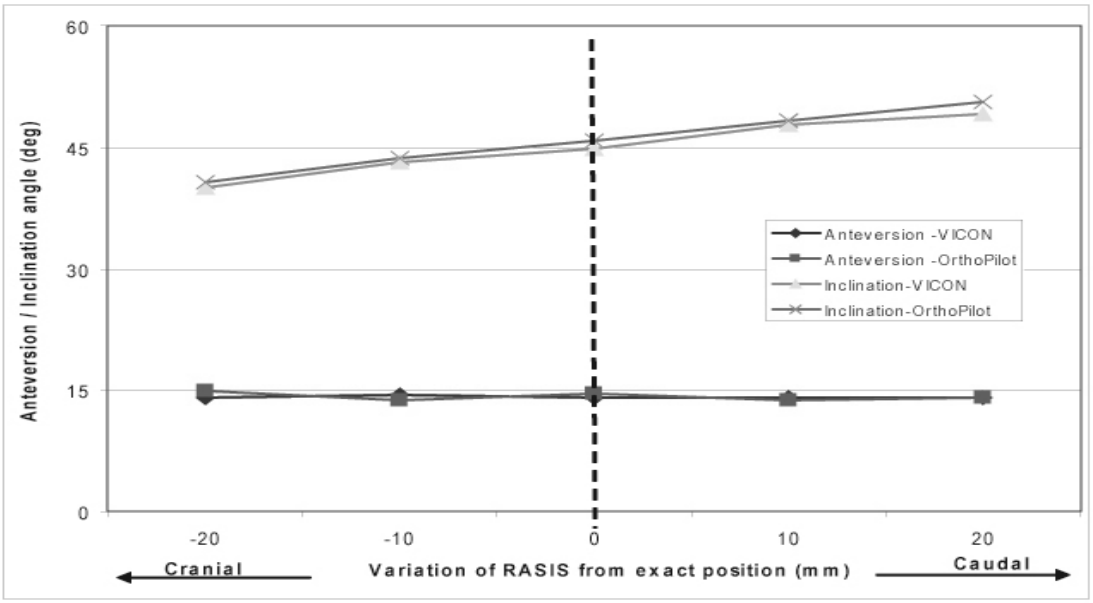

Figure 4. Graphical representation of the acetabular angle variation when RASIS changes along Caudal and Cranial directions

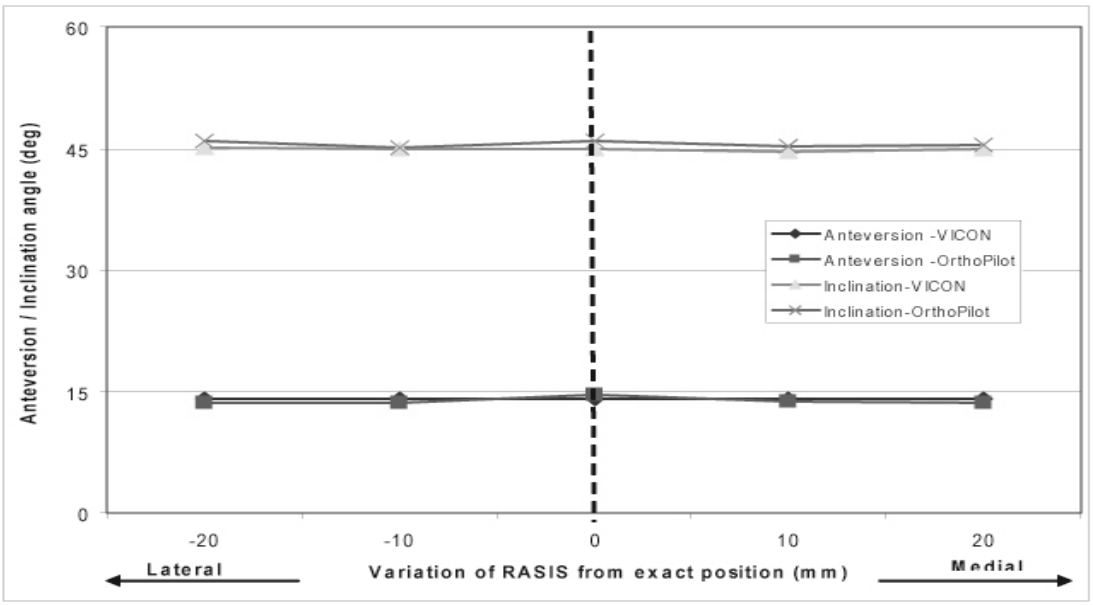

Figure 5. Graphical representation of the acetabular angle variation when RASIS changes along Medial and Lateral directions

When the landmark position of the *RASIS* varied along the caudal and cranial directions by 10 mm and 20 mm (Figure 4), the inclination angle deviated considerably compare to the inclination angle value of the pelvic phantom, when the APP was exactly on *RASIS*, *LASIS* and *PS*. No such deviation in anteversion angle was observed. Moving the *RASIS* towards the caudal direction increased the inclination angle significantly, while the anteversion angle remained unchanged. When landmarks moved in the cranial direction, inclination angle significantly decreased, but the anteversion angle was unchanged. When, the position of *RASIS*

moves along the medial or lateral directions, both anteversion and inclination angles did not change as shown in Figure 5.

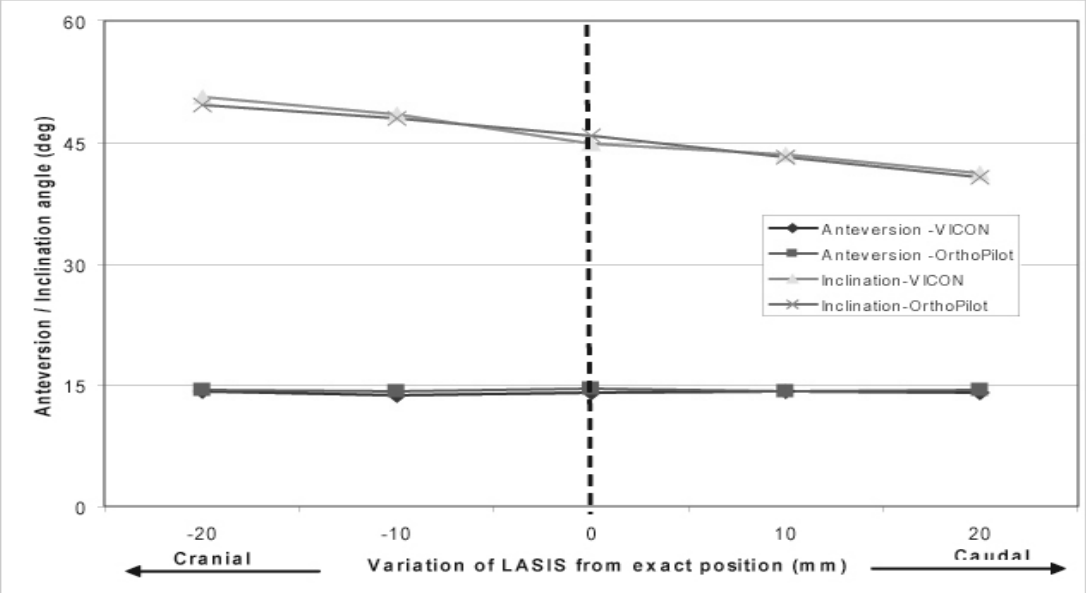

Figure 6 Graphical representation of the acetabular angle variation when LASIS changes along Caudal and Cranial directions

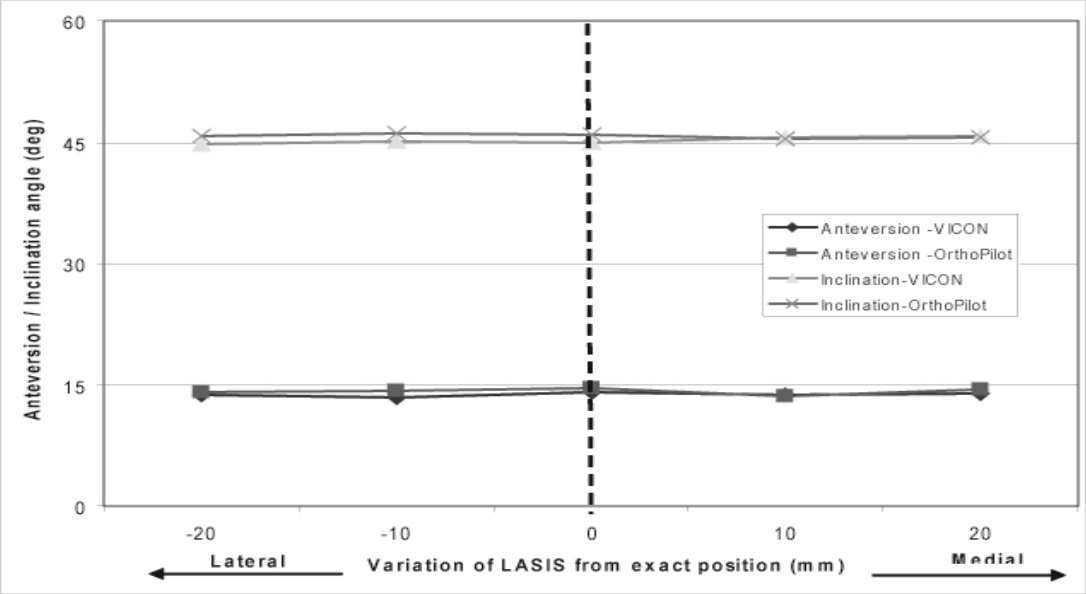

Figure 7. Graphical representation of the acetabular angle variation when LASIS changes along Medial and Lateral directions

When the *LASIS* was moved in the caudal/ cranial directions again the inclination angle changed considerably from its original value, but with no deviation in anteversion angle (Figure 6). Moving the *LASIS* towards the caudal direction decreased the inclination angles significantly. Moving in the cranial direction increased the inclination angle. In addition, no significant changes occur in

anteversion or inclination angles when LASIS moved along the medial and lateral axes as seen in Figure 7.

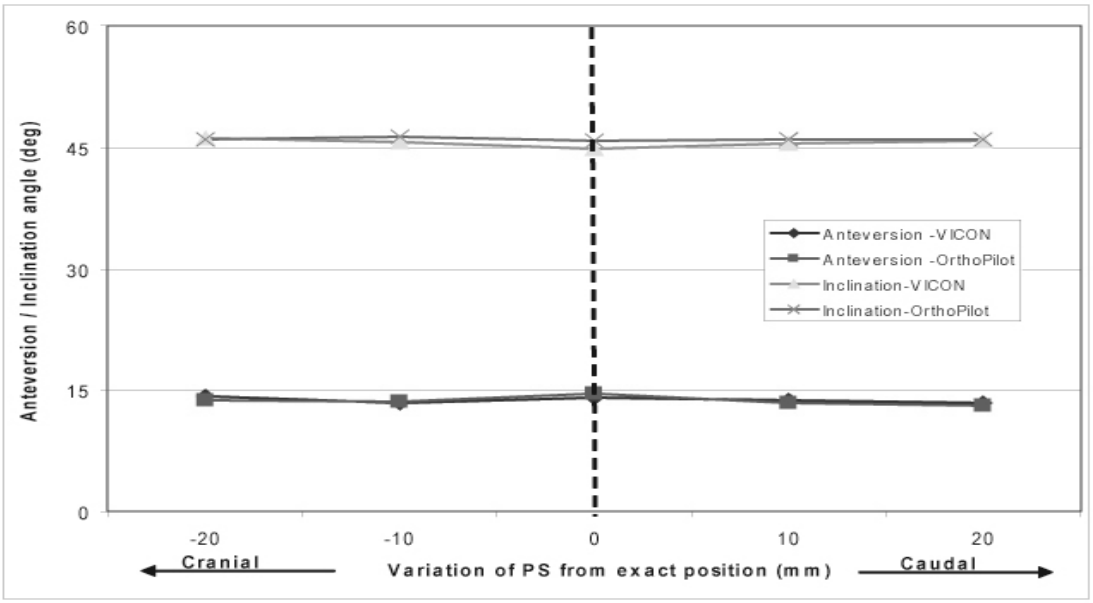

Figure 8. Graphical representation of the acetabular angle variation when PS changes along Caudal and Cranial directions

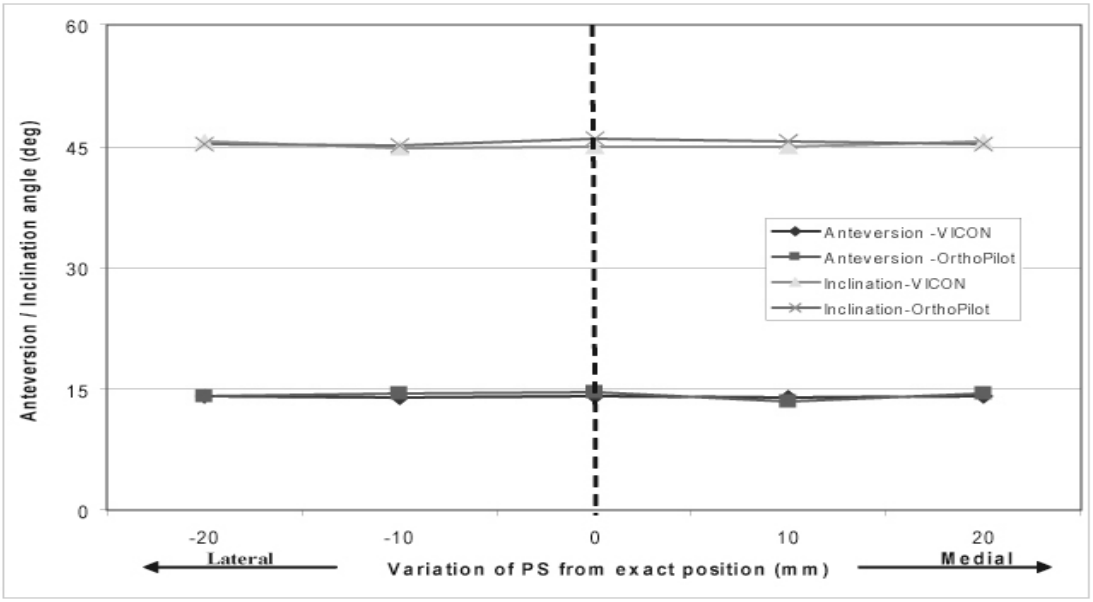

Figure 9. Graphical representation of the acetabular angle variation when PS changes along Medial and Lateral directions

When the landmark position of PS changes along the caudal and cranial axis (Figure 8) or the medial and lateral axis (Figure 9), little change in inclination and anteversion angle were observed.

The inclination angle deviation observed, due to the landmark changes at the LASIS and RASIS along caudal/cranial direction can be explained as reference to the figure 10.

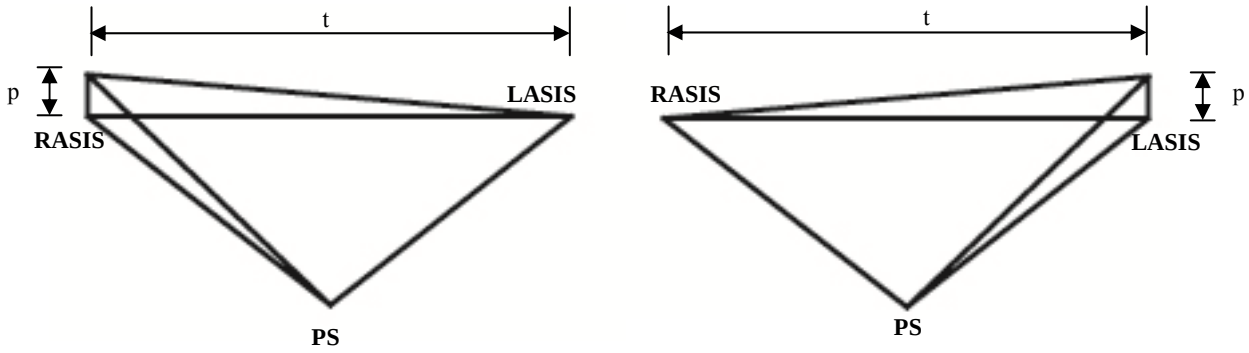

Figure 10. APP variations, (a) when changing the landmark of RASIS along caudal and cranial direction, (b) when changing the landmark of LASIS along caudal and cranial direction.

If the APP changes with an angle (θ_{APP}), then $\theta_{APP} = \tan^{-1}(\frac{p}{t})$. When p = 10 mm and t = 230 mm, $\theta_{APP} = 3^0$. This means, inclination angle also changes by ± 3^0 when either LASIS or RASIS position changes by 10 mm in the caudal- cranial axis. Similarly, when p = 20mm $\theta_{APP} = 5^0$ and inclination angle changes by ± 5^0. The above-observed relationship can be expressed as; the APP changing angle equals to the amount of deviation of the inclination angle.

If, the small size APP (APP1) is taken for the above condition, when t = 170 mm and p = 10 mm and 20 mm, then $\theta_{APP} = 4^0$ and 7^0 respectively. In addition, for the large size APP (APP3), t = 290 mm, and p = 10 mm and 20 mm, then $\theta_{APP} = 2^0$ and 4^0 respectively.

Discussion

This research study was conducted to validate the accuracy of a CT free navigation system (OrthoPilot hip navigation) process from an engineering point of view. According to the manufacturer's technical specification, the accuracy of the system is defined as ± 2mm and ± 2^0. The accuracy of this system required to be determined independently of the manufactures. The clinical validation contains many sources of error or deviation from an ideal outcome in terms of the surgeons' use of the system, inaccurate palpation of landmarks, variation in actual cup position from that given by the navigation system and measurement of the final cup position. Small deviations in locating landmarks can lead to significant errors for anatomical reference frames, therefore, the degree of point registration accuracy plays considerably important role in different surgical steps **(9)**. For an example, in APP registration, a 20mm deviation of the exact landmark position of RASIS or LASIS along caudal - cranial direction can leads to deviate the inclination angle by 5^0 for average size APPs. This inclination angle deviation a can be further increased with small size APPs. It is therefore not possible to validate the claims of the OrthoPilot manufacturer about the accuracy of the system easily from this data. Therefore, it is important to evaluate the

technical accuracy of the system i.e. the ability of the system to measure known inputs.

Data for the distance between the anatomical landmarks were within the range of ± 2 mm to the exact distance reading. All the distance results were observed to have small standard deviations. Small standard deviations represent the precision of the OrthoPilot results. According to the OrthoPilot manufacture's technical specification distance accuracy is ± 2 mm and was verified with the distance data recorded. Therefore, it can be stated here that the OrthoPilot instrument position data are accurate and repeatable enough for the real world surgical operations.

Data for the acetabular angles were within the range of $\pm 1^0$ to the exact acetabular angle readings of the pelvic phantom. All these results were observed with small standard deviations by representing the precision of the OrthoPilot results. According to the OrthoPilot manufacture's technical specification angular accuracy is $\pm 2^0$ and which is verified by the experimental results. Therefore, it can be stated here that the Cup navigation algorithm produces accurate and repeatable angle results.

The results from this study shows that errors introduced during landmark palpation can have a substantial effect on the final cup orientation and hence on impingement, dislocation, wear and loosening **(10)**. Lee et al (2008) discussed the acetabular angle errors introduced due to fat tissue thickness. Fat tissue thickness introduces coordinates errors mainly in the anterior axis **(11)**. However, this aside, errors can be introduced with incorrect landmark registration due to deviation of the exact anatomical landmark in the coronal plane. These factors may cause the surgeon to position the implant incorrectly. This can be clearly seen from the acetabular angles we recorded, when varying the anterior pelvic plane in the coronal plane. Therefore, changing the landmark positions of RASIS and LASIS along caudal-cranial axis deviate the APP resulting in deviations of the inclination angle. However, errors in the landmark position along the medial-lateral axis do not affect either anteversion or inclination angles to any measurable degree. When similar changes occur at the landmark position of PS, they do not change anteversion or inclination angles. Therefore, care should be taken when registering the anatomical landmarks at RASIS and LASIS to avoid deviations along the caudal- cranial axis.

Conclusions

It is cleared that the distances obtained from the OrthoPilot are almost comparable to them obtained from the gold standard VICON system and the calibrated distances of the phantom. Also, small standard deviations of less than 1% of actual value illustrate the precision of data capturing. This concludes that, the OrthoPilot data capturing is accurate and repeatable. Acetabular angles obtained from the OrthoPilot are almost equivalent to these obtained from the VICON and the calibrated phantom angles, when the APP was exactly on *RASIS*, *LASIS* and *PS*. Also, with small standard deviations of less than 1% of actual angle values, those are obtained for the acetabulum of the pelvic phantom. These findings conclude that, the OrthoPilot cup navigation algorithm produces accurate and repeatable results.

An error in ASIS landmark palpation in excess of 10mm along caudal / cranial direction leads to considerable deviations of the acetabular orientation. Therefore, it is advisable to avoid the possible excess pointer palpations along caudal-cranial directions and care should be taken to palpate the exact anatomical landmark, especially with the small size pelvis. From above mentioned concluding remarks, it can be ultimately concluded that data palpation from OrthoPilot system and acetabular angle calculation algorithm, if used correctly, are sufficiently accurate enough for the real world clinical applications.

Appendix

Experimental Set up

The experimental environment can be clearly visualized from the Figure 11. Both systems were under the same experimental conditions and capable of capturing the passive transmitters. The author was very careful in arranging both systems without disturbing each other, specially the VICON cameras. The pelvic phantom was positioned on a table in the supine position of the pelvic. In addition, the reference tracker was attached to a Goniometer and placed at the operated side of the pelvic phantom.

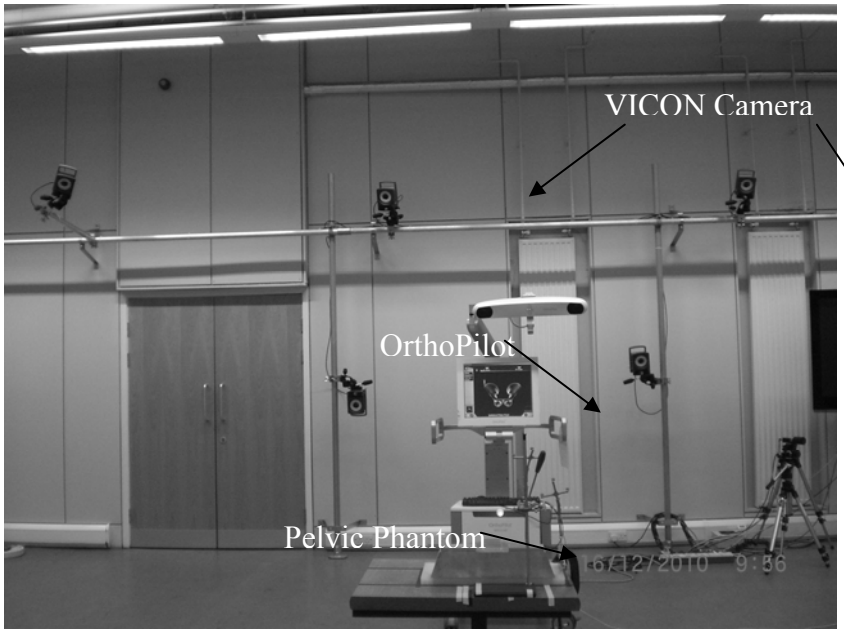

Figure 11 Simultaneous data recording from OrthoPilot and VICON systems

Angle calculation algorithm

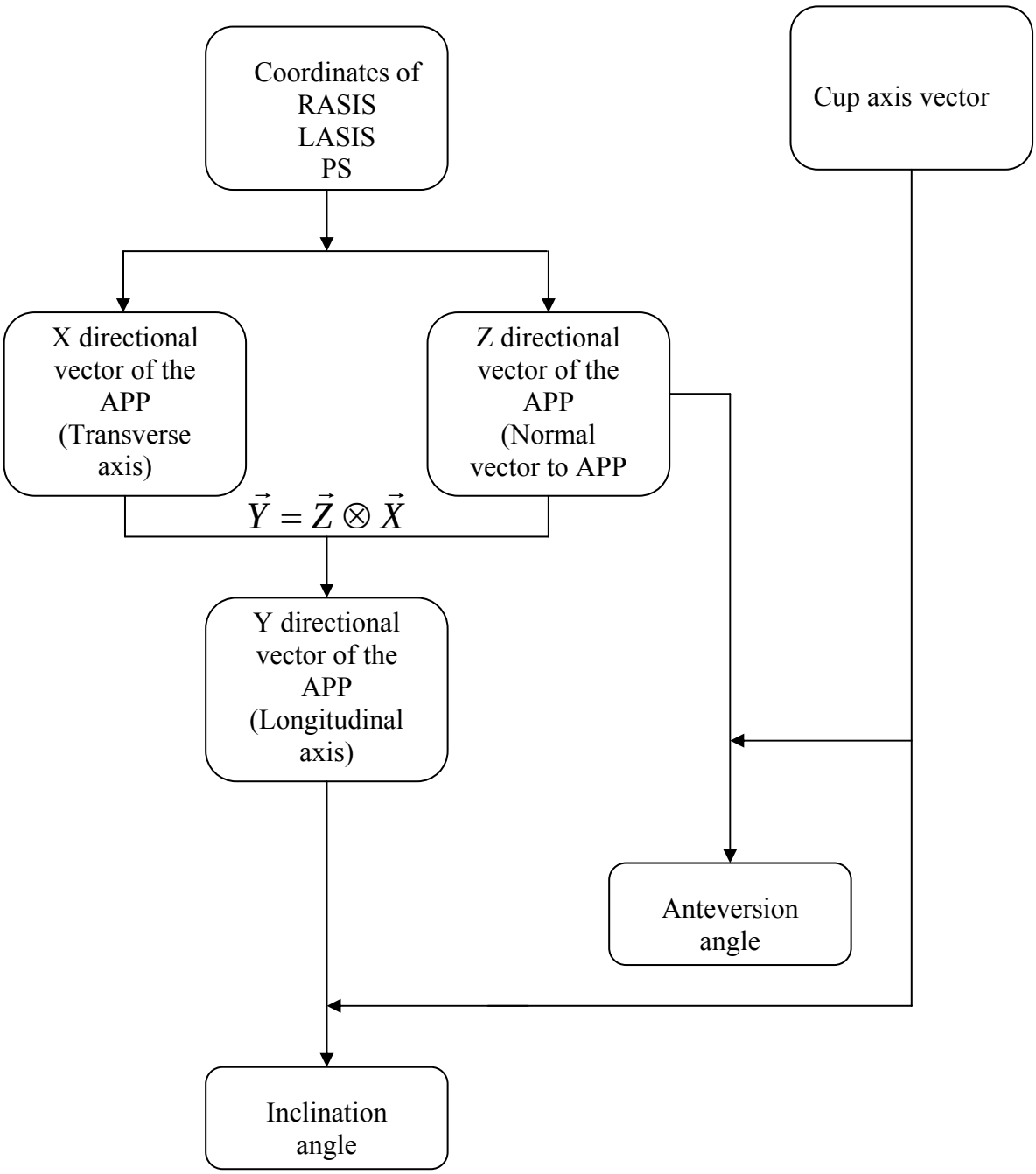

Figure 12. Flow chart of angle calculation algorithm

Reference

1. Erhardt K. Report of joint meeting of the sections of Geriatrics & Gerentology and Rheumatology & Rehabilitation. Osteoarthritis in old age. J. R. Soc. Med. 1995; 88: 539 - 542.

2. Frankel S, Eachus J, Pearson N, Greenwood R, Chan P, Peters TJ, et. al Population requirements for primary hip replacement surgery: a cross sectional study. The Lancet 1999; 353(9161): 1304 - 1309.
3. Sugano N., Computer-assisted orthopedic surgery, Journal of Orthopaedic Science, The Japanese Orthopaedic association 2003; 8:442–448
4. Tran HH, Matsumiya K, Masamune K, Sakuma I, Dohi1 T , Liao H, Interactive 3D Navigation System for Image-guided Surgery, The International Journal of Virtual Reality, 2009; 8(1): 9-16
5. Kelley TC, Swank M L, Role of Navigation in Total Hip Arthroplasty, The Journal of Bone & Joint surgery 2009; volume 91-A
6. DiGioia III AM, Jaramaz B, Plakseychuk AY, Moody JE, Nikou C, LaBarca RS, et al, Comparison of a Mechanical Acetabular Alignment Guide With Computer Placement of the Socket. The Journal of Arthroplasty 2003; Vol. 17
7. Kalteis T, Handel M, Bäthis H, Perlick L, Tingart M, Grifka J, Imageless navigation for insertion of the acetabular component in total hip arthroplasty, J Bone Joint Surg [Br]2006;88-B:163-7
8. Kiefer H, OrthoPilot cup navigation – How to optimize cup positioning, International Orthopaedics (SICOT) , 2003 - 27 (Suppl.1):S37–S42
9. Clarke J.V, Deakin A.H, Nicol A.C, Picard F, Measuring the positional accuracy of computer assisted surgical tracking systems, Computer Aided Surgery, 2010, 15(1-3):13-18,
10. Wolf A, DiGioia III AM, Mor AB, Jaramaz B, Cup alignment error model for THA, Clinical orthopaedic and related research, 2005 - 437, pp 132-137.
11. Lee YS and Yoon TR, Error in acetabular socket alignment due to the thick anterior pelvic soft tissues, The Journal of Arthroplasty, 2008, Vol. 23 No. 5, pp 699-705
12. Świątek-Najwer E, Będziński R, Krowicki P, Krysztoforski K, Keppler P, Kozak J, Improving surgical precision-application of navigation system in orthopedic surgery. Acta of Bioengineering and Biomechanics 2008; Vol. 10, No. 4.
13. Liaw CK, Yang RS, Hou SM, Wu TY, Fuh CS, A simple mathematical standardized measurement of acetabulum anteversion after total hip arthroplasty. Computational and Mathematical Methods in Medicine June 2008; Vol. 9, No. 2, 105–119.
14. D.W. Murray. The Definition and Measurement of Acetabular Orientation. The Journal of Bone and Joint Surgery 1993; 75-B: 228-32.

Appendix A

The file bellow presents the palpated data obtained from the pelvic phantom, which was used in the experiments and further explained in Chapter 4.

OrthoPilot data

{

AcetabulumRecorder: {

Ant.: *0.24474* ← Anteversion angle in radiant

Incl.: *0.793349* ← Inclination angle in radiant

Size: *48* ← Cup size

Orientation of the native acetabulum

(

(0.461132, -0.403778, 0.790139, -0.0500267),

(-0.306433, 0.763217, 0.568857, 0.18792),

(-0.832739, -0.504443, 0.228213, -0.0302264)

)

}

Anterior Pelvic plane derived from the palpated land marks

AnteriorPlane: (

(0.00702326, -0.987928, -0.154752, 0),

(0.0150834, 0.154843, -0.987824, 0),

(0.999862, 0.00460356, 0.0159888, 0)

)

Transformation matrix of the mid point of pubic Symphysis (PS)

Central: (

(0.985226, 0.160173, 0.0606231, -0.21121),

(-0.161793, 0.986561, 0.0228034, 0.150647),

(-0.0561559, -0.0322749, 0.9979, 0.0122076)

)

Transformation matrix of the mid point of ASIS at operated side (RASIS)

Colateral: (

(0.995084, 0.0956381, 0.0257105, -0.110942),

(-0.0975693, 0.991236, 0.0890607, 0.0445087),

(-0.0169676, -0.0911315, 0.995694, 0.013104)

)

Transformation matrix of the mid point of ASIS at other side (LASIS)

Controlateral: (

(0.996303, 0.00990057, 0.085331, -0.338059),

(-0.0206411, 0.991825, 0.125923, 0.0801058),

(-0.0833867, -0.127219, 0.988363, 0.0141628)

)

Implants: {

Approach: ANTERIOR ← Surgical Approach

Cup: "PLASMACUP SC" ← Implant type

"Cup cementless": YES

"Cup size": 48

"Head Diameter": 28

"Head Material": GENERIC

"Head Neck Size": M

"Inlay Material": CHIRULEN

"Inlay Shape":SYMMETRICAL

Position:SUPINE ← Patient's position during the surgery

Serial:PASSIVE ← Instrument type

Stem: ""

"Stem CCD": 135

"Stem antetorsion": 0

"Stem cementless": NO

"Stem size": 0

Taper: 12/14

}

Transformation matrix of the medial wall point

MedialWallPoint: (

(

(-0.0395222, -0.688025, 0.72461, -0.079106),

(0.556417, 0.587186, 0.587889, 0.160514),

(-0.829963, 0.426419, 0.359622, -0.0490489)

)

)

Patient: {

BirthDate: "1999-12-31T00:00:00"

DepartmentName: "B.BRAUN AESCULAP WORKSHOP-SYSTEM"

Gender: FEMALE

PatientFirstName: "TEST TEN MEAN RAD"

PatientLastName: "T TEN"

SurgeonName:DR.D

}

ReamerSelection: {

Position: 0

Reamer: 0

}

SurgeryData: {

InstrumentSetName: ""

IsLeftSide: NO ← Operated side -Right

}

Step 1

Converting the coordinates value from reference plane to lab coordinate frame,

$$T_r = R \bullet T$$

Position coordinate matrix of the PS

$$\begin{bmatrix} 0.980968 & 0.188141 & 0.0480092 & -0.211681 \\ -0.190308 & 0.980672 & 0.0454404 & 0.150213 \\ -0.038532 & -0.0537121 & 0.997813 & 0.0121988 \end{bmatrix}$$

According to the equation 2.10

$$\begin{bmatrix} x_p \\ y_p \\ z_p \end{bmatrix} = -\left[R\right]^{-1} * \left[T\right]$$

$$= -\begin{bmatrix} 0.980968 & 0.188141 & 0.0480092 \\ -0.190308 & 0.980672 & 0.0454404 \\ -0.038532 & -0.0537121 & 0.997813 \end{bmatrix}^{-1} * \begin{bmatrix} -0.211681 \\ 0.150213 \\ 0.0121988 \end{bmatrix}$$

$$= -\begin{bmatrix} 0.980968 & -0.190308 & -0.038532 \\ 0.188141 & 0.980672 & -0.0537121 \\ 0.0480092 & 0.0454404 & 0.997813 \end{bmatrix} * \begin{bmatrix} -0.211681 \\ 0.150213 \\ 0.0121988 \end{bmatrix}$$

$$\begin{bmatrix} x_p \\ y_p \\ z_p \end{bmatrix} = \begin{bmatrix} -0.236709 \\ 0.106829 \\ 0.008835 \end{bmatrix}$$

Transformation of the rotational matrix to lab coordinate frame R_{p_new}

$$\left[R_r\right]^{-1} * \left[R_p\right] = \left[R_{p\_new}\right]$$

$$\begin{bmatrix} -0.06347 & 0.101321 & 0.992827 \\ -0.48943 & 0.863822 & -0.11944 \\ -0.86973 & -0.4935 & -0.00524 \end{bmatrix}^{-1} * \begin{bmatrix} 0.780871 & -0.62378 & 0.033799 \\ 0.621014 & 0.78099 & 0.066194 \\ -0.06769 & -0.0307 & 0.997234 \end{bmatrix} = \begin{bmatrix} -0.05384 & 0.088243 & 0.994643 \\ 0.162346 & 0.983608 & -0.07848 \\ -0.98526 & 0.15725 & -0.06728 \end{bmatrix}$$

Position coordinates with respect to lab coordinate frame

$$\begin{bmatrix} x_f \\ y_f \\ z_f \end{bmatrix} = -\left[R_{p\_new}\right]^{-1} * \left[T\right]_r$$

$$\begin{bmatrix} x_p \\ y_p \\ z_p \end{bmatrix} = \begin{bmatrix} \frac{x_f}{z_f} \\ \frac{y_f}{z_f} \\ z_f \\ \end{bmatrix}$$

$$\begin{bmatrix} x_f \\ y_f \\ z_f \end{bmatrix} = \left[\begin{bmatrix} -0.05384 & 0.088243 & 0.994643 \\ 0.162346 & 0.983608 & -0.07848 \\ -0.98526 & 0.15725 & -0.06728 \end{bmatrix}\right]^{-1} * \begin{bmatrix} -0.1106 \\ 0.3018 \\ -0.01869 \end{bmatrix} = \begin{bmatrix} 0.073391 \\ 0.284114 \\ -0.13289 \end{bmatrix}$$

$$\begin{bmatrix} x_p \\ y_p \\ z_p \end{bmatrix} = \begin{bmatrix} \frac{0.073391}{-0.13289} \\ \frac{0.284114}{-0.13289} \\ -0.13289 \\ \end{bmatrix}$$

$$\begin{bmatrix} x_p \\ y_p \\ z_p \end{bmatrix} = \begin{bmatrix} -0.5527 \\ -2.13797 \\ -0.13289 \end{bmatrix}$$

Above steps has explained the position coordinate calculation for the Pubic symphysis and same procedure is used to calculate all other position coordinates.

Distance between Anatomical landmarks

$$RASIS - LASIS = \sqrt{\left(T_{x\_col} - T_{x\_con}\right)^2 + \left(T_{y\_col} - T_{y\_con}\right)^2 + \left(T_{z\_col} - T_{z\_con}\right)^2}$$

$$RASIS - LASIS = \sqrt{\left(-0.1109 - (-0.3381)\right)^2 + \left(0.0445 - 0.0801\right)^2 + \left(0.0131 - 0.0142\right)^2}$$

$$RASIS - LASIS = 0.230m$$

$$RASIS - PS = \sqrt{\left(T_{x\_col} - T_{x\_cen}\right)^2 + \left(T_{y\_col} - T_{y\_cen}\right)^2 + \left(T_{z\_col} - T_{z\_cen}\right)^2}$$

$$RASIS - PS = \sqrt{\left(-0.1109 - (-0.2102)\right)^2 + \left(0.0445 - 0.1506\right)^2 + \left(0.0131 - 0.0122\right)^2}$$

$$RASIS - PS = 0.145m$$

$$LASIS - PS = \sqrt{\left(T_{x\_con} - T_{x\_cen}\right)^2 + \left(T_{y\_con} - T_{y\_cen}\right)^2 + \left(T_{z\_con} - T_{z\_cen}\right)^2}$$

$$LASIS - PS = \sqrt{\left(-0.1109 - (-0.3381)\right)^2 + \left(0.0445 - 0.0801\right)^2 + \left(0.0131 - 0.0142\right)^2}$$

$$LASIS - PS = 0.146m$$

Acetabular angle calculation for the neutral position of the APP

Anteversion angle calculations

Position coordinates in millimetres

$RASIS = (-85.744, 97.052, 827.210)$

$LASIS = (142.567, 98.080, 830.674)$

$PS = (42.118, 17.656, 828.526)$

Normal vector to the APP is used in anteversion angle calculations

$$\vec{Z} = \begin{bmatrix} x_{col} - x_{con} & y_{col} - y_{con} & z_{col} - z_{con} \\ x_{col} - x_{cen} & y_{col} - y_{cen} & z_{col} - z_{cen} \end{bmatrix}$$

When substitute above coordinates values,

$$\vec{Z} = \begin{bmatrix} -228.311 & -1.027 & -3.454 \\ -127.861 & 79.397 & -1.306 \end{bmatrix}$$

By considering the mode of the above $\vec{Z}$

$$Z_{x_{apc}} = \begin{vmatrix} -1.027 & -3.454 \\ 79.397 & -1.306 \end{vmatrix}$$

$$Z_{x_{apc}} = [((-1.027) * (-1.306)) - ((-3.454) * (79.397))]$$

$$Z_{x_{apc}} = 275.608$$

$$Z_{y_{apc}} = \begin{vmatrix} \text{-228.311} & \text{-3.454} \\ \text{-127.861} & \text{-1.306} \end{vmatrix}$$

$$Z_{y_{apc}} = [((\text{-228.311}) * (\text{-1.306})) - ((\text{-3.454}) * (\text{-127.861}))]$$

$$Z_{y_{apc}} = -143.398$$

$$Z_{z_{apc}} = \begin{vmatrix} \text{-228.311} & \text{-1.027} \\ \text{-127.861} & 17.656 \end{vmatrix}$$

$$Z_{z_{apc}} = [((\text{-228.311}) * (\text{-1.027})) - ((\text{-127.861}) * (79.397))]$$

$$Z_{z_{apc}} = -18252.629$$

Cup axis vector

According to C. K. Liaw et al (2008), cup axis vector can be derived for known acetabular angles. From that, bellow vector was derived for 14^0 of *Ant* and 45^0 of *Inc*

$$(a, b, c) = [(\sin(Inc) * \cos(Ant)), \text{-}(\cos(Inc) * \cos(Ant)), \sin(Ant)]$$

$$(a, b, c) = (0.6861, \text{-}0.6861, 0.2419)$$

From equation 2.23

$$ant\_ang = \sin^{-1}\left(\frac{\left(Z_{x_{apc}} * a\right) + \left(Z_{y_{apc}} * b\right) + \left(Z_{z_{apc}} * c\right)}{\sqrt{\left(Z_{x_{apc}}\right)^2 + \left(Z_{y_{apc}}\right)^2 + \left(Z_{x_{apc}}\right)^2} * \sqrt{a^2 + b^2 + c^2}} \right)$$

By substituting the above obtained values,

$$Ant\_ang = \sin^{-1}\left|\frac{(275.608*0.6861)+(-143.398*\text{-}0.6861)+(-18252.629*0.2419)}{\sqrt{(275.608)^2+(-143.398)^2+(-18252.629)^2}*\sqrt{0.6861^2+(\text{-}0.6861)^2+0.2419^2}}\right|$$

$$Ant\_ang = \sin^{-1} 0.2369$$

$$Ant\_ang = 13.81^{\circ}$$

Inclination angle calculations

$$\vec{Y} = \begin{bmatrix} Z_{x_{apc}} & Z_{y_{apc}} & Z_{z_{apc}} \\ x_{col}-x_{con} & y_{col}-y_{con} & z_{col}-z_{con} \end{bmatrix}$$

$$\vec{Y} = \begin{pmatrix} Y_{x_{apc}} & Y_{y_{apc}} & Y_{z_{apc}} \end{pmatrix}$$

$$\vec{Y} = \begin{bmatrix} 275.608 & -143.398 & -18252.629 \\ -228.311 & -1.0269 & -3.454 \end{bmatrix}$$

By considering the mode of the above $\vec{Y}$

$$Y_{x_{apc}} = \begin{vmatrix} -143.398 & -18252.629 \\ -1.0269 & -3.454 \end{vmatrix}$$

$$Y_{x_{apc}} = [((-143.398)*(-3.454))-((-18252.629)*(-1.0269))]$$

$$Y_{x_{apc}} = -18254.04$$

$$Y_{y_{apc}} = \begin{vmatrix} 275.608 & -18252.629 \\ -228.311 & -3.454 \end{vmatrix}$$

$$Y_{y_{apc}} = [((275.608)*(-3.454)) - ((-18252.629)*(-228.311))]$$

$$Y_{y_{apc}} = -4169604.044$$

$$Y_{z_{apc}} = \begin{vmatrix} 275.608 & -143.398 \\ -228.311 & -1.0269 \end{vmatrix}$$

$$Y_{z_{apc}} = [((275.608)*(-1.0269)) - ((-143.398)*(-228.311))]$$

$$Y_{z_{apc}} = -33022.342$$

From equation 2.24

$$Inc - ang = \cos^{-1}\left(\frac{\left(Y_{x_{apc}} * (a/c)\right) + \left(Y_{y_{apc}} * (b/c)\right) + \left(Y_{z_{apc}} * c\right)}{\sqrt{\left(Y_{x_{apc}}\right)^2 + \left(Y_{y_{apc}}\right)^2 + \left(Y_{z_{apc}}\right)^2} * \sqrt{\left(a/c\right)^2 + \left(b/c\right)^2 + c^2}} \right)$$

By substituting the above obtained values,

$$Inc - ang = \cos^{-1}\left| \frac{\left(-0.182 * (2.8360)\right) + \left(-41.696 * (-2.8360)\right) + \left(-0.330 * 0.2419\right)}{\sqrt{\left(-0.182\right)^2 + \left(-41.696\right)^2 + \left(-0.330\right)^2} * \sqrt{\left(2.8360\right)^2 + \left(-2.8360\right)^2 + 0.2419^2}} \right|$$

$$Inc - ang = \cos^{-1} 0.7022$$

$$Inc - ang = 45.34^{\circ}$$

Acetabular angle calculation for the tilted APP

When tilting the APP along anterior direction;

New position coordinates in millimetres

$RASIS = (96.524, 8.486, 131.365)$

$LASIS = (324.305, 5.930, 134.348)$

$PS = (213.127, -69.284, 131.638)$

Normal vector to the APP is used in anteversion angle calculations,

if APP tilts in anterior direction,

$$\vec{Z}_{tilt} = \begin{bmatrix} x_{col} - x_{con} & y_{col} - y_{con} + l_1 \cos\theta & z_{col} - z_{con} - l_1 \sin\theta \\ x_{col} - x_{cen} & y_{col} - y_{cen} + l_2 \cos\theta & z_{col} - z_{cen} - l_2 \sin\theta \end{bmatrix}$$

Where, θ is the tilting angle towards the anterior direction and l_1 is the magnitude of vector along $\overrightarrow{RASIS - LASIS}$ and l_2 is the magnitude of vector along $\overrightarrow{RASIS - PS}$

$l_1 = \overrightarrow{RASIS - LASIS} = 227.781$

$l_2 = \overrightarrow{RASIS - PS} = 140.159$

When substitute above coordinates values for $\theta = 5^\circ$,

$$\vec{Z}_{a\,tilt} = \begin{bmatrix} -227.781 & 229.503 & -22.846 \\ -116.603 & 217.395 & -12.493 \end{bmatrix}$$

By considering the mode of the above $\vec{Z}_{a\,tilt}$ and by following the same steps shown in the anteversion angle calculation for the neutral position of the APP

$$Z_{x_{apc}} = \begin{vmatrix} 229.503 & -22.846 \\ 217.395 & -12.493 \end{vmatrix}$$

$$Z_{x_{apc}} = [((229.503) * (-12.493)) - ((-22.846) * (217.395))]$$

$$Z_{x_{apc}} = 2099.324$$

$$Z_{y_{apc}} = \begin{vmatrix} -227.781 & -22.846 \\ -116.603 & -12.493 \end{vmatrix}$$

$$Z_{y_{apc}} = [((-227.781) * (-12.493)) - ((-22.846) * (-116.603))]$$

$$Z_{y_{apc}} = 181.816$$

$$Z_{z_{apc}} = \begin{vmatrix} -227.781 & 229.503 \\ -116.603 & 217.395 \end{vmatrix}$$

$$Z_{z_{apc}} = [((-227.781) * (217.395)) - ((229.503) * (-116.603))]$$

$$Z_{z_{apc}} = -22757.642$$

From equation 2.23, anteversion angle, when APP tilts 5^0 towards the anterior direction.

$$Ant\_ang = \sin^{-1} \left| \frac{(2099.324 * 0.6861) + (181.816 * -0.6861) + (-22757.642 * 0.2419)}{\sqrt{(2099.324)^2 + (181.816)^2 + (-22757.642)^2} * \sqrt{0.6861^2 + (-0.6861)^2 + 0.2419^2}} \right|$$

$$Ant\_ang = \sin^{-1} 0.1724$$

$$Ant\_ang = 9.93^{\circ}$$

Inclination angle calculations

if APP tilts in anterior direction,

$$\vec{Y}_{a\,tilt} = \begin{bmatrix} Z_{x_{apc}} & Z_{y_{apc}} & Z_{z_{apc}} \\ x_{col} - x_{con} & y_{col} - y_{con} + l_1 \cos\theta & z_{col} - z_{con} - l_1 \sin\theta \end{bmatrix}$$

$$\vec{Y}_{a\,tilt} = \begin{bmatrix} 2099.324 & 181.816 & -22757.642 \\ -227.781 & 229.503 & -22.846 \end{bmatrix}$$

By considering the mode of the above $\vec{Y}_{a\,tilt}$ and obtained the values for $\vec{Y}_{x_{app}}, \vec{Y}_{y_{app}}, \vec{Y}_{z_{app}}$. Then, those values were substituted in equation 2.24 and inclination angle was obtained by following the same steps shown in the inclination angle calculation for the neutral position of the APP.

From equation 2.24

$$Inc - ang = \cos^{-1} 0.7062$$

$$Inc - ang = 45.07^{\circ}$$

When tilting the APP along posterior direction;

New position coordinates in millimetres

$$RASIS = (96.524, 8.486, 131.365)$$
$$LASIS = (324.305, 5.930, 134.348)$$
$$PS = (213.127, -69.284, 131.638)$$

Normal vector to the APP is used in anteversion angle calculations,

if APP tilts in posterior direction,

$$\vec{Z}_{p\,tilt} = \begin{bmatrix} x_{col} - x_{con} & y_{col} - y_{con} + l_1 \cos\theta & z_{col} - z_{con} + l_1 \sin\theta \\ x_{col} - x_{cen} & y_{col} - y_{cen} + l_2 \cos\theta & z_{col} - z_{cen} + l_2 \sin\theta \end{bmatrix}$$

Where, θ is the tilting angle towards the anterior direction and l_1 is the magnitude of vector along $\overrightarrow{RASIS - LASIS}$ and l_2 is the magnitude of vector along $\overrightarrow{RASIS - PS}$

$l_1 = \overrightarrow{RASIS - LASIS} = 227.781$

$l_2 = \overrightarrow{RASIS - PS} = 140.159$

When substitute above coordinates values,

$$\vec{Z}_{p\,tilt} = \begin{bmatrix} \text{-227.781} & 229.503 & 16.881 \\ \text{-116.603} & 217.395 & 11.948 \end{bmatrix}$$

By considering the mode of the above $\vec{Z}_{p\,tilt}$ and by following the same steps shown in the anteversion angle calculation for the neutral position of the APP;

From equation 2.23, anteversion angle, when APP tilts 5^0 towards the anterior direction.

$$Ant\_ang = \sin^{-1}\left| \frac{(-927.749 * 0.6861) + (-753.145 * \text{-}0.6861) + (-22757.642 * 0.2419)}{\sqrt{(-927.749)^2 + (-753.145)^2 + (-22757.642)^2} * \sqrt{0.6861^2 + (\text{-}0.6861)^2 + 0.2419^2}} \right|$$

$Ant\_ang = \sin^{-1} 0.2922$

$Ant\_ang = 16.98^{\circ}$

Inclination angle calculations

if APP tilts in posterior direction,

$$\vec{Y}_{p\,tilt} = \begin{bmatrix} Z_{x_{apc}} & Z_{y_{apc}} & Z_{z_{apc}} \\ x_{col} - x_{con} & y_{col} - y_{con} + l_1 \cos\theta & z_{col} - z_{con} + l_1 \sin\theta \end{bmatrix}$$

$$\vec{Y}_{p\,tilt} = \begin{bmatrix} -927.749 & -753.145 & -22757.642 \\ -227.781 & 229.503 & 16.881 \end{bmatrix}$$

By considering the mode of the above $\vec{Y}_{p\,tilt}$ and obtained the values for $\vec{Y}_{x_{app}}, \vec{Y}_{y_{app}}, \vec{Y}_{z_{app}}$. Then, those values were substituted in equation 2.24 and inclination angle was obtained by following the same steps shown in the inclination angle calculation for the neutral position of the APP.

From equation 2.24

$$Inc - ang = \cos^{-1} 0.6805$$

$$Inc - ang = 47.12^{\circ}$$

When tilting the APP along lateral direction;

New position coordinates in millimetres

$$RASIS = (3.800, 200.472, 88.290)$$
$$LASIS = (234.326, 205.048, 91.146)$$
$$PS = (111.711, 122.482, 89.069)$$

Normal vector to the APP is used in anteversion angle calculations,

if APP tilts in lateral direction,

$$\vec{Z}_{l\,tilt} = \begin{bmatrix} x_{col} - x_{con} + l_1 \cos\theta & y_{col} - y_{con} & z_{col} - z_{con} - l_1 \sin\theta \\ x_{col} - x_{cen} + l_2 \cos\theta & y_{col} - y_{cen} & z_{col} - z_{cen} - l_2 \sin\theta \end{bmatrix}$$

Where, θ is the tilting angle towards the anterior direction and l_1 is the magnitude of vector along $\overrightarrow{RASIS - LASIS}$ and l_2 is the magnitude of vector along $\overrightarrow{RASIS - PS}$

$l_1 = \overrightarrow{RASIS - LASIS} = 230.554$

$l_2 = \overrightarrow{RASIS - PS} = 133.145$

When substitute above coordinates values for the $\theta = 5^\circ$,

$$\vec{Z}_{l\,tilt} = \begin{bmatrix} -230.346 & -4.576 & 22.958 \\ -107.826 & 77.989 & -12.388 \end{bmatrix}$$

By considering the mode of the above $\vec{Z}_{l\,tilt}$ and following the same steps shown in the anteversion angle calculation for the neutral position of the APP;
From equation 2.23, anteversion angle was calculated, when APP tilts 5^0 towards the anterior direction.

$$ant\_ang = \sin^{-1}\left(\frac{\left(Z_{x_{apc}} * a\right) + \left(Z_{y_{apc}} * b\right) + \left(Z_{z_{apc}} * c\right)}{\sqrt{\left(Z_{x_{apc}}\right)^2 + \left(Z_{y_{apc}}\right)^2 + \left(Z_{x_{apc}}\right)^2} * \sqrt{a^2 + b^2 + c^2}} \right)$$

$Ant\_ang = \sin^{-1} 0.1584$

$Ant\_ang = 9.11^\circ$

Inclination angle calculations

if APP tilts in lateral direction,

$$\vec{Y}_{l\,tilt} = \begin{bmatrix} Z_{x_{apc}} & Z_{y_{apc}} & Z_{z_{apc}} \\ x_{col} - x_{con} + l_1 \cos\theta & y_{col} - y_{con} & z_{col} - z_{con} - l_1 \sin\theta \end{bmatrix}$$

$$\vec{Y}_{l\,tilt} = \begin{bmatrix} 1847.205 & 378.094 & -18457.920 \\ -230.346 & -4.576 & -22.958 \end{bmatrix}$$

By considering the mode of the above $\vec{Y}_{l\,tilt}$ and obtained the values for $\vec{Y}_{x_{app}}, \vec{Y}_{y_{app}}, \vec{Y}_{z_{app}}$. Then, those values were substituted in equation 2.24 and inclination angle was obtained by following the same steps shown in the inclination angle calculation for the neutral position of the APP.

From equation 2.24

$$Inc - ang = \cos^{-1} 0.6907$$

$$Inc - ang = 46.31^{\circ}$$

When tilting the APP along medial direction;

New position coordinates in millimetres

$$RASIS = (87.458, 10.174, 130.633)$$
$$LASIS = (346.600, 12.199, 133.766)$$
$$PS = (213.980, -70.444, 131.861)$$

Normal vector to the APP is used in anteversion angle calculations,

if APP tilts in medial direction,

$$\vec{Z}_{m\,ilt} = \begin{bmatrix} x_{col} - x_{con} + l_1 \cos\theta & y_{col} - y_{con} & z_{col} - z_{con} + l_1 \sin\theta \\ x_{col} - x_{cen} + l_2 \cos\theta & y_{col} - y_{cen} & z_{col} - z_{cen} + l_2 \sin\theta \end{bmatrix}$$

Where, θ is the tilting angle towards the anterior direction and l_1 is the magnitude of vector along $\overrightarrow{RASIS - LASIS}$ and l_2 is the magnitude of vector along $\overrightarrow{RASIS - PS}$

$l_1 = \overrightarrow{RASIS - LASIS} = 259.169$

$l_2 = \overrightarrow{RASIS - PS} = 150.029$

When substitute above coordinates values for the $\theta = 5^\circ$,

$$\vec{Z}_{m\,tilt} = \begin{bmatrix} -258.978 & -2.025 & 19.464 \\ -126.427 & 80.619 & 11.854 \end{bmatrix}$$

By considering the mode of the above $\vec{Z}_{m\,tilt}$ and by following the same steps shown in the anteversion angle calculation for the neutral position of the APP;
From equation 2.23, anteversion angle was calculated, when APP tilts 5^0 towards the anterior direction.

$$ant\_ang = \sin^{-1}\left(\frac{\left(Z_{x_{apc}} * a\right) + \left(Z_{y_{apc}} * b\right) + \left(Z_{z_{apc}} * c\right)}{\sqrt{\left(Z_{x_{apc}}\right)^2 + \left(Z_{y_{apc}}\right)^2 + \left(Z_{x_{apc}}\right)^2} * \sqrt{a^2 + b^2 + c^2}} \right)$$

$Ant\_ang = \sin^{-1} 0.3124$

$Ant\_ang = 18.20^\circ$

Inclination angle calculations

if APP tilts in lateral direction,

$$\vec{Y}_{m\,tilt} = \begin{bmatrix} Z_{x_{apc}} & Z_{y_{apc}} & Z_{z_{apc}} \\ x_{col} - x_{con} + l_1 \cos\theta & y_{col} - y_{con} & z_{col} - z_{con} - l_1 \sin\theta \end{bmatrix}$$

$$\vec{Y}_{m\,tilt} = \begin{bmatrix} -1593.207 & -608.956 & -21134.418 \\ -258.978 & -2.025 & 19.465 \end{bmatrix}$$

By considering the mode of the above $\vec{Y}_{m\,tilt}$ and obtained the values for $\vec{Y}_{x_{app}}, \vec{Y}_{y_{app}}, \vec{Y}_{z_{app}}$. Then, those values were substituted in equation 2.24 and inclination angle was obtained by following the same steps shown in the inclination angle calculation for the neutral position of the APP.

From equation 2.24

$$Inc - ang = \cos^{-1} 0.7078$$

$$Inc - ang = 44.94^{\circ}$$

Changing the landmark position in coronal plane

Changing the landmark position of RASIS along caudal direction by 1 cm.

New position coordinates in millimetres

$$RASIS = (\text{-}96.927, 156.021, 825.722)$$
$$LASIS = (131.310, 162.804, 828.376)$$
$$PS = (16.666, 89.253, 825.618)$$

Normal vector to the APP is used in anteversion angle calculations,

$$\vec{Z} = \begin{bmatrix} x_{col} - x_{con} & y_{col} + 10 - y_{con} & z_{col} - z_{con} \\ x_{col} - x_{cen} & y_{col} + 10 - y_{cen} & z_{col} - z_{cen} \end{bmatrix}$$

When substitute above coordinates values,

$$\vec{Z} = \begin{bmatrix} \text{-}228.238 & \text{-}6.782 & \text{-}2.654 \\ \text{-}113.593 & 66.768 & 0.104 \end{bmatrix}$$

By considering the mode of the above $\vec{Z}$ and following the same steps shown in the anteversion angle calculation for the neutral position of the APP. From equation 2.23, anteversion angle, when RASIS moves towards the caudal direction by 1 cm.

$$ant\_ang = \sin^{-1}\left|\left(\frac{(176.531*0.6861)+(-325.330*-0.6861)+(-16009.366*0.2419)}{\sqrt{(176.531)^2+(-325.330)^2+(-16009.366)^2}*\sqrt{(0.6861)^2+(-0.6861)^2+(0.2419)^2}}\right)\right|$$

$$Ant\_ang = \sin^{-1} 0.2482$$

$$Ant\_ang = 14.37^{\circ}$$

Inclination angle calculations

$$\vec{Y} = \begin{bmatrix} Z_{x_{apc}} & Z_{y_{apc}} & Z_{z_{apc}} \\ x_{col}-x_{con} & y_{col}-y_{con} & z_{col}-z_{con} \end{bmatrix}$$

$$\vec{Y} = \begin{bmatrix} 127.5312 & -325.33 & -16009.366 \\ -228.238 & -6.7822 & -2.654 \end{bmatrix}$$

By considering the mode of the above $\vec{Y}$ and obtained the values for $\vec{Y}_{x_{app}}, \vec{Y}_{y_{app}}, \vec{Y}_{z_{app}}$. Then, those values were substituted in equation 2.24 and inclination angle was obtained for, when RASIS moves towards the cranial direction by 1 cm.

From equation 2.24

$$Inc-ang = \cos^{-1}\left|\frac{\left(-1.077*\left(2.8360\right)\right)+\left(-36.544*\left(-2.8360\right)\right)+\left(-0.754*0.2419\right)}{\sqrt{\left(-1.077\right)^2+\left(-36.544\right)^2+\left(-0.754\right)^2}*\sqrt{\left(2.8360\right)^2+\left(-2.8360\right)^2+0.2419^2}}\right|$$

$$Inc-ang = \cos^{-1} 0.6723$$

$$Inc-ang = 47.75^{\circ}$$

Changing the landmark position of RASIS along cranial direction by 1 cm.

New position coordinates in millimetres

$RASIS = (\text{-}93.811, 180.595, 825.382)$

$LASIS = (134.481, 172.019, 827.204)$

$PS = (24.082, 96.614, 824.521)$

Normal vector to the APP is used in anteversion angle calculations,

$$\vec{Z} = \begin{bmatrix} x_{col} - x_{con} & y_{col} - 10 - y_{con} & z_{col} - z_{con} \\ x_{col} - x_{cen} & y_{col} - 10 - y_{cen} & z_{col} - z_{cen} \end{bmatrix}$$

When substitute above coordinates values,

$$\vec{Z} = \begin{bmatrix} \text{-}228.293 & 8.576 & \text{-}1.822 \\ \text{-}117.894 & 83.981 & 0.861 \end{bmatrix}$$

By considering the mode of the above $\vec{Z}$ matrix, $\vec{Z}_{x_{app}}, \vec{Z}_{y_{app}}, \vec{Z}_{z_{app}}$ values were obtained by followed the same steps shown in the anteversion angle calculation for the neutral position of the APP. Then, those values were substituted in equation 2.23 and Anteversion angle was obtained for, when RASIS moves towards the cranial direction by 1 cm,

$$ant\_ang = \sin^{-1}\left|\left(\frac{(160.4*0.6861)+(-411.385*-0.6861)+(-18161.182*0.2419)}{\sqrt{(160.4)^2+(-411.385)^2+(-18161.182)^2}*\sqrt{(0.6861)^2+(-0.6861)^2+(0.2419)^2}}\right)\right|$$

$Ant\_ang = \sin^{-1} 0.2468$

$Ant\_ang = 14.29^{\circ}$

Inclination angle calculations

$$\vec{Y} = \begin{bmatrix} Z_{x_{apc}} & Z_{y_{apc}} & Z_{z_{apc}} \\ x_{col} - x_{con} & y_{col} - y_{con} & z_{col} - z_{con} \end{bmatrix}$$

$$\vec{Y} = \begin{bmatrix} 160.4 & -411.385 & -18161.1856 \\ -228.238 & 8.576 & -1.822 \end{bmatrix}$$

By considering the mode of the above $\vec{Y}$ and obtained the values for $\vec{Y}_{x_{app}}, \vec{Y}_{y_{app}}, \vec{Y}_{z_{app}}$ by following the same steps shown in the anteversion angle calculation for the neutral position of the APP. Then inclination angle was obtained for, when RASIS moves towards the cranial direction by 1 cm.

From equation 2.24

$$Inc-ang = \cos^{-1}\left|\frac{\left(1.565*\left(2.8360\right)\right)+\left(-41.464*\left(-2.8360\right)\right)+\left(-0.925*0.2419\right)}{\sqrt{\left(1.565\right)^2+\left(-41.464\right)^2+\left(-0.925\right)^2}*\sqrt{\left(2.8360\right)^2+\left(-2.8360\right)^2+0.2419^2}}\right|$$

$$Inc-ang = \cos^{-1} 0.7304$$

$$Inc-ang = 43.08^{\circ}$$

Changing the landmark position of RASIS along medial direction by 1 cm.

New position coordinates in millimetres

$$RASIS = \left(-86.048, 114.380, 825.928\right)$$
$$LASIS = \left(134.238, 116.626, 826.775\right)$$
$$PS = \left(11.122, 30.773, 825.872\right)$$

Normal vector to the APP is used in anteversion angle calculations,

$$\vec{Z} = \begin{bmatrix} x_{col}+10-x_{con} & y_{col}-y_{con} & z_{col}-z_{con} \\ x_{col}+10-x_{cen} & y_{col}-y_{cen} & z_{col}-z_{cen} \end{bmatrix}$$

When substitute above coordinates values,

$$\vec{Z} = \begin{bmatrix} -217.285 & -2.246 & -0.848 \\ -97.170 & 83.9606 & 0.056 \end{bmatrix}$$

By considering the mode of the above $\vec{Z}$ matrix, $\vec{Z}_{x_{app}}, \vec{Z}_{y_{app}}, \vec{Z}_{z_{app}}$ values were obtained by followed the same steps shown in the anteversion angle calculation for the neutral position of the APP. Then, those values were substituted in equation 2.23 and Anteversion angle was obtained for, when RASIS moves towards the medial direction by 1 cm,

$$ant\_ang = \sin^{-1}\left|\left(\frac{(70.740*0.6861)+(-94.442*-0.6861)+(-18384.710*0.2419)}{\sqrt{(70.740)^2+(-94.442)^2+(-18384.710)^2}*\sqrt{(0.6861)^2+(-0.6861)^2+(0.2419)^2}}\right)\right|$$

$$Ant\_ang = \sin^{-1} 0.2428$$

$$Ant\_ang = 14.05^{\circ}$$

Inclination angle calculations

$$\vec{Y} = \begin{bmatrix} Z_{x_{apc}} & Z_{y_{apc}} & Z_{z_{apc}} \\ x_{col}-x_{con} & y_{col}-y_{con} & z_{col}-z_{con} \end{bmatrix}$$

$$\vec{Y} = \begin{bmatrix} 70.740 & -94.442 & -18384.710 \\ -217.285 & -2.246 & -0.848 \end{bmatrix}$$

By considering the mode of the above $\vec{Y}$ and obtained the values for $\vec{Y}_{x_{app}}, \vec{Y}_{y_{app}}, \vec{Y}_{z_{app}}$ by following the same steps shown in the anteversion angle calculation for the neutral position of the APP. Then inclination angle was obtained for, when RASIS moves towards the medial direction by 1 cm.

From equation 2.24

$$Inc-ang = \cos^{-1}\left|\frac{((-0.412)*(2.8360))+((-39.948)*(-2.8360))+((-0.207)*0.2419)}{\sqrt{(-0.412)^2+(-39.948)^2+(-0.207)^2}*\sqrt{(2.8360)^2+(-2.8360)^2+0.2419^2}}\right|$$

$$Inc-ang = \cos^{-1} 0.7082$$

$$Inc-ang = 44.91^{\circ}$$

Changing the landmark position of RASIS along lateral direction by 1 cm.

New position coordinates in millimetres

$RASIS = (\text{-}94.117, 183.860, 825.813)$

$LASIS = (133.978, 175.948, 826.563)$

$PS = (26.600, 91.548, 825.359)$

Normal vector to the APP is used in anteversion angle calculations,

$$\vec{Z} = \begin{bmatrix} x_{col} - 10 - x_{con} & y_{col} - y_{con} & z_{col} - z_{con} \\ x_{col} - 10 - x_{cen} & y_{col} - y_{cen} & z_{col} - z_{cen} \end{bmatrix}$$

When substitute above coordinates values,

$$\vec{Z} = \begin{bmatrix} \text{-}228.096 & 7.913 & \text{-}0.749 \\ \text{-}120.718 & 92.313 & 0.454 \end{bmatrix}$$

By considering the mode of the above $\vec{Z}$ matrix, $\vec{Z}_{x_{app}}, \vec{Z}_{y_{app}}, \vec{Z}_{z_{app}}$ values were obtained by followed the same steps shown in the anteversion angle calculation for the neutral position of the APP. Then, those values were substituted in equation 2.23 and Anteversion angle was obtained for, when RASIS moves towards the lateral direction by 1 cm,

$$ant\_ang = \sin^{-1}\left|\left(\frac{(72.776*0.6861)+((-194.037)*-0.6861)+((-20100.927)*0.2419)}{\sqrt{(72.776)^2+(-194.037)^2+(-20100.927)^2}*\sqrt{(0.6861)^2+(-0.6861)^2+(0.2419)^2}}\right)\right|$$

$$Ant\_ang = \sin^{-1} 0.2460$$

$$Ant\_ang = 14.24^{\circ}$$

Inclination angle calculations

$$\vec{Y} = \begin{bmatrix} Z_{x_{apc}} & Z_{y_{apc}} & Z_{z_{apc}} \\ x_{col} - x_{con} & y_{col} - y_{con} & z_{col} - z_{con} \end{bmatrix}$$

$$\vec{Y} = \begin{bmatrix} 70.740 & -94.442 & -18384.710 \\ -217.285 & -2.246 & -0.848 \end{bmatrix}$$

By considering the mode of the above $\vec{Y}$ and obtained the values for $\vec{Y}_{x_{app}}, \vec{Y}_{y_{app}}, \vec{Y}_{z_{app}}$ by following the same steps shown in the anteversion angle calculation for the neutral position of the APP. Then inclination angle was obtained for, when RASIS moves towards the lateral direction by 1 cm. by substituting the above obtained values in

equation 2.24

$$Inc - ang = \cos^{-1} 0.7103$$
$$Inc - ang = 45.26^{\circ}$$

Changing the landmark position of LASIS along caudal direction by 1 cm.

New position coordinates in millimetres

$$RASIS = (-87.364, 159.345, 825.950)$$
$$LASIS = (131.387, 152.566, 828.400)$$
$$PS = (28.709, 86.693, 825.897)$$

Normal vector to the APP is used in anteversion angle calculations,

$$\vec{Z} = \begin{bmatrix} x_{col} - x_{con} & y_{col} - y_{con} + 10 & z_{col} - z_{con} \\ x_{col} - x_{cen} & y_{col} - y_{cen} & z_{col} - z_{cen} \end{bmatrix}$$

When substitute above coordinates values,

$$\vec{Z} = \begin{bmatrix} -218.749 & -6.778 & -2.446 \\ -116.074 & 72.652 & 0.054 \end{bmatrix}$$

By considering the mode of the above $\vec{Z}$ and following the same steps shown in the anteversion angle calculation for the neutral position of the APP. From equation 2.23, anteversion angle, when LASIS moves towards the caudal direction by 1 cm.

$$ant\_ang = \sin^{-1}\left|\left(\frac{\left((0.178)*0.6861\right)+\left((-0.296)*-0.6861\right)+\left((-15.105)*0.2419\right)}{\sqrt{\left(0.178\right)^2+\left(-0.296\right)^2+\left(-15.105\right)^2}*\sqrt{(0.6861)^2+(-0.6861)^2+(0.2419)^2}}\right)\right|$$

$$Ant\_ang = \sin^{-1} 0.2472$$

$$Ant\_ang = 14.31^{\circ}$$

Inclination angle calculations

$$\vec{Y} = \begin{bmatrix} Z_{x_{apc}} & Z_{y_{apc}} & Z_{z_{apc}} \\ x_{col}-x_{con} & y_{col}-y_{con} & z_{col}-z_{con} \end{bmatrix}$$

$$\vec{Y} = \begin{bmatrix} 178.113 & -295.681 & -15105.805 \\ -218.749 & 6.778 & -2.445 \end{bmatrix}$$

By considering the mode of the above $\vec{Y}$ and obtained the values for $\vec{Y}_{x_{app}}, \vec{Y}_{y_{app}}, \vec{Y}_{z_{app}}$. Then, those values were substituted in equation 2.24 and inclination angle was obtained for, when LASIS moves towards the caudal direction by 1 cm.

From equation 2.24

$$Inc-ang = \cos^{-1}\left|\frac{\left(1.031*\left(2.8360\right)\right)+\left(-33.048*\left(-2.8360\right)\right)+\left(-0.635*0.2419\right)}{\sqrt{\left(1.031\right)^2+\left(-33.048\right)^2+\left(-0.635\right)^2}*\sqrt{\left(2.8360\right)^2+\left(-2.8360\right)^2+0.2419^2}}\right|$$

$$Inc-ang = \cos^{-1} 0.7262$$

$$Inc-ang = 43.43^{\circ}$$

Changing the landmark position of LASIS along cranial direction by 1 cm.

New position coordinates in millimetres

$RASIS = (\text{-}81.461, 168.644, 824.717)$

$LASIS = (141.812, 178.166, 827.894)$

$PS = (31.728, 84.243, 826.504)$

Normal vector to the APP is used in anteversion angle calculations,

$$\vec{Z} = \begin{bmatrix} x_{col} - x_{con} & y_{col} - y_{con} - 10 & z_{col} - z_{con} \\ x_{col} - x_{cen} & y_{col} - y_{cen} & z_{col} - z_{cen} \end{bmatrix}$$

When substitute above coordinates values,

$$\vec{Z} = \begin{bmatrix} \text{-}223.273 & \text{-}9.522 & \text{-}3.178 \\ \text{-}113.188 & 84.401 & \text{-}1.787 \end{bmatrix}$$

By considering the mode of the above $\vec{Z}$ matrix, $\vec{Z}_{x_{app}}, \vec{Z}_{y_{app}}, \vec{Z}_{z_{app}}$ values were obtained by followed the same steps shown in the anteversion angle calculation for the neutral position of the APP. Then, those values were substituted in equation 2.23 and Anteversion angle was obtained for, when LASIS moves towards the caudal direction by 1 cm,

$$ant\_ang = \sin^{-1}\left| \left(\frac{(285.209 * 0.6861) + (39.419 * -0.6861) + (-19922.285 * 0.2419)}{\sqrt{(285.209)^2 + (39.419)^2 + (-19922.285)^2} * \sqrt{(0.6861)^2 + (-0.6861)^2 + (0.2419)^2}} \right) \right|$$

$$Ant\_ang = \sin^{-1} 0.2307$$

$$Ant\_ang = 13.39^{\circ}$$

Inclination angle calculations

$$\vec{Y} = \begin{bmatrix} Z_{x_{apc}} & Z_{y_{apc}} & Z_{z_{apc}} \\ x_{col} - x_{con} & y_{col} - y_{con} & z_{col} - z_{con} \end{bmatrix}$$

$$\vec{Y} = \begin{bmatrix} 285.209 & 39.419 & -19922.285 \\ -223.273 & -9.522 & -3.176 \end{bmatrix}$$

By considering the mode of the above $\vec{Y}$ and obtained the values for $\vec{Y}_{x_{app}}, \vec{Y}_{y_{app}}, \vec{Y}_{z_{app}}$ by following the same steps shown in the anteversion angle calculation for the neutral position of the APP. Then inclination angle was obtained for, when LASIS moves towards the cranial direction by 1 cm.

From equation 2.24

$$Inc - ang = \cos^{-1}\left| \frac{\left((-18.982)*(2.8360)\right) + \left((-444.901)*(-2.8360)\right) + (0.608*0.2419)}{\sqrt{(-18.982)^2 + (-444.901)^2 + (0.608)^2} * \sqrt{(2.8360)^2 + (-2.8360)^2 + 0.2419^2}} \right|$$

$$Inc - ang = \cos^{-1} 0.6752$$

$$Inc - ang = 47.53^{\circ}$$

Changing the landmark position of LASIS along medial direction by 1 cm.

New position coordinates in millimetres

$$RASIS = (99.939, 17.223, 130.115)$$

$$LASIS = (323.661, 17.172, 132.330)$$

$$PS = (216.880, -69.653, 131.699)$$

Normal vector to the APP is used in anteversion angle calculations,

$$\vec{Z} = \begin{bmatrix} x_{col} - x_{con} + 10 & y_{col} - y_{con} & z_{col} - z_{con} \\ x_{col} - x_{cen} & y_{col} - y_{cen} & z_{col} - z_{cen} \end{bmatrix}$$

When substitute above coordinates values,

$$\vec{Z} = \begin{bmatrix} \text{-223.722} & 0.051 & \text{-2.215} \\ \text{-116.941} & 86.876 & \text{-1.584} \end{bmatrix}$$

By considering the mode of the above $\vec{Z}$ matrix, $\vec{Z}_{x_{app}}, \vec{Z}_{y_{app}}, \vec{Z}_{z_{app}}$ values were obtained by followed the same steps shown in the anteversion angle calculation for the neutral position of the APP. Then, those values were substituted in equation 2.23 and Anteversion angle was obtained for, when LASIS moves towards the medial direction by 1 cm,

$$ant\_ang = \sin^{-1}\left|\left(\frac{(192.326*0.6861)+(95.459*-0.6861)+(-19430.128*0.2419)}{\sqrt{(192.326)^2+(95.459)^2+(-19430.128)^2}*\sqrt{(0.6861)^2+(-0.6861)^2+(0.2419)^2}}\right)\right|$$

$$Ant\_ang = \sin^{-1} 0.2318$$

$$Ant\_ang = 13.40^{\circ}$$

Inclination angle calculations

$$\vec{Y} = \begin{bmatrix} Z_{x_{apc}} & Z_{y_{apc}} & Z_{z_{apc}} \\ x_{col} - x_{con} & y_{col} - y_{con} & z_{col} - z_{con} \end{bmatrix}$$

$$\vec{Y} = \begin{bmatrix} 192.326 & 95.460 & -19430.128 \\ -223.722 & 0.051 & -2.215 \end{bmatrix}$$

By considering the mode of the above $\vec{Y}$ and obtained the values for $\vec{Y}_{x_{app}}, \vec{Y}_{y_{app}}, \vec{Y}_{z_{app}}$ by following the same steps shown in the anteversion angle calculation for the neutral position of the APP. Then inclination angle was obtained for, when LASIS moves towards the medial direction by 1 cm.

From equation 2.24

$$Inc-ang=\cos^{-1}\left|\frac{\left((0.784)*\left(2.8360\right)\right)+\left((-4347.370)*\left(-2.8360\right)\right)+\left((21.366)*0.2419\right)}{\sqrt{\left(0.784\right)^2+\left(-4347.370\right)^2+\left(21.366\right)^2}*\sqrt{\left(2.8360\right)^2+\left(-2.8360\right)^2+0.2419^2}}\right|$$

$$Inc-ang=\cos^{-1}0.7062$$

$$Inc-ang=45.07^{\circ}$$

Changing the landmark position of RASIS along lateral direction by 1 cm.

New position coordinates in millimetres

$$RASIS=\left(92.129,12.459,130.610\right)$$

$$LASIS=\left(320.704,10.017,133.548\right)$$

$$PS=\left(216.956,-70.144,131.823\right)$$

Normal vector to the APP is used in anteversion angle calculations,

$$\vec{Z}=\begin{bmatrix} x_{col}-x_{con}-10 & y_{col}-y_{con} & z_{col}-z_{con} \\ x_{col}-x_{cen} & y_{col}-y_{cen} & z_{col}-z_{cen} \end{bmatrix}$$

When substitute above coordinates values,

$$\vec{Z}=\begin{bmatrix} -228.575 & 2.448 & -2.938 \\ -124.826 & 82.604 & -1.213 \end{bmatrix}$$

By considering the mode of the above $\vec{Z}$ matrix, $\vec{Z}_{x_{app}},\vec{Z}_{y_{app}},\vec{Z}_{z_{app}}$ values were obtained by followed the same steps shown in the anteversion angle calculation for the neutral position of the APP. Then, those values were substituted in equation 2.23 and Anteversion angle was obtained for, when RASIS moves towards the lateral direction by 1 cm,

$$ant\_ang = \sin^{-1}\left|\left(\frac{(2.397*0.6861)+((-0.895)*-0.6861)+((-185.75)*0.2419)}{\sqrt{(2.397)^2+(0.954)^2+(-185.75)^2}*\sqrt{(0.6861)^2+(-0.6861)^2+(0.2419)^2}}\right)\right|$$

$$Ant\_ang = \sin^{-1} 0.2364$$

$$Ant\_ang = 13.67^{\circ}$$

Inclination angle calculations

$$\vec{Y} = \begin{bmatrix} Z_{x_{apc}} & Z_{y_{apc}} & Z_{z_{apc}} \\ x_{col}-x_{con} & y_{col}-y_{con} & z_{col}-z_{con} \end{bmatrix}$$

$$\vec{Y} = \begin{bmatrix} 239.707 & -89.467 & -18575.451 \\ -228.575 & 2.448 & -2.938 \end{bmatrix}$$

By considering the mode of the above $\vec{Y}$ and obtained the values for $\vec{Y}_{x_{app}}, \vec{Y}_{y_{app}}, \vec{Y}_{z_{app}}$ by following the same steps shown in the anteversion angle calculation for the neutral position of the APP. Then inclination angle was obtained for, when RASIS moves towards the lateral direction by 1 cm. by substituting the above obtained values in

equation 2.24

$$Inc-ang = \cos^{-1}\left|\frac{((0.457)*(2.8360))+((-42.466)*(-2.8360))+((-0.199)*0.2419)}{\sqrt{(0.457)^2+(-42.466)^2+(-0.199)^2}*\sqrt{(2.8360)^2+(-2.8360)^2+0.2419^2}}\right|$$

$$Inc-ang = \cos^{-1} 0.7131$$

$$Inc-ang = 44.52^{\circ}$$

Changing the landmark position of PS along caudal direction by 1 cm.

New position coordinates in millimetres

$RASIS = (\text{-}135.847, 167.916, 1135.893)$

$LASIS = (192.528, 165.474, 1142.473)$

$PS = (27.191, 17.008, 1139.054)$

Normal vector to the APP is used in anteversion angle calculations,

$$\vec{Z} = \begin{bmatrix} x_{col} - x_{con} & y_{col} - y_{con} & z_{col} - z_{con} \\ x_{col} - x_{cen} & y_{col} - y_{cen} + 10 & z_{col} - z_{cen} \end{bmatrix}$$

When substitute above coordinates values,

$$\vec{Z} = \begin{bmatrix} \text{--}328.376 & 2.442 & \text{-}6.581 \\ \text{-}163.039 & 150.908 & \text{-}3.161 \end{bmatrix}$$

By considering the mode of the above $\vec{Z}$ and following the same steps shown in the anteversion angle calculation for the neutral position of the APP. From equation 2.23, anteversion angle, when PS moves towards the caudal direction by 1 cm.

$$ant\_ang = \sin^{-1}\left| \left(\frac{((9.853)*0.6861)+((-0.348)*-0.6861)+((-491.563)*0.2419)}{\sqrt{(9.853)^2+(-0.348)^2+(-491.563)^2}*\sqrt{(0.6861)^2+(-0.6861)^2+(0.2419)^2}} \right) \right|$$

$$Ant\_ang = \sin^{-1} 0.2286$$

$$Ant\_ang = 13.51^{\circ}$$

Inclination angle calculations

$$\vec{Y} = \begin{bmatrix} Z_{x_{apc}} & Z_{y_{apc}} & Z_{z_{apc}} \\ x_{col} - x_{con} & y_{col} - y_{con} & z_{col} - z_{con} \end{bmatrix}$$

$$\vec{Y} = \begin{bmatrix} 985.339 & -34.847 & -49156.334 \\ -328.376 & 2.442 & -6.581 \end{bmatrix}$$

By considering the mode of the above $\vec{Y}$ and obtained the values for $\vec{Y}_{x_{app}}, \vec{Y}_{y_{app}}, \vec{Y}_{z_{app}}$. Then, those values were substituted in equation 2.24 and inclination angle was obtained for, when PS moves towards the caudal direction by 1 cm.

From equation 2.24

$$Inc - ang = \cos^{-1} \left| \frac{\left(12.026 * \left(2.8360\right)\right) + \left(-0.002 * \left(-2.8360\right)\right) + \left(-0.904 * 0.2419\right)}{\sqrt{\left(12.026\right)^2 + \left(-0.002\right)^2 + \left(-0.904\right)^2} * \sqrt{\left(2.8360\right)^2 + \left(-2.8360\right)^2 + 0.2419^2}} \right|$$

$$Inc - ang = \cos^{-1} 0.7110$$

$$Inc - ang = 44.68^{\circ}$$

Changing the landmark position of PS along cranial direction by 1 cm.

New position coordinates in millimetres

$$RASIS = \left(-78.043, 103.383, 826.592\right)$$
$$LASIS = \left(143.835, 100.715, 830.472\right)$$
$$PS = \left(25.101, 21.010, 827.564\right)$$

Normal vector to the APP is used in anteversion angle calculations,

$$\vec{Z} = \begin{bmatrix} x_{col} - x_{con} & y_{col} - y_{con} & z_{col} - z_{con} \\ x_{col} - x_{cen} & y_{col} - y_{cen} - 10 & z_{col} - z_{cen} \end{bmatrix}$$

When substitute above coordinates values,

$$\vec{Z} = \begin{bmatrix} \text{-221.878} & 2.667 & \text{-3.880} \\ \text{-103.145} & 82.287 & -0.972 \end{bmatrix}$$

By considering the mode of the above $\vec{Z}$ matrix, $\vec{Z}_{x_{app}}, \vec{Z}_{y_{app}}, \vec{Z}_{z_{app}}$ values were obtained by followed the same steps shown in the anteversion angle calculation for the neutral position of the APP. Then, those values were substituted in equation 2.23 and Anteversion angle was obtained for, when LASIS moves towards the cranial direction by 1 cm,

$$ant\_ang = \sin^{-1}\left| \left(\frac{(0.317*0.6861)+(-0.185*-0.6861)+(-17.982*0.2419)}{\sqrt{(0.317)^2+(-0.185)^2+(-17.982)^2}*\sqrt{(0.6861)^2+(-0.6861)^2+(0.2419)^2}} \right) \right|$$

$$Ant\_ang = \sin^{-1} 0.2368$$

$$Ant\_ang = 13.70^{\circ}$$

Inclination angle calculations

$$\vec{Y} = \begin{bmatrix} Z_{x_{apc}} & Z_{y_{apc}} & Z_{z_{apc}} \\ x_{col} - x_{con} & y_{col} - y_{con} & z_{col} - z_{con} \end{bmatrix}$$

$$\vec{Y} = \begin{bmatrix} 316.712 & -184.631 & -17982.575 \\ -221.878 & 2.667 & -3.880 \end{bmatrix}$$

By considering the mode of the above $\vec{Y}$ and obtained the values for $\vec{Y}_{x_{app}}, \vec{Y}_{y_{app}}, \vec{Y}_{z_{app}}$ by following the same steps shown in the anteversion angle calculation for the neutral position of the APP. Then inclination angle was obtained for, when PS moves towards the cranial direction by 1 cm.

From equation 2.24

$$Inc-ang=\cos^{-1}\left|\frac{\left((0.487)*(2.8360)\right)+\left((-39.912)*(\text{-}2.8360)\right)+\left(-0.401*0.2419\right)}{\sqrt{(0.487)^2+(-39.912)^2+(-0.401)^2}*\sqrt{(2.8360)^2+(\text{-}2.8360)^2+0.2419^2}}\right|$$

$$Inc-ang=\cos^{-1}0.7137$$

$$Inc-ang=44.46^{\circ}$$

Changing the landmark position of PS along medial direction by 1 cm.

New position coordinates in millimetres

$$RASIS=(\text{-}58.110,101.287,826.512)$$
$$LASIS=(153.330,97.489,831.024)$$
$$PS=(32.158,22.740,827.364)$$

Normal vector to the APP is used in anteversion angle calculations,

$$\vec{Z}=\begin{bmatrix} x_{col}-x_{con} & y_{col}-y_{con} & z_{col}-z_{con} \\ x_{col}-x_{cen}+10 & y_{col}-y_{cen} & z_{col}-z_{cen} \end{bmatrix}$$

When substitute above coordinates values,

$$\vec{Z}=\begin{bmatrix} \text{-}211.441 & 3.798 & \text{-}4.512 \\ \text{-}90.268 & 78.547 & \text{-}0.852 \end{bmatrix}$$

By considering the mode of the above $\vec{Z}$ matrix, $\vec{Z}_{x_{app}},\vec{Z}_{y_{app}},\vec{Z}_{z_{app}}$ values were obtained and followed the same steps shown in the anteversion angle calculation for the neutral position of the APP. Then, those values were substituted in equation 2.23 and Anteversion angle was obtained for, when PS moves towards the medial direction by 1 cm,

$$ant\_ang = \sin^{-1}\left|\left(\frac{(0.351*0.6861)+((-0.227)*-0.6861)+((-16.265)*0.2419)}{\sqrt{(0.351)^2+(-0.227)^2+(-16.265)^2}*\sqrt{(0.6861)^2+(-0.6861)^2+(0.2419)^2}}\right)\right|$$

$$Ant\_ang = \sin^{-1} 0.2366$$

$$Ant\_ang = 13.69^{\circ}$$

Inclination angle calculations

$$\vec{Y} = \begin{bmatrix} Z_{x_{apc}} & Z_{y_{apc}} & Z_{z_{apc}} \\ x_{col}-x_{con} & y_{col}-y_{con} & z_{col}-z_{con} \end{bmatrix}$$

$$\vec{Y} = \begin{bmatrix} 351.214 & -227.246 & -16265.137 \\ -211.441 & 3.798 & -4.512 \end{bmatrix}$$

By considering the mode of the above $\vec{Y}$ and obtained the values for $\vec{Y}_{x_{app}}, \vec{Y}_{y_{app}}, \vec{Y}_{z_{app}}$ by following the same steps shown in the anteversion angle calculation for the neutral position of the APP. Then inclination angle was obtained for, when PS moves towards the medial direction by 1 cm.

From equation 2.24

$$Inc-ang = \cos^{-1}\left|\frac{((0.628)*(2.8360))+((-34.407)*(-2.8360))+((-0.467)*0.2419)}{\sqrt{(0.628)^2+(-34.407)^2+(-0.467)^2}*\sqrt{(2.8360)^2+(-2.8360)^2+0.2419^2}}\right|$$

$$Inc-ang = \cos^{-1} 0.7177$$

$$Inc-ang = 44.14^{\circ}$$

Changing the landmark position of PS along lateral direction by 1 cm.

New position coordinates in millimetres

$RASIS = (102.651, 7.597, 131.692)$

$LASIS = (330.215, 4.626, 134.815)$

$PS = (210.992, -67.180, 131.253)$

Normal vector to the APP is used in anteversion angle calculations,

$$\vec{Z} = \begin{bmatrix} x_{col} - x_{con} & y_{col} - y_{con} & z_{col} - z_{con} \\ x_{col} - x_{cen} - 10 & y_{col} - y_{cen} & z_{col} - z_{cen} \end{bmatrix}$$

When substitute above coordinates values,

$$\vec{Z} = \begin{bmatrix} -227.564 & 2.971 & -3.123 \\ -108.341 & 74.778 & 0.439 \end{bmatrix}$$

By considering the mode of the above $\vec{Z}$ matrix, $\vec{Z}_{x_{app}}, \vec{Z}_{y_{app}}, \vec{Z}_{z_{app}}$ values were obtained by followed the same steps shown in the anteversion angle calculation for the neutral position of the APP. Then, those values were substituted in equation 2.23 and Anteversion angle was obtained for, when PS moves towards the lateral direction by 1 cm,

$$ant\_ang = \sin^{-1}\left| \left(\frac{(0.235 * 0.6861) + ((-0.438) * -0.6861) + ((-16.695) * 0.2419)}{[\sqrt{(0.235)^2 + (-0.438)^2 + (-16.695)^2}] * [\sqrt{(0.6861)^2 + (-0.6861)^2 + (0.2419)^2}]} \right) \right|$$

$$Ant\_ang = \sin^{-1} 0.2502$$

$$Ant\_ang = 14.48^{\circ}$$

Inclination angle calculations

$$\vec{Y} = \begin{bmatrix} Z_{x_{apc}} & Z_{y_{apc}} & Z_{z_{apc}} \\ x_{col} - x_{con} & y_{col} - y_{con} & z_{col} - z_{con} \end{bmatrix}$$

$$\vec{Y} = \begin{bmatrix} 234.828 & -438.347 & -16694.841 \\ -227.564 & 2.971 & -3.123 \end{bmatrix}$$

By considering the mode of the above $\vec{Y}$ and obtained the values for $\vec{Y}_{x_{app}}, \vec{Y}_{y_{app}}, \vec{Y}_{z_{app}}$ by following the same steps shown in the anteversion angle calculation for the neutral position of the APP. Then inclination angle was obtained for, when PS moves towards the lateral direction by 1 cm. by substituting the above obtained values in equation 2.24

$$Inc-ang = \cos^{-1}\left|\frac{\left((0.510)*\left(2.8360\right)\right)+\left((-37.999)*\left(-2.8360\right)\right)+\left((-0.991)*0.2419\right)}{\sqrt{\left(0.510\right)^2+\left(-37.999\right)^2+\left(-0.991\right)^2}*\sqrt{\left(2.8360\right)^2+\left(-2.8360\right)^2+0.2419^2}}\right|$$

$$Inc-ang = \cos^{-1} 0.7134$$

$$Inc-ang = 44.48^{\circ}$$

Appendix B

Preparation of VICON environment.

VICON enviroment should be prepared prior to the data capturing process. First step is to prepare VICON system, including MX cameras. At this stage, Nexus is in Live mode. Calibration object was selected as *5 marker wand & L-frame* from *system preparation* tools pane.

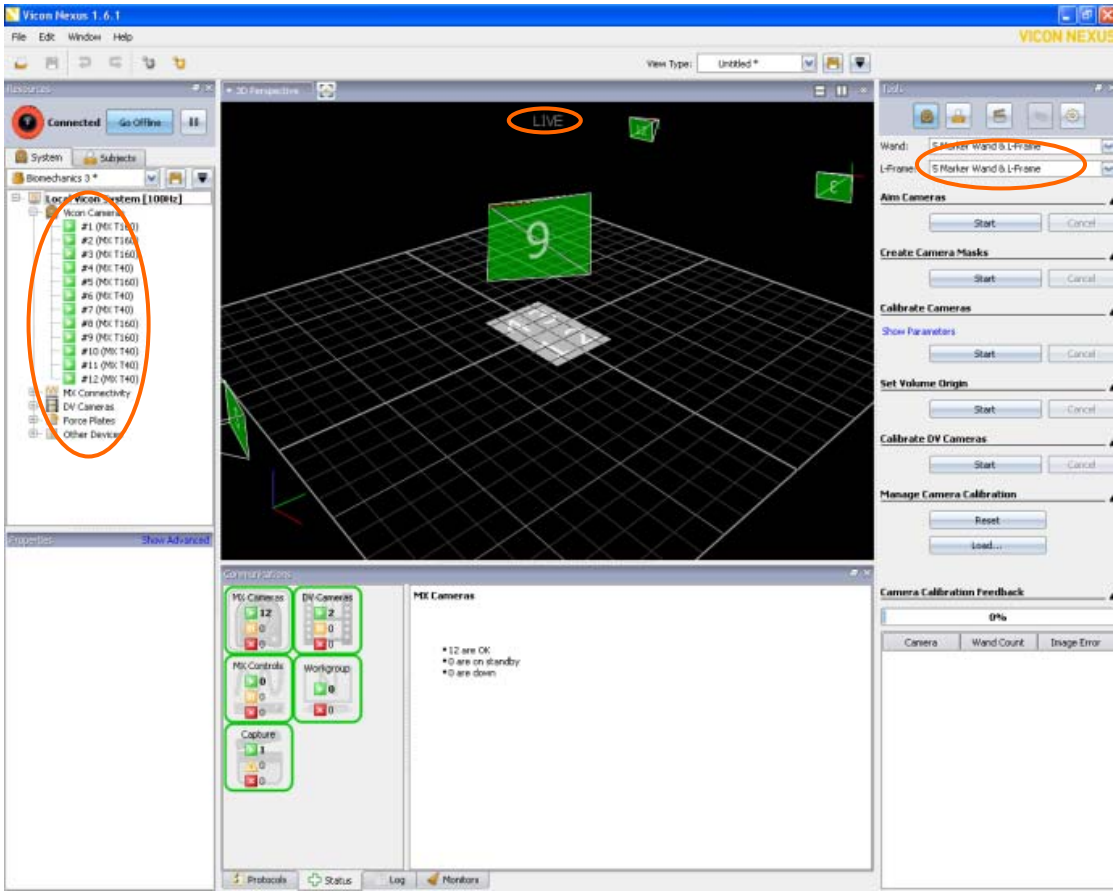

Next step was MX camera calibration. Camera calibration was started by switching the *start* button and then wand was waved with in the capture volume. At this stage, Nexus started to identify the calibration object in each camera view, and then *stat* button was switched to *stop* mode.

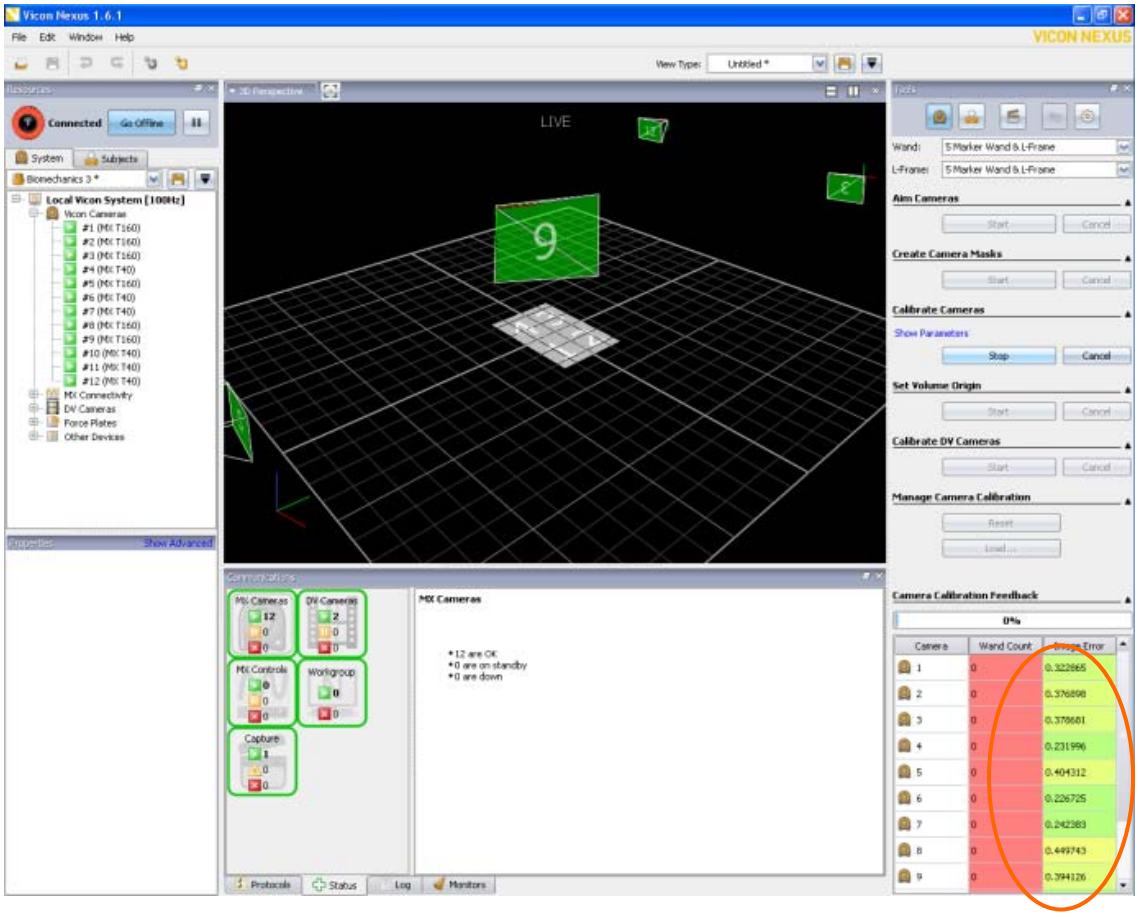

After switching to stop mode at camera calibration, camera calibration feed back was loaded. It shows the number of wand counts and image error data. Wand count identify the number of frames it has captured containing the calibration object. When Nexus has acquired enough wand data to calibrate that camera (typically 1000 frames), entry for the number of frames was turned green from red. Image error indicates the accuracy of 3D reconstruction of the marker.

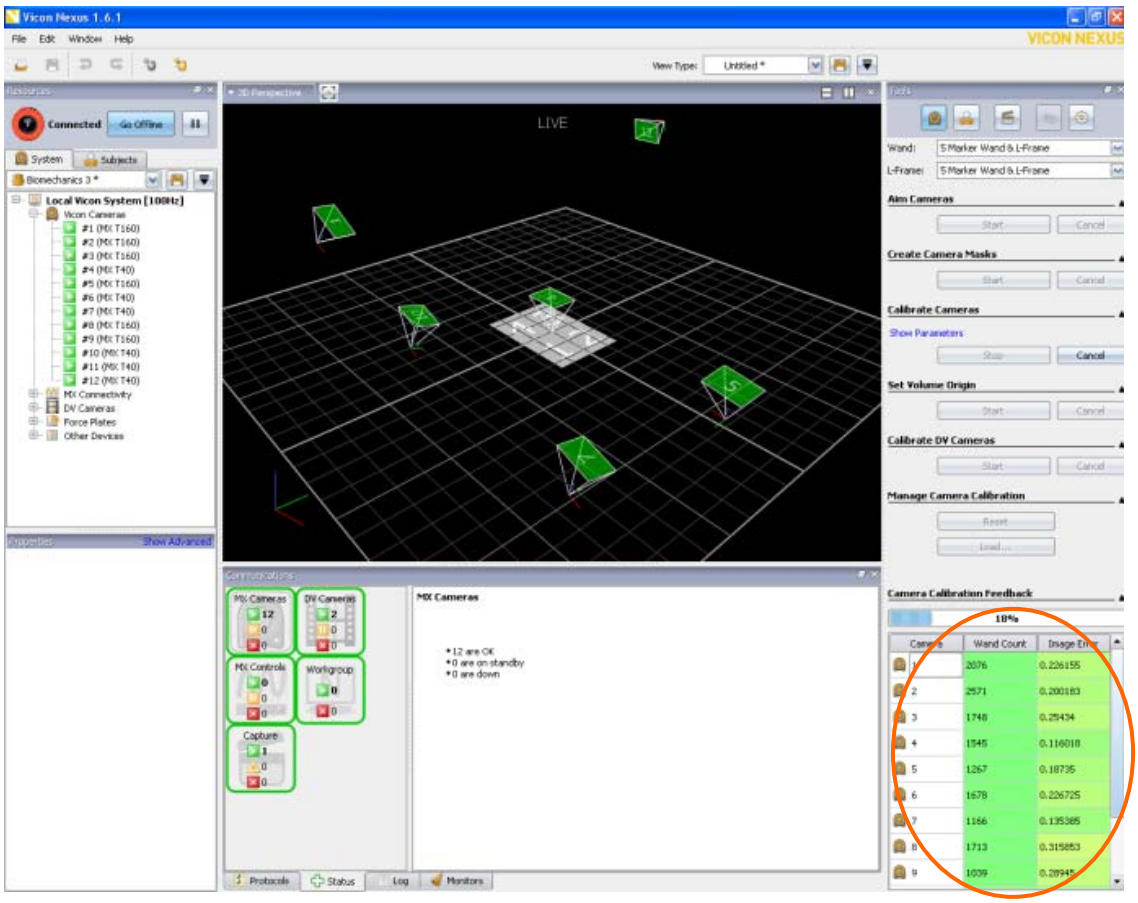

Set origin

Next sept was setting the volume origin. Origin of the VICON coordinate frame was set by placing five marker want in the middle of the force plate. Once, wand was placed there, *set origin* button was switched on. With that, system defines the origin of the lab coordinate frame.

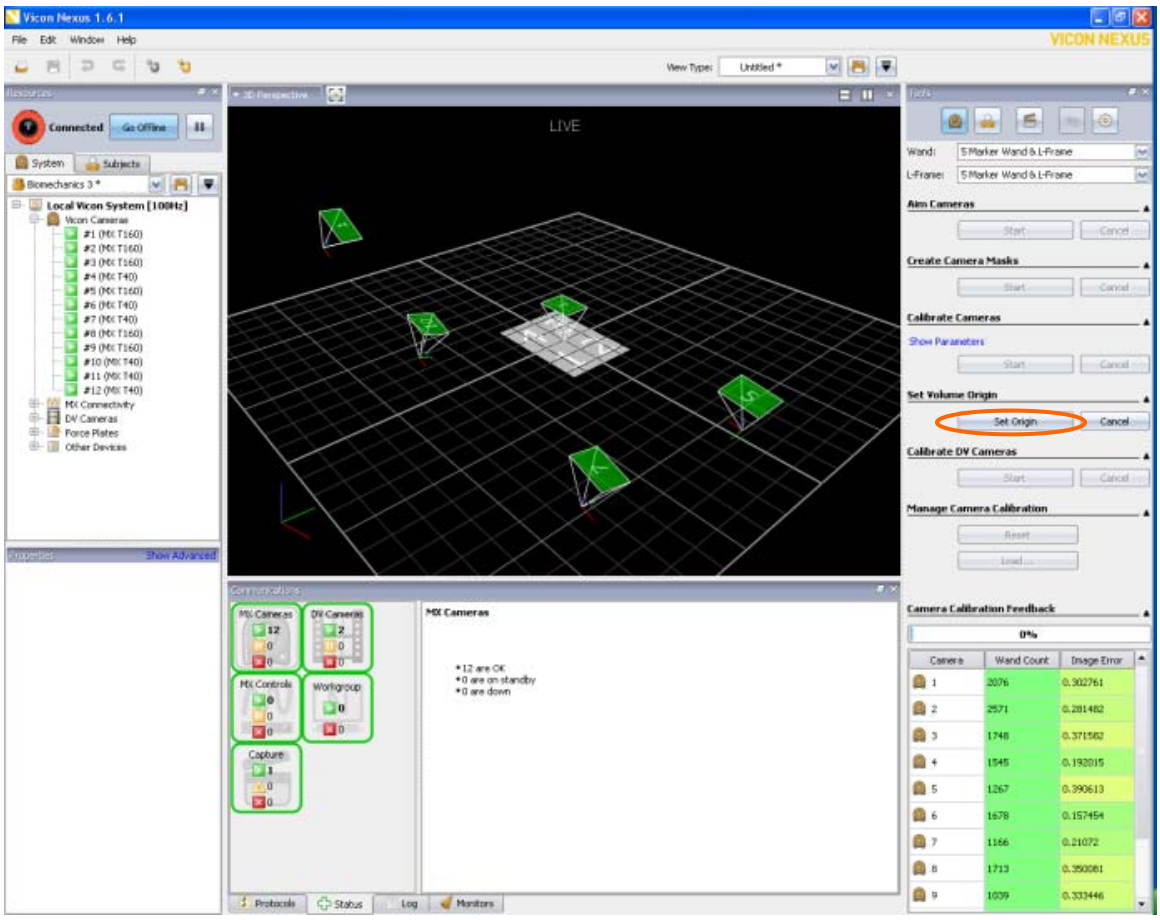
Vicon Nexus 1.6.1
File Edit Window Help
VICON NEXUS
View Type: Untitled *
Connected
Go Offline
System
Subjects
Biomechanics 3 *
Local Vicon System [100Hz]
Vicon Cameras
#1 (MX T160)
#2 (MX T160)
#3 (MX T160)
#4 (MX T40)
#5 (MX T160)
#6 (MX T40)
#7 (MX T40)
#8 (MX T160)
#9 (MX T160)
#10 (MX T40)
#11 (MX T40)
#12 (MX T40)
MX Connectivity
DV Cameras
Force Plates
Other Devices
Properties
Show Advanced
3D Perspective
LIVE
Tools
Wand: 5 Marker Wand & L-Frame
L-Frame: 5 Marker Wand & L-Frame
Aim Cameras
Start
Cancel
Create Camera Masks
Start
Cancel
Calibrate Cameras
Show Parameters
Start
Cancel
Set Volume Origin
Set Origin
Cancel
Calibrate DV Cameras
Start
Cancel
Manage Camera Calibration
Reset
Load...
Camera Calibration Feedback
0%
Camera
Wand Count
Image Error
1 2076 0.302761
2 2571 0.281482
3 1748 0.371582
4 1545 0.192015
5 1267 0.390613
6 1678 0.157454
7 1166 0.21072
8 1713 0.350081
9 1039 0.333446
Communications
MX Cameras
12
0
0
DV Cameras
2
0
0
MX Controls
0
0
0
Workgroup
0
0
Capture
1
0
0
MX Cameras
* 12 are OK
* 0 are on standby
* 0 are down
Protocols
Status
Log
Monitors

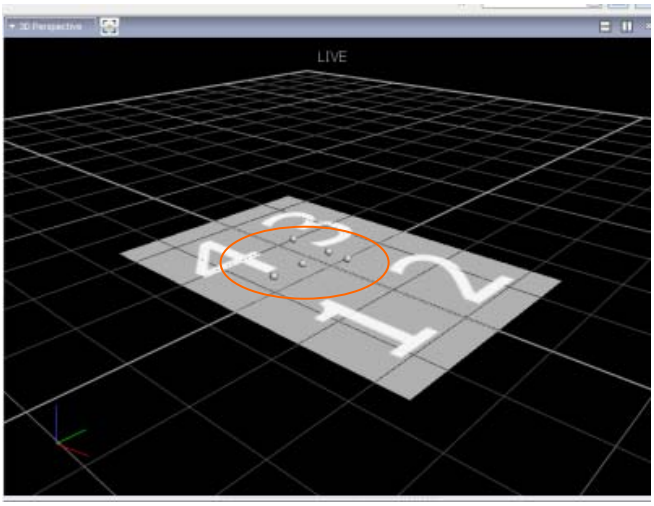
3D Perspective
LIVE

Appendix C

BodyBuilder code

Mod file used to get the pointer coordnates from VICON data.

```
{*Start of macro section*}
{*======================*}

macro SUBSTITUTE4(p1,p2,p3,p4)
{*Replaces any point missing from set of four fixed in a segment*}

s234 = [p3,p2-p3,p3-p4]
p1V = Average(p1/s234)*s234
s341 = [p4,p3-p4,p4-p1]
p2V = Average(p2/s341)*s341
s412 = [p1,p4-p1,p1-p2]
p3V = Average(p3/s412)*s412
s123 = [p2,p1-p2,p2-p3]
p4V = Average(p4/s123)*s123

p1 = p1 ? p1V
p2 = p2 ? p2V
p3 = p3 ? p3V
p4 = p4 ? p4V
endmacro

macro SEGVIS(Segment)
{*outputs a visual representation of the segment to be viewed in the Workspace*}
{*0(Segment) is the origin of the segment*}

ORIGIN#Segment=0(Segment)
XAXIS#Segment=0(Segment)+(1(Segment)*10)
YAXIS#Segment=0(Segment)+(2(Segment)*10)
ZAXIS#Segment=0(Segment)+(3(Segment)*10)
OUTPUT(ORIGIN#Segment,XAXIS#Segment,YAXIS#Segment,ZAXIS#Segment)
endmacro

macro POINTER(Anatomy, Segment)

{*Calculates the position of the end of the pointer for calibration in the technical
frame it belongs to*}
{*1st determine the "point" in the Global system and outputs it as point#Calib. Then
converts the point into*}
{*the appropriate technical reference frame and stores it as parameter
$%#point#Calib*}
```

```
unitPointer=((POI1-POI2)/DIST(POI1,POI2))
Anatomy#Calib=POI1+123*unitPointer
OUTPUT(Anatomy#Calib)
PARAM(Anatomy#Calib)
%#Anatomy#Calib=Anatomy#Calib/Segment
PARAM(%#Anatomy#Calib)
endmacro

{*End of macro section*}

XC=(p1(1)+p2(1)+p3(1)+p4(1))/4
YC=(p1(2)+p2(2)+p3(2)+p4(2))/4
ZC=(p1(3)+p2(3)+p3(3)+p4(3))/4

CENT_p={XC,YC,ZC}

OUTPUT(CENT_p)

pAXES=[CENT_p,p1-p2,p3-p4,zyx]

SEGVIS(pAXES)

%p_TIP={17.335,29.529,-313.705}
p_TIP=%p_TIP*pAXES

OUTPUT(p_TIP)

p_EDGE={(XC+17.335),(YC+29.529),(ZC-313.705)}

OUTPUT(p_EDGE)
```

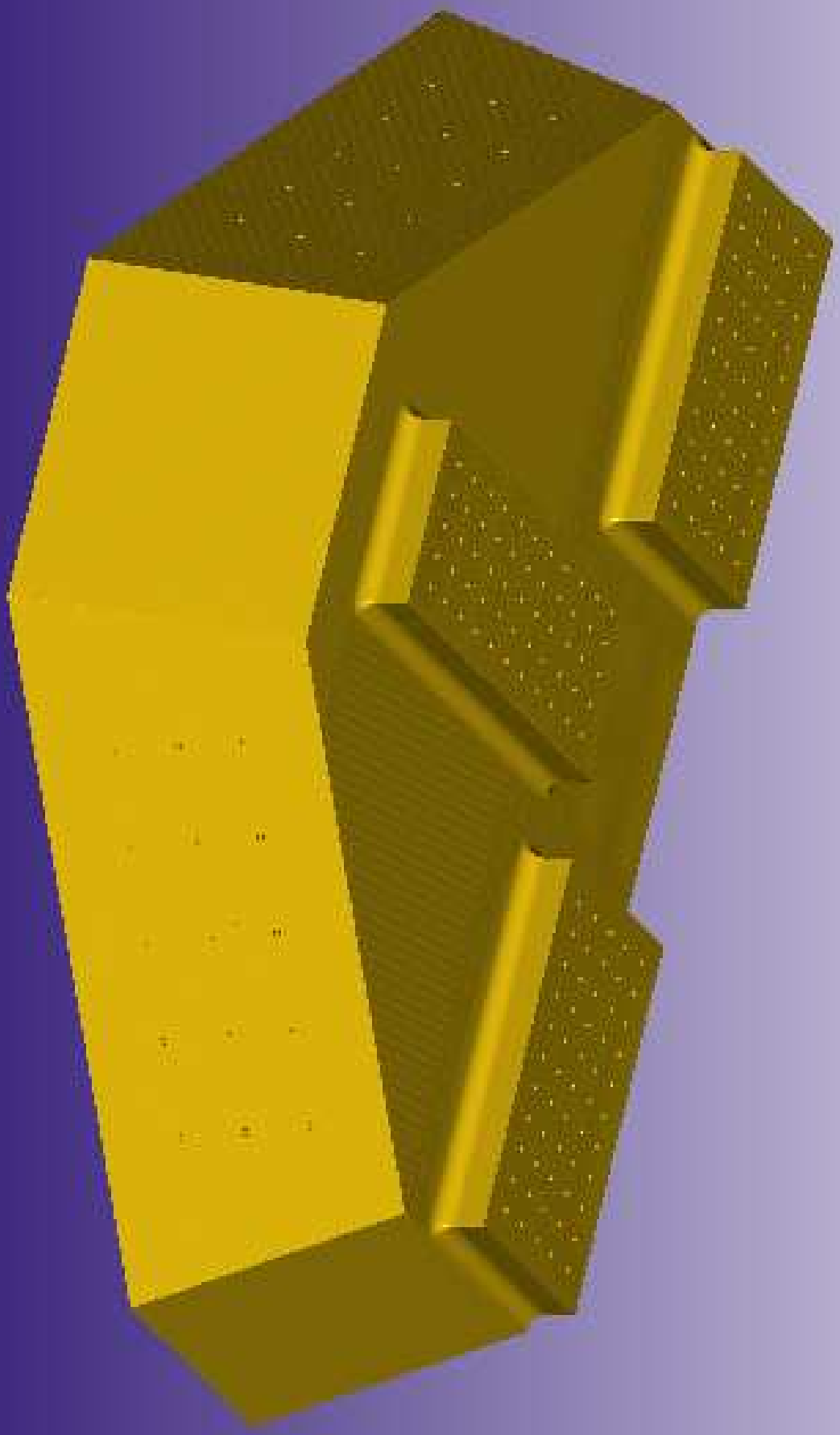

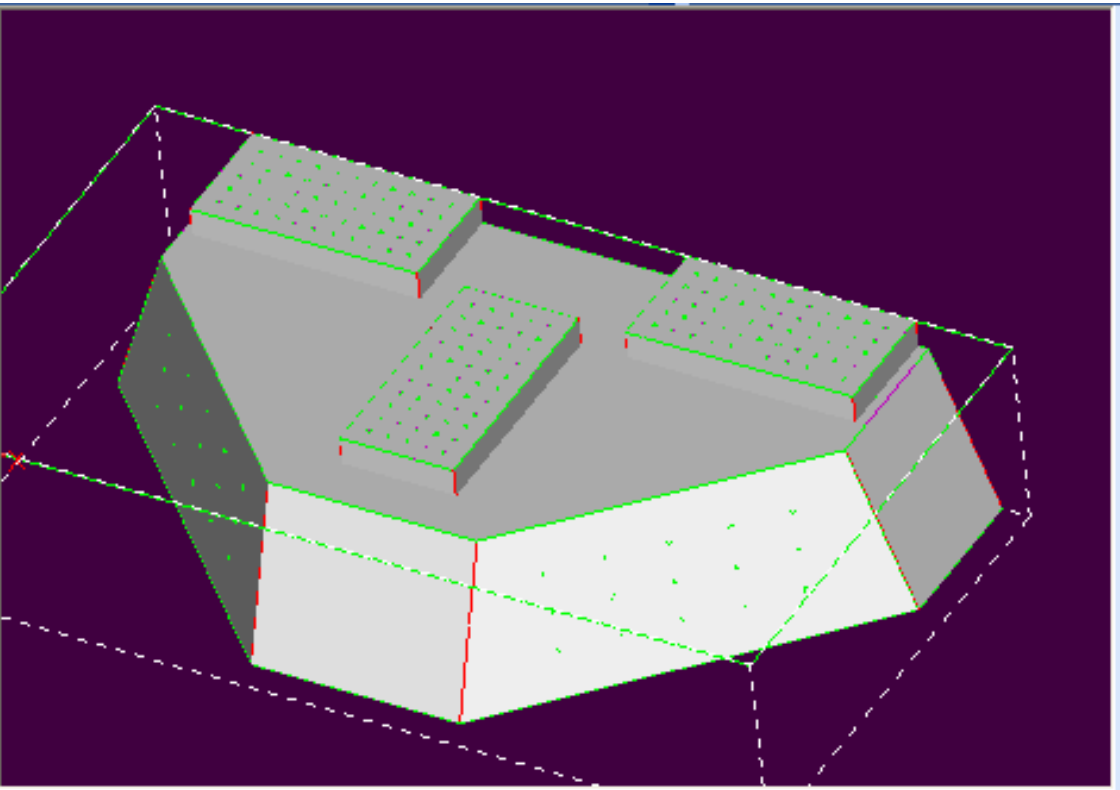

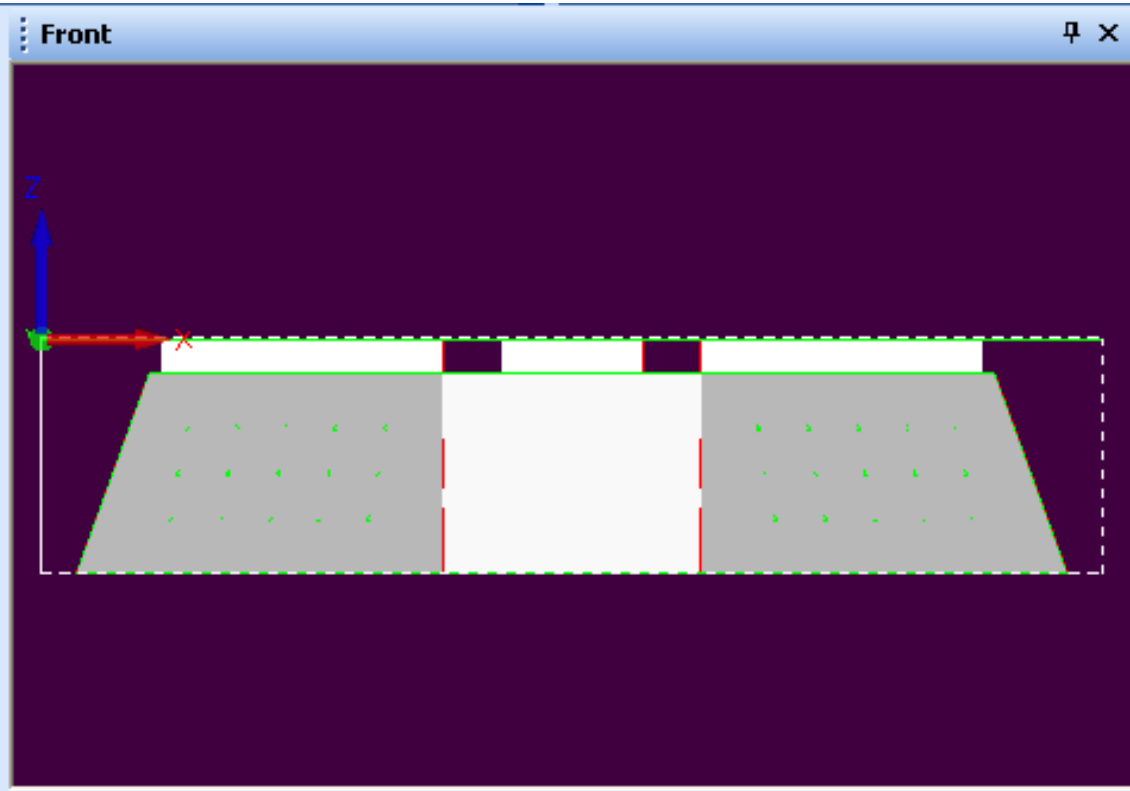
Front
Z
X

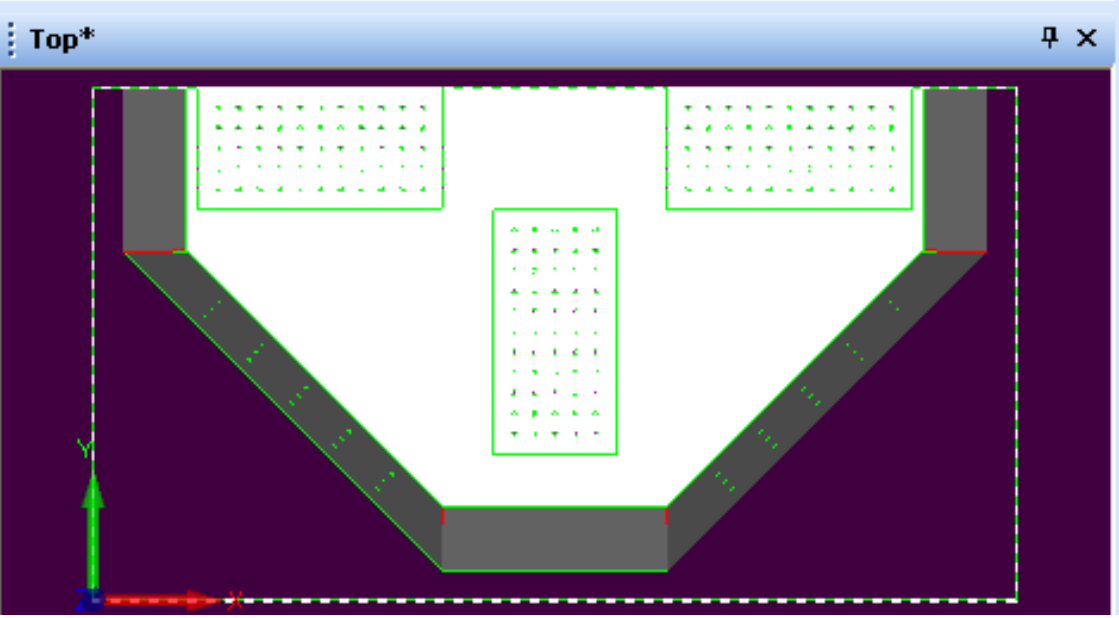
Top*
Y
X

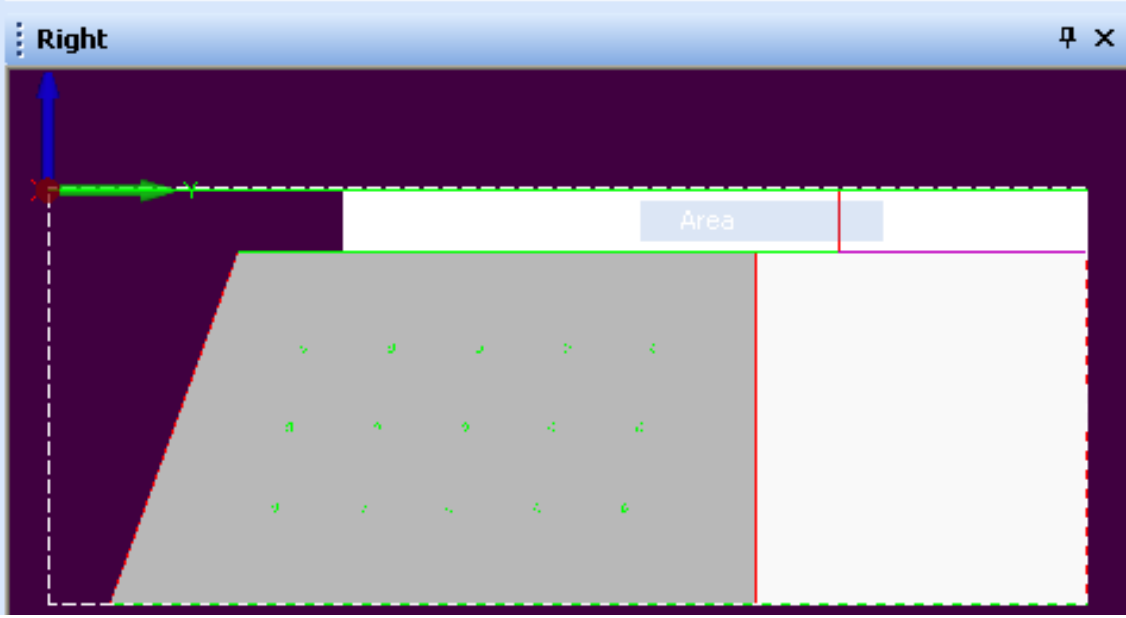
Right
Y
X
Area

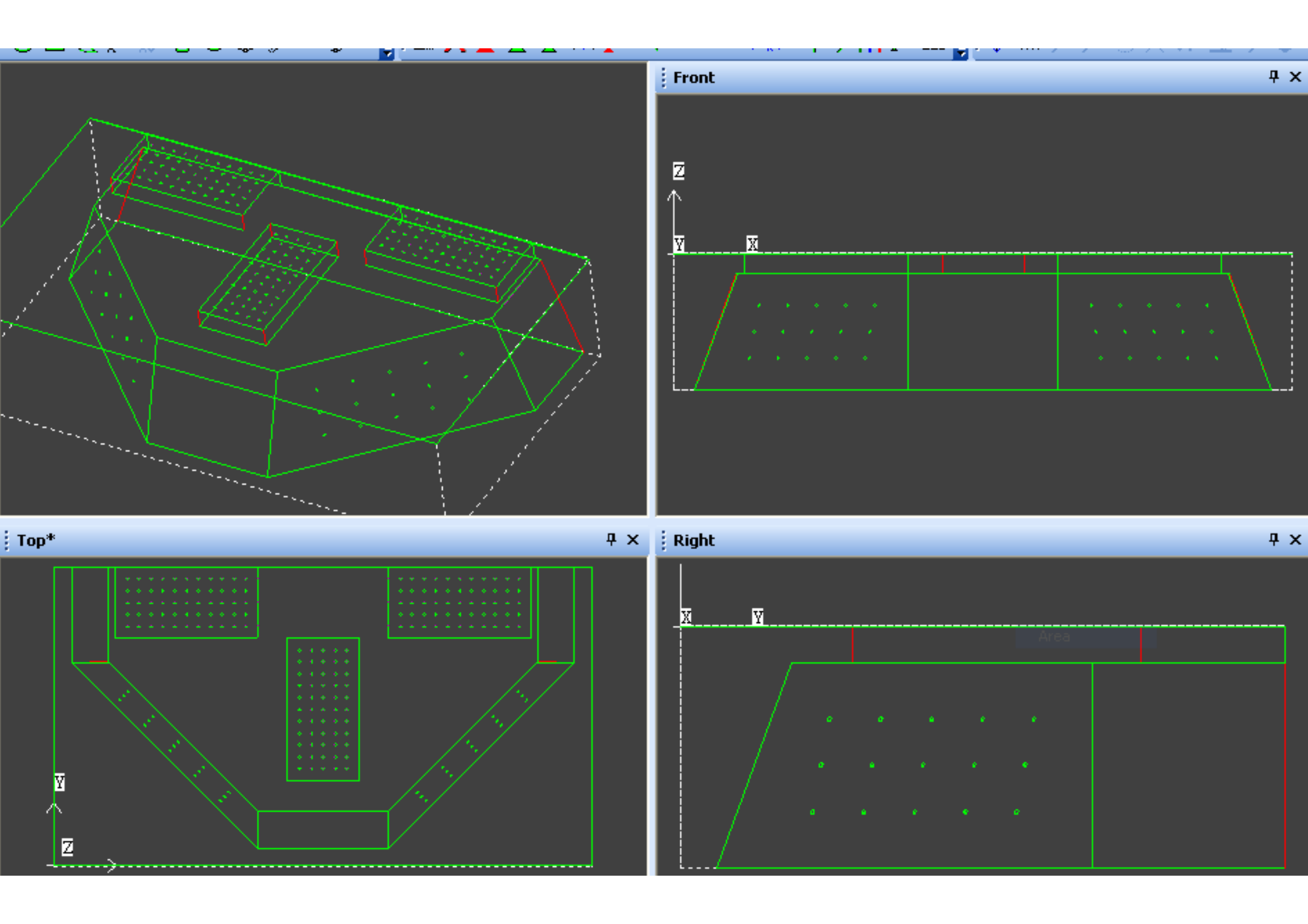
Front
Z
Y
X
Top*
Y
Z
Right
X
Y